

# Shipboard Smoke Control Tests Using Forced Counterflow Air Supply

F. W. WILLIAMS

*Navy Technology Center for Safety and Survivability, Chemistry Division*

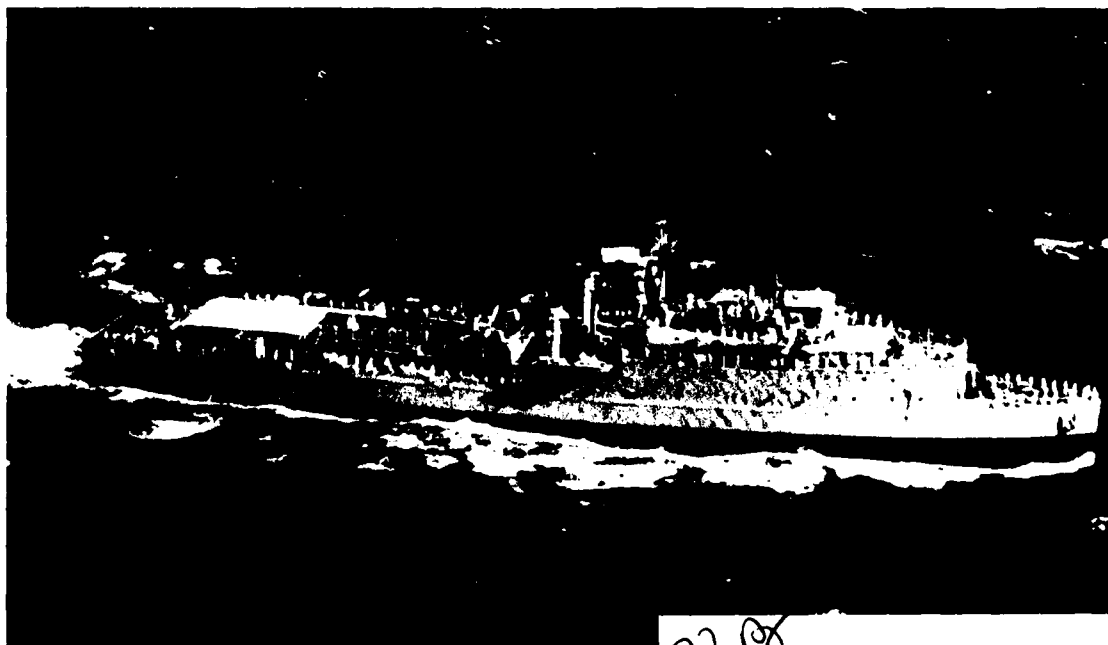
E. W. FORSELL, P. J. DiNENNO, C. L. BEYLER

*Hughes Associates, Inc., Columbia, MD 21045*

P. LAIN

*Naval Sea Systems Command, Washington, DC 20362-5101*

September 16, 1994



Approved for public release; distribution unlimited.

7218 94-31904



AD-A285 409



REPORT DOCUMENTATION PAGE			Form Approved OMB No. 0704-0188	
Public reporting burden for this collection of information is estimated to average 1 hour per response, including the time for reviewing instructions, searching existing data sources, gathering and maintaining the data needed, and completing and reviewing this collection of information. Send comments regarding this burden estimate or any other aspect of this collection of information, including suggestions for reducing this burden, to Washington Headquarters Services, Directorate for Information Operations and Reports, 1215 Jefferson Davis Highway, Suite 1204, Arlington, VA 22202-4302, and to the Office of Management and Budget, Paperwork Reduction Project (0704-0188), Washington, DC 20503.				
1. AGENCY USE ONLY (Leave Blank)		2. REPORT DATE  September 8, 1994		3. REPORT TYPE AND DATES COVERED
4. TITLE AND SUBTITLE  Shipboard Smoke Control Tests Using Forced Counterflow Air Supply			5. FUNDING NUMBERS	
6. AUTHOR(S)  F. W. Williams, E. W. Forssell,* P. J. DiNenno,* C. L. Beyler,* and P. Lain**				
7. PERFORMING ORGANIZATION NAME(S) AND ADDRESS(ES)  Naval Research Laboratory Washington, DC 20375-5320			8. PERFORMING ORGANIZATION REPORT NUMBER  NRL/MR/6180-94-7616	
9. SPONSORING/MONITORING AGENCY NAME(S) AND ADDRESS(ES)  Naval Sea Systems Command Washington, DC 20362-5101			10. SPONSORING/MONITORING AGENCY REPORT NUMBER	
11. SUPPLEMENTARY NOTES  *Hughes Associates, Inc., Columbia, MD **Naval Sea Systems Command, Washington, DC 20362-5101				
12a. DISTRIBUTION/AVAILABILITY STATEMENT  Approved for public release; distribution unlimited.			12b. DISTRIBUTION CODE	
13. ABSTRACT (Maximum 200 words)  A full-scale experimental investigation of smoke movement in horizontal passages and vertical trunks has been conducted to correlate minimum opposed air flows and buoyancy of the smoke. A series of experiments were carried out on the ex-USS SHADWELL. The correlation between minimum opposed air flow velocity and smoke propagation is presented in terms of Froude numbers. The experimental results of the present work shows that the relatively modest air velocities are able to limit the movement of smoke in either the horizontal passageway or the vertical trunk. On the basis of present results, a smoke exhaust system can be designed with large openings to provide a means of restricting the movement of smoke from fires. Recommendations are made for further research on smoke exhaust system testing to establish a correlation between fire size, extent of upstream smoke migration and air flow velocity.				
14. SUBJECT TERMS  Smoke                      Froude modeling Control                    Control shipboard smoke control Fire induced flow        Damage			15. NUMBER OF PAGES  72	
			16. PRICE CODE	
17. SECURITY CLASSIFICATION OF REPORT  UNCLASSIFIED	18. SECURITY CLASSIFICATION OF THIS PAGE  UNCLASSIFIED	19. SECURITY CLASSIFICATION OF ABSTRACT  UNCLASSIFIED	20. LIMITATION OF ABSTRACT  UL	

## Table of Contents

Section	Page
1.0 Introduction . . . . .	1
1.1 Background . . . . .	1
1.2 Previous Shipboard Experiments . . . . .	4
2.0 Present Objectives . . . . .	4
3.0 Experimental Test Facilities . . . . .	4
4.0 Test Fires . . . . .	7
5.0 Experimental Procedure . . . . .	12
5.1 Sequence of Experiments . . . . .	13
6.0 Instrumentation and Apparatus . . . . .	13
6.1 Smoke Temperature Measurement . . . . .	13
6.2 Air Velocity Measurement (Vent Flows) . . . . .	14
6.3 Smoke Density Measurement . . . . .	14
6.4 Gas Sampling . . . . .	15
6.5 Chemical Species Concentration Measurement . . . . .	15
6.6 Pressure Differential Measurement . . . . .	15
6.7 Visualization of Smoke Filling . . . . .	15
7.0 Experimental Results . . . . .	16
7.1 Results for Horizontal Passage Smoke Movement Test Series . . . . .	16
7.2 Results for Vertical Trunk Smoke Movement Test Series . . . . .	26
8.0 Discussion . . . . .	61
9.0 Conclusions . . . . .	62
10.0 Recommendations for Future Research . . . . .	63
11.0 References . . . . .	64

Accession For	
NTIS · CRA&I	<input checked="" type="checkbox"/>
DTIC TAB	<input type="checkbox"/>
Unannounced	<input type="checkbox"/>
Justification	
By	
Distribution /	
Availability Codes	
Dist	Avail and / or Special

A-1

## List of Figures

Figure	Page
1    01 level stateroom complex - geometry and instrumentation scheme for horizontal passageway tests . . . . .	6
2    Vertical Trunk 3-29-1-T geometry and instrumentation scheme — main deck . . . . .	8
3    Vertical trunk test series instrumentation scheme - second deck . . . . .	9
4    Vertical trunk test series instrumentation scheme - third deck . . . . .	10
5    Vertical trunk test series instrumentation scheme - elevation detail . . . . .	11
6    Required air velocity to halt upstream smoke migration during horizontal corridor tests with fire in location 1 . . . . .	18
7    Required air velocity to halt upstream smoke migration during horizontal tests with fire in location 2 . . . . .	19
8    Required air velocity at station 6 to halt smoke migration during horizontal corridor tests with fire in location 1 . . . . .	20
9    Required air velocity at station 6 to halt upstream smoke migration during horizontal tests with fire in location 2 . . . . .	21
10   Air velocity effects on upstream and downstream average temperatures in horizontal corridor with 620 kW fire in location 1 . . . . .	22
11   Air velocity effects on upstream and downstream maximum temperatures in horizontal corridor with 620 kW fire in location 1 . . . . .	23
12   Air velocity effects on upstream and downstream average temperatures in horizontal corridor with 720 kW fire in location 2 . . . . .	24
13   Air velocity effects on upstream and downstream maximum temperatures in horizontal corridor with 720 kW fire in location 2 . . . . .	25
14   Froude Number correlation based on hot layer temperature depth and average velocity at smoke location with fire in location 1 . . . . .	27
15   Froude Number correlation based on hot layer temperature depth and average velocity at smoke location with fire in location 2 . . . . .	28

## List of Figures

Figure	Page
16 Froude Number correlation based on ceiling temperature difference and velocity at smoke location with fire in location 1 . . . . .	29
17 Froude Number correlation based on ceiling temperature difference and velocity at smoke location with fire in location 2 . . . . .	30
18 Check of Heskestad and Spaulding correlation during horizontal corridor tests with fire in location 1 . . . . .	31
19 Check of Heskestad and Spaulding correlation during horizontal corridor tests with fire in location 2 . . . . .	32
20 Froude Number correlation based on fire size, downstream temperature, and velocity at smoke location with fire in location 1 . . . . .	33
21 Froude Number correlation based on fire size, downstream temperature, and velocity at smoke location with fire in location 2 . . . . .	34
22 Froude Number correlation based on fire size, downstream temperature, and velocity at station 6 with fire in location 1 . . . . .	35
23 Froude Number correlation based on fire size, downstream temperature, and velocity at station 6 with fire in location 2 . . . . .	36
24 Required air velocity to halt upstream smoke migration during vertical trunk tests with fire in location 1 . . . . .	39
25 Required air velocity to halt upstream smoke migration during vertical tests with fire in location 2 . . . . .	40
26 Required air velocity at main deck to halt smoke migration during vertical trunk tests with fire in location 1 . . . . .	41
27 Required air velocity at main deck hatch to halt upstream smoke migration during vertical tests with fire in location 2 . . . . .	42
28 Main deck hatch air velocity effects on average temperatures with 650 kW fire in location 1 . . . . .	43
29 Main deck hatch air velocity effects on maximum temperatures with 650 kW fire in location 1 . . . . .	44

## List of Figures

Figure	Page
30 Main deck hatch air velocity effects on average temperatures with 670 kW fire in location 2 . . . . .	45
31 Main deck hatch air velocity effects on maximum temperatures with 670 kW fire in location 2 . . . . .	46
32 Froude Number correlation based on center (trunk) tree hot layer temperature, depth and average velocity at smoke location with fire in location 1 . . . . .	47
33 Froude Number correlation based on center (trunk) tree hot layer temperature, depth and average velocity at smoke location with fire in location 2 . . . . .	48
34 Froude Number correlation based on side trunk tree hot layer temperature, depth and average velocity at smoke location with fire in location 1 . . . . .	49
35 Froude Number correlation based on side trunk tree hot layer temperature, depth and average velocity at smoke location with fire in location 2 . . . . .	50
36 Froude Number correlation based on center trunk tree temperature difference, height and velocity at smoke location with fire in location 1 . . . . .	51
37 Froude Number correlation based on center trunk tree temperature difference, height and velocity at smoke location with fire in location 2 . . . . .	52
38 Froude Number correlation based on side trunk tree temperature difference, height and velocity at smoke location with fire in location 1 . . . . .	53
39 Froude Number correlation based on side trunk tree temperature difference, height and velocity at smoke location with fire in location 2 . . . . .	54
40 Froude Number correlation based on hatch trees temperature difference, height and velocity at smoke location with fire in location 1 . . . . .	55

## List of Figures

Figure		Page
41	Froude Number correlation based on hatch trees temperature difference, height and velocity at smoke location with fire in location 2 . . . . .	56
42	Froude Number correlation based on fire size, downstream temperature and velocity at smoke location with fire in location 1 . . . . .	57
43	Froude Number correlation based on fire size, downstream temperature and velocity at smoke location with fire in location 2 . . . . .	58
44	Froude Number correlation based on fire size, downstream temperature and velocity at smoke location with fire in location 1 . . . . .	59
45	Froude Number correlation based on fire size, downstream temperature and velocity at main deck hatch with fire in location 2 . . . . .	60

## List of Tables

Table		Page
1	Preliminary Shipboard Experimental Results: Critical Air Flow Velocities	5
2	Shipboard Experimental Results: Horizontal Passages . . . . .	17
3	Shipboard Experimental Results: Vertical Trunks . . . . .	37



## **SHIPBOARD SMOKE CONTROL TESTS USING FORCED COUNTERFLOW AIR SUPPLY**

### **1.0 INTRODUCTION**

Control of smoke generation and smoke movement during shipboard fire incidents is a major concern. Unmanaged smoke spread exacerbates the effects of the fire, severely impacts damage control operations, and may result in significant nonthermal secondary damage, particularly to vital electronics equipment.

The concept of using high supply air flows to form a high air velocity barrier countercurrent to the buoyancy-driven smoke spread has been well established [1]. Some preliminary testing of this concept in a shipboard context was previously conducted and demonstrated the potential efficacy of this approach [2]. More quantitative data was needed on the relationship between fire size, counter flow air velocity, and the effects of shipboard geometry was needed in order to advance the concept. This was the primary objective of these tests.

High flow rate supply air sources include machinery space supply fans, portable blower arrays, and/or reconfigured normal shipboard ventilation fans. On CPS equipped ships, high pressure high flow rate supply air fans are also available. Hence, this concept had potential significant utility for application to both existing and new design ships.

One of the potential risks associated with using high counterflow air velocities to limit smoke migration is possible enhancement of fire growth rates. In addition, it is necessary to provide an exhaust path downstream of the smoke source, and therefore, conditions in the exhaust path must be understood. The tests were also designed to evaluate these parameters.

In order to quantify the performance of a shipboard smoke exhaust system a correlation relating the extent of upstream smoke migration to air flow velocities, fire parameters, and geometric factors, was required.

### **1.1 Background**

The purpose of this experimental study is to evaluate the use of counterflow smoke control in horizontal passages and vertical trunks.

Froude (atmospheric) modeling techniques have been used in a number of practical applications involving fire induced flow in compartments. Turbulent free convection flows are governed by buoyancy inertial and viscous forces. However for fully turbulent flows viscous effects are usually unimportant except possibly near flow boundaries. These viscous forces can also be unimportant even near flow boundaries if the boundaries are sufficiently rough. Froude modeling takes advantage of this simplification. If the migration of smoke has been stopped by an opposing air flow velocity, then a balance of the driving forces will exist, i.e., buoyancy and inertia forces. Specifically, the Froude number "Fr", representing the balance between buoyant and inertial forces should equal 1 at the point the smoke is stopped. The Froude number is defined as follows:

$$Fr = \frac{V}{\left(2gd \frac{\rho_c - \rho_h}{\rho_c}\right)^{\frac{1}{2}}} = \frac{V}{\left(2gd \frac{T_h - T_c}{T_c}\right)^{\frac{1}{2}}} \quad (1)$$

where

V	=	apposing air velocity to prevent smoke backflow,
g	=	acceleration of gravity,
d	=	depth of the hot smoke layer,
$\rho_c$	=	density of the ambient air,
$\rho_h$	=	density of the hot smoke,
$T_c$	=	temperature of the ambient air,
$T_h$	=	temperature of the hot smoke.

In practice, the Froude number can not be determined at the point where the migration of smoke is halted as both forces are equal to zero. Instead, both the buoyancy and the inertial force are determined independently at points of minimum interaction. This results in the determined Froude number being dependent upon geometric factors, wall heat loss properties, and the flow profiles of both the smoke and air.

An investigation by Thomas in 1968 [3] using a wind tunnel and methanol pool fires and an electric heater led to the following correlation between heat release rate and the opposed air flow velocities resulting in no movement of smoke [4].

$$\frac{V}{\left(g \frac{Q}{W C_p T_{ha} \rho_c}\right)^{\frac{1}{3}}} = 1 \quad (2)$$

where

Q	=	heat release rate,
W	=	wind tunnel width,
$C_p$	=	specific heat of air at constant pressure,
$T_{ha}$	=	average temperature downstream of the fire.

If the heat release rate in this correlation is substituted for the following:

$$Q = W H V \rho_c C_p \frac{T_{ha} - T_c}{n_o} \quad (3)$$

where  $H$  = wind tunnel height,  
 $n_o$  = fraction of the heat released that is transferred to the air (nominally 0.8 for methanol fires).

The Thomas [3] correlation can then be put in the form of a Froude number as follows:

$$Fr = \frac{V}{\left( 2 g H \frac{T_{ha} - T_c}{T_{ha}} \right)^{\frac{1}{2}}} = \frac{1}{(2 n_o)^{\frac{1}{2}}} \quad (4)$$

Heskestad and Spaulding [5] found similar correlations when studying apertures in both walls and ceilings. For apertures in walls, the resulting correlation was as follows:

$$Fr = \frac{V}{(2 g H \phi_H)^{\frac{1}{2}}} = C \int_0^1 \left( \int_{\frac{y}{H}}^1 \left( \frac{\phi}{\phi_H} \right) d \left( \frac{y}{H} \right) \right)^{\frac{1}{2}} d \left( \frac{y}{H} \right) \quad (5)$$

where

$$\phi = \frac{T_h - T_c}{T_h}$$

$C$  = dimensionless flow coefficient of the aperture,  
 $y$  = height in the aperture,  
 $H$  = aperture height,  
 $\phi_H$  =  $\phi$  evaluated at the height of the aperture.

The temperature on the hot side,  $T_h$ , is evaluated away from the aperture where there is no effect of the cold air flow. The double integral in this correlation is a result of the temperature profile on the hot side of the aperture and its corresponding effects on the opposing air flow through the aperture.

For apertures in ceilings, they found the following correlation [5]:

$$Fr = \frac{V}{(2 g W \phi_{cl})^{1/2}} = \begin{matrix} 0.23 \text{ for } Gr > 1 \times 10^7 \\ 0.38 \text{ for } Gr < 5 \times 10^6 \end{matrix} \quad (6)$$

where

$$Gr = \frac{g \rho_c^2 \phi_{cl} W^3}{\mu^2}$$

- Gr = Grashof number,
- W = aperture width (smaller dimension of the aperture),
- $\mu$  = viscosity of air evaluated at a mean temperature,
- $\phi_{cl}$  =  $\phi$  evaluated at the ceiling away from the aperture.

## 1.2 Previous Shipboard Experiments

A series of experiments was conducted on board of the U.S. Navy full scale damage control research ship ex-USS SHADWELL [6] to establish minimum opposing air velocities and flow rates to prevent upstream migration of smoke for a limited range of conditions [2]. The primary results of these experiments are given in Table 1.

## 2.0 PRESENT OBJECTIVES

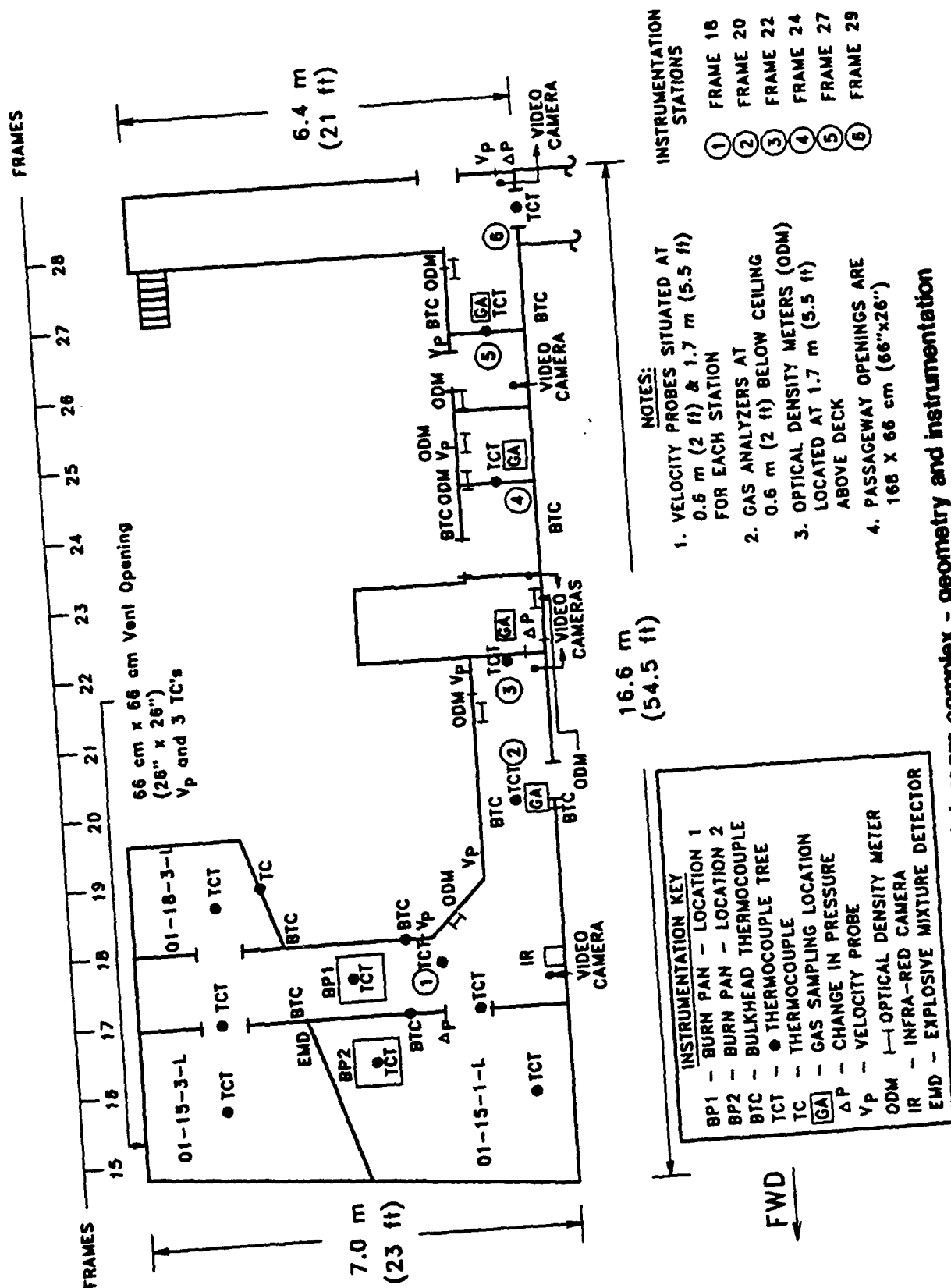
The objectives of this test series was to correlate the opposing air velocity required to contain or stop smoke migration to the buoyancy of the smoke for both horizontal passages and vertical trunks and to evaluate the feasibility of forced counterflow air movement as a shipboard smoke control method.

## 3.0 EXPERIMENTAL TEST FACILITIES

These tests were conducted on board the ex-USS SHADWELL in Mobile Bay, Mobile, Alabama [6]. The tests involving a horizontal passageway were conducted in the 01 level stateroom complex. All of the staterooms were closed off with the exceptions of staterooms 01-15-1-L and 01-15-3-L. This results in an "L" shaped corridor 1.2 m (4 ft) wide, 2.3 m (7.5 ft) high, 13.7 m (45 ft) in length and 7 m (23 ft) across as shown in Figure 1. There are two nominally 0.6 x 1.8 m (2 x 6 ft) archways in this passageway, one at frame 22 and the other in the thwart ships passageway forward of frame 29.

Table 1. Preliminary Shipboard Experimental Results: Critical Air Flow Velocities [2]

Test ID	Location	Fire Size (kW)	Temperature Upstream-Downstream (°C)	Critical Velocity (fpm)	Critical Flow Rate (cfm)
2-1	01 Level	500	140 - 350	375 - 400	4350 - 4630
2-2	01 Level	1000	200 - 500	450 - 510	5190 - 5910
2-3	CIC	1000	--	(200)	(2200)
2-4	CIC	2000	--	186 - 195 at FR 22	2160 - 2260
2-5	CIC	1000	--	527 - 536	6120 - 6220



Tests involving a vertical trunk were conducted in trunk 3-29-1-T between the main deck and hold levels. This trunk is nominally 8.8 m (29 ft) in height, 1.2 m (4 ft) square with two 0.76 m (2.5 ft) square hatches. It contains two vestibules, one 1.3 x 3.7 x 2.8 m (4.4 x 12 x 9.2 ft) on the main deck and one 1.2 x 3.8 x 3.0 m (4 x 12.5 x 9.8 ft) on the third deck or hold level, as shown in Figures 2 through 5.

Two fire locations were used in horizontal testing. The first location was in the passageway between the doorways of the two open staterooms. The other fire location was in stateroom 01-15-1-L.

Two fire locations were also used in vertical testing. The first location was in the lower vestibule 1.4 m (4.5 ft) centerline to centerline from the trunk. The other location was centered underneath the trunk.

Supply air for the horizontal passage testing was provided by the ship's machinery space supply fan. A supply air path was configured by securing doors and openings such that flow was directed into the 01 level passageway from port and starboard side ladderways from second deck. Flow rates were adjusted by varying the fan speed and by controlling the amount of supply air vented overboard. The exhaust path on the 01 level was a 0.66 m (2.2 ft) square vent in the starboard bulkhead of the 01 level (01-15-3-L) downstream of the fire location (reference Fig. 1).

For the vertical trunk tests, the counterflow air supply was developed by the machinery space exhaust fan. Air was pulled through an opening to weather through passageways and into trunk 3-29-1-T on the main deck, down the trunk through the second deck level and out of the trunk on the third deck. The exhaust gas flowed into the machinery space on the third deck and was then exhausted by the machinery space exhaust fan. The exhaust flow rate was varied by adjusting the fan speed and by providing exhaust flow relief area between the main deck passage and the main deck directly, bypassing the trunk and hence reducing the flow through the trunk.

#### **4.0 TEST FIRES**

Propene gas fires were used in both the horizontal passageway tests and the vertical trunk tests (Apachi gas was used in the horizontal tests and Matheson propene gas was used in the vertical tests). The propene gas was burned in a 0.6 m (2 ft) square stainless steel sand type burner located as described in the previous section. A small pan, nominally 5 cm (2 in.) in diameter, was filled with heptane and ignited in order to initiate the sand burner.

The propene was drawn as a liquid from two cylinders which were manifolded together. In addition to the cylinder valves, two quarter turn valves, one on each line from the cylinders, were used to isolate the liquid feed. The fuel was fed from the 1.3 cm (0.5 in) NPS manifold to an Alternate Energy Systems direct fired vaporizer where the phase change was accomplished. A two stage pressure regulator was attached to the vapor



**Fig. 2 - Vertical Trunk 3-29-1-T geometry and instrumentation scheme - main deck**



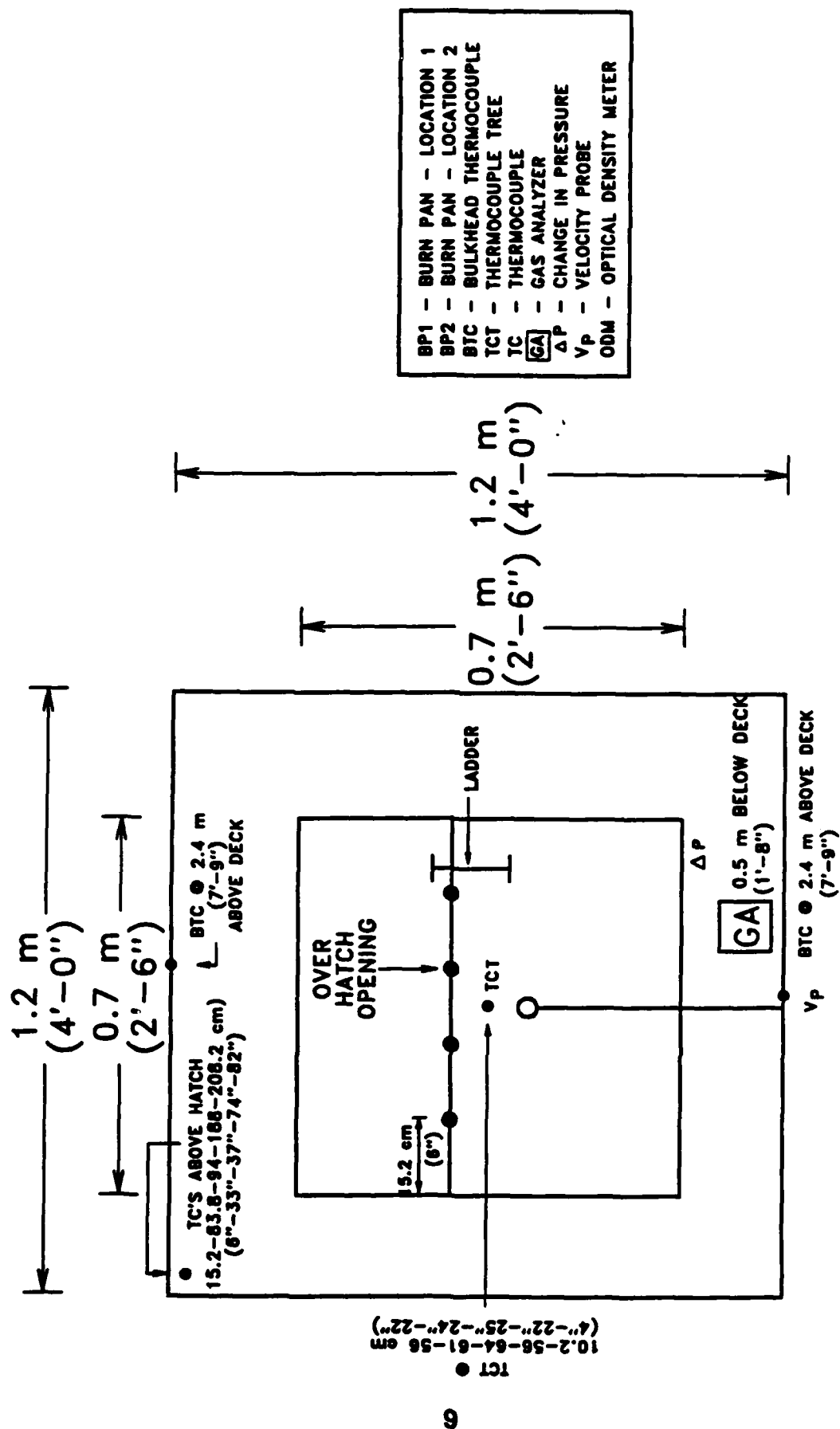
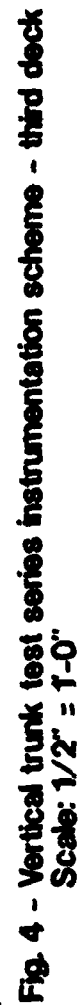


Fig. 3 - Vertical trunk test series instrumentation scheme - see second deck  
Scale: 1" = 1'-0"



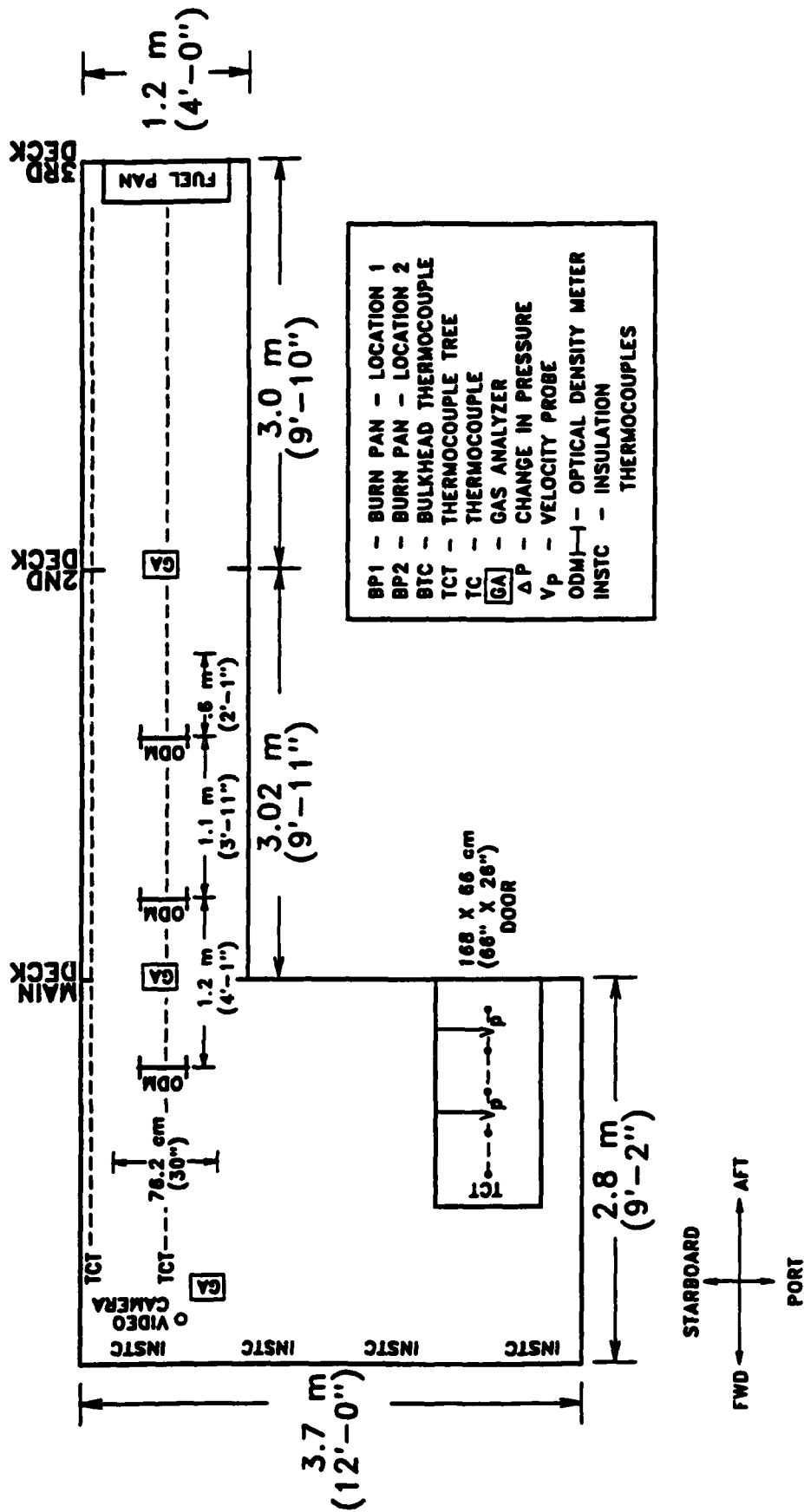


Fig. 5 - Vertical trunk test series instrumentation scheme - elevation detail  
Scale: 1/4" = 1'-0"

outlet of the vaporizer. The fuel then passed through both a quarter turn valve and a normally closed solenoid valve controlled from the main control room on the O2 level of the ex-USS SHADWELL to provide for rapid shutdown of the burner. The fuel flow rate was controlled using a Dwyer model RMC-108-SSV valve and rotameter which has a range of 5.1-51 SCMh of air (180-1800 SCFH of air).

The rotameter reading requires a correction factor in order to measure propene flows as follows [7]:

$$V_p = V_D \left( \frac{\rho_{air}}{\rho_p} \right)^{\frac{1}{2}} = V_D * 0.83 \quad (7)$$

where

$V_p$	=	volumetric flow rate of propene gas,
$V_D$	=	reading from the Dwyer rotameter,
$\rho_{air}$	=	density of the ambient air,
$\rho_p$	=	density of the propene gas.

The fuel flow rate was also monitored by an orifice meter with a 2.54 cm (1 in.) diameter orifice in 5 cm (2 in.) NPS schedule 40 pipe with flange taps. The equation for this orifice meter is as follows [8]:

$$V_p = C \left( \frac{\rho_{air}}{\rho_p} \right)^{\frac{1}{2}} (P_s \Delta P)^{\frac{1}{2}} = C * 0.83 (P_s \Delta P)^{\frac{1}{2}} \quad (8)$$

where

$P_s$	=	absolute static pressure,
$\Delta P$	=	pressure difference across path, and
$C$	=	orifice flow constant = 4.545 (dimensionless flow coefficient).

An MKS Baratron differential pressure transducer model 220CD with a range of 0-1.33 kPa (0-10 mm Hg) was used to measure the pressure differential.

During tests with horizontal passageways, both cylinders, vaporizer, regulator, meters and controls were located on the forecastle with 3.8 cm (1.5 in.) NPS schedule 40 steel pipe transiting from the orifice meter to the burner location. During tests with vertical trunks, they were located in the well deck aft of frame 35 with 3.8 cm (1.5 in.) NPS schedule 40 steel pipe transiting from the orifice meter to the burner location.

## 5.0 EXPERIMENTAL PROCEDURE

In testing both horizontal corridors and vertical trunks, opposing air velocities were varied while the extent of smoke migration, and layer temperatures were recorded for three sizes of propene fires; nominally 350, 650, and 1300 kW (150 and 1000 kW fires were sometimes tested). These tests were repeated with the test fire moved.

## **5.1 Sequence of Experiments**

- A Ventilation system secured, doors checked, fire watch stationed.
- B Data logging initiated and 1 minute of background recorded.
- C Heptane poured and ignited.
- D Propene flow started and burner ignited approximately 30 seconds after heptane ignited. Ventilation system started.
- E Ventilation adjusted until smoke migration is stopped at desired location, that is, (station 1, station 2, in horizontal testing or third deck hatch, main deck hatch in vertical testing).
- F Set data flag and measure reference velocity.
- G Step E is repeated until all feasible locations have been obtained.
- H Propene flow is secured, data logging is terminated, ventilation is configured for maximum flow.
- I Fire watch is dismissed when test area has cooled.

## **6.0 INSTRUMENTATION AND APPARATUS**

The instrumentation design for both the horizontal and vertical series of smoke movement tests was developed to characterize the movement of smoke within the compartment. Measurements collected include temperature, air velocity, smoke obscuration, gas analysis, and pressure differential. The instrumentation locations for both series of tests are shown in Figures 1 through 5.

### **6.1 Smoke Temperature Measurement**

Thermocouples were the primary means of collecting compartment air and fire temperatures for both the horizontal and vertical series of smoke movement tests.

Detailed temperature profiles were obtained by primarily using type K glass braid thermocouples arranged in vertical tiers with thermocouples in evenly spaced intervals, starting 15 cm (6 in.) below the passageway overhead. Fourteen thermocouple trees were utilized to obtain temperatures at each of the six stations, through each passageway and in critical room areas. In addition, four Inconel-sheathed thermocouples were used to measure fire temperatures above the burn pan for each fire scenario. Surface temperatures of the exposed steel bulkheads along the horizontal and vertical passageways were measured. These thermocouples were welded to the bulkhead and at each of the instrumentation collection stations.

Thermocouple trees were also utilized for the vertical trunk hatch series of tests. Two vertical thermocouple trees were run continuously throughout the trunk hatch located as shown in Figures 2 through 5. Vertical tiers of thermocouples were also installed in the two passageways and above the burn pan. Three horizontal sets of four evenly spaced thermocouples were set-up across each hatch opening. Thermocouples were also placed in the overhead insulation.

## 6.2 Air Velocity Measurement (Vent Flows)

Air velocity measurements were taken using bidirectional flow probes located at 0.8 m (2.5 ft) and 1.5 m (5 ft) above the deck for the horizontal flow tests. A string of thermocouples were purposely located adjacent to these bidirectional probes to measure vent flows. These bidirectional probes measure the differences in pressure through a passageway and with the thermocouples taking temperature measurements, accurate vent flows across a passageway can be computed. The following equation gives the air velocity in the vent [9],

$$V = \frac{1}{1.08} \sqrt{\frac{2\Delta P}{\rho}} \quad (9)$$

where  $V$  = air flow velocity,  
 $\Delta P$  = pressure difference across path,  
 $\rho$  = density.

A calibration factor of 1.08 is used for the bidirectional probes in the above equation. Using the temperature distribution and the pressure readings from the bidirectional probes in the vent, the following equation is used [8],

$$V = 0.0813 \sqrt{T\Delta P} \quad (10)$$

where  $T$  = temperature, K.

The velocity probe heads had a 19 mm (0.75 in.) O.D. and a 16 mm (0.63 in.) opening. These heads were welded to 4.8 mm (0.19 in.) O.D. stainless steel tubing.

These air velocity measurements were also obtained, using the same methodology discussed previously, for the vertical trunk test series. See Figures 1 through 5 for the location of these velocity probes.

## 6.3 Smoke Density Measurement

Smoke obscuration measurements were obtained using optical density meters designed specifically for this series of testing. These meters were made of aluminum framing with a 0.5 m (1.5 ft) path length. An infrared emitting diode was used as a source. The source intensity was monitored with one PIN photodiode and a second PIN photodiode at the other end of the optical path measured the reduction in IR transmission due to smoke. With these measurements, the ability to monitor the movement of smoke throughout the horizontal and vertical testing series was achieved. These devices were located 1.7 m (5.5 ft) above the deck along the horizontal passageway between

instrumentation stations 1 and 6. See Figures 2 through 5 for the locations of the smoke obscuration meters for the vertical trunk smoke movement tests.

#### **6.4 Gas Sampling**

Gas analyzers were installed to measure oxygen and carbon dioxide at the compartment sampling points shown in Figures 1 through 5 for both the horizontal and vertical smoke movement tests. The gas sampling device in the compartment was designed using a stainless steel funnel with two layers of ceramic filter paper and a swab of glass wool/Kaowool to be used as a filter, connected to 9.5 mm (0.375 in.) copper tubing. The gas sampling points for the horizontal compartment smoke movement tests were located in the center of the compartment 0.6 m (2 ft) below the ceiling. The locations for the vertical trunk and horizontal passage tests are shown in Figures 1 through 5.

#### **6.5 Chemical Species Concentration Measurement**

An MSA Instruments Combustible Gas Sensor was used for each series of testing to detect unsafe concentrations of combustible gases. This sensor was located on the deck in the corner of stateroom 01-15-3-L for the horizontal compartment test series and at the entrance to the passageway on the Third Deck near the burn pan for the vertical compartment tests. The sensor was monitored at the test control room and would activate an audio alarm if greater than 1% propane was detected.

#### **6.6 Pressure Differential Measurement**

Pressure transducers were used to determine the pressure differential readings across a door opening to estimate mass flow rates out of a compartment. For the horizontal flow tests, pressure differentials were continuously measured throughout tests 1-8 across the doorway at station 3, Frame 22. Pressure differentials were also monitored at the doorway leading out from stateroom 01-15-1-L and at the station 6 doorway for tests 6-8.

The vertical trunk tests measured pressure differentials across each trunk hatch opening and at the doorway at the third deck.

#### **6.7 Visualization of Smoke Filling**

The smoke movement and fire burner characteristics were remotely recorded using both infra-red and video cameras. For each test series the I/R camera was situated so that the fire source could be monitored closely and the initial fire sequence could be noted. The horizontal test series utilized four video cameras located throughout the compartment as shown in Figure 1. The vertical trunk test series used three video cameras with one of them being mounted horizontally above the center of the trunk hatch. See Figures 2 through 5 for the other vertical trunk camera locations.

## 7.0 EXPERIMENTAL RESULTS

### 7.1 Results for Horizontal Passageway Smoke Movement Test Series

The results of the tests involving horizontal passage flows are given in Table 2. The hot gas layer temperature and depth was determined at the instrumentation station (reference Fig. 1), preceding (closer to the fire) the instrumentation location noted, except when the smoke was located at instrumentation station 1; in this case, the same station was used. The hot gas layer was defined as the portion of the corridor with a temperature of at least 20 percent higher than the ambient temperature in the corridor at the beginning of the test. In the tests with the fire in location 2, the thermocouple tree in the fire room door was used instead of the tree at station 1. The opposing air velocity was determined at the same instrumentation station as the smoke location. The measured oxygen and carbon dioxide concentrations (percent by volume) are given for the same location as the hot layer temperature and depth determination. This table also presents the hand held anemometer readings ( $Vel_a$ ), the location of these readings ( $Vel_a$  Loc.), and the determined air flow readings from the bi-directional probes ( $Vel_b$ ) at the same location for comparison. The measured pressure differential at both instrumentation stations 3 and 6 were included in this table. These measurements give an indication of the variation in required air flow to hold the smoke at the various locations in the corridor. The air velocity ( $Vel_b$ ) determined at station 6 was also included for this reason.

The opposing air velocity required to halt upstream smoke migration is shown in Figures 6 and 7 for the test fires in locations 1 and 2 respectively. The dominant features in these tests are the arches at station 3 and at station 6 and the entrance to the corridor between stations 5 and 6. The former features disturb the flow field on both sides of the arches, and since the velocity was measured at the smoke location, the required opposing air velocity at those locations was relatively high. Wisps of smoke in turbulent eddies were noted passing through the arch. The air velocity was increased until no smoke flowed through the arch due to the local eddy effects. This may have had the effect of resulting in a much higher counterflow air velocity at station 3. The velocity measurements at station 5 are severely affected by the passageway entrance effects causing low (sometimes negative) and unstable readings. Figures 8 and 9 show the required air velocity measured at the arch at station 6 to hold the smoke at the various stations. This demonstrates the relative differences in required air velocities to halt upstream smoke migration at the 6 instrumentation stations.

Figures 10 through 13 show the effects of increased air flow through the test corridor on both upstream and downstream temperatures for the 620 kW fire in location 1 and the 720 kW fire in location 2. Temperatures measured toward the end of a test were higher than those measured with similar conditions toward the beginning of a test due to increases in boundary temperatures. In Figures 10 and 11, the downstream temperature at the highest flow rate (first measurement in test 4) is high due to a fuel flow adjustment prior to these measurements.



Table 2. Shipboard Experimental Results: Horizontal Passages

Test No.	Fire Size (kW)	Smoke Location	Dist (m)	Temp (°C)	Depth (m)	O <sub>2</sub> (%)	CO <sub>2</sub> (%)	Vel (m/s)	$\Delta P_3$ (Pa)	Vel <sub>3</sub> (m/s)	Vel <sub>6</sub> Loc.	Vel <sub>6</sub> (m/s)	$\Delta P_6$ (Pa)
1	170	Stn. 1	1.52	57	1.07	--	--	0.67	2.788	2.45	M. Space	--	--
1	170	Stn. 3	7.62	70	1.07	21.01	0.00	1.47	0.612	1.25	M. Space	--	--
1	169	Stn. 2	5.18	67	2.29	--	--	1.12	2.788	2.45	M. Space	--	--
3	323	Stn. 1	1.52	55	2.29	--	--	1.56	7.417	2.79	Stn. 3	4.06	3.96
3	325	Stn. 3	7.62	84	1.37	21.03	0.03	0.96	0.921	1.09	Stn. 3	0.96	1.55
3	324	Stn. 2	5.18	94	2.29	--	--	0.81	1.740	1.35	Stn. 3	2.16	2.18
3	322	Stn. 4	10.67	85	0.91	20.76	0.07	0.36	0.734	0.98	Stn. 6	1.29	1.29
3	322	Stn. 5	13.41	46	0.55	20.87	0.12	-0.14	0.518	0.99	Stn. 6	1.14	1.14
3	320	Stn. 4	10.67	86	0.91	19.52	0.76	0.53	0.933	1.07	Stn. 6	1.40	1.40
4	634	Stn. 1	1.52	70	2.29	--	--	1.58	6.695	2.20	Stn. 3	3.99	4.07
4	624	Stn. 2	5.18	123	2.29	--	--	1.43	4.630	2.18	Stn. 3	3.40	3.53
4	646	Stn. 4	10.67	119	0.91	18.67	1.42	0.86	1.003	1.22	Stn. 6	1.80	1.80
4	670	Stn. 5	13.41	52	0.55	20.42	0.67	-0.43	0.704	1.17	Stn. 6	1.62	1.62
4	590	Stn. 3	7.62	91	1.37	17.46	2.39	2.83	3.136	1.74	Stn. 3	2.83	2.95
5	1300	Stn. 1	1.52	99	2.29	--	--	2.00	10.080	2.89	Stn. 3	4.85	4.55
6	360	Stn. 2	6.10	132	1.98	--	--	2.44	11.151	2.78	Stn. 3	4.96	4.81
6	357	Stn. 3	8.53	112	1.68	20.99	0.00	1.80	1.747	1.26	Stn. 3	1.80	1.97
6	350	Stn. 4	11.58	168	0.91	17.36	2.38	0.67	1.033	1.16	Stn. 6	1.61	1.61
7	716	Stn. 2	6.10	223	1.98	--	--	2.87	14.735	3.59	Stn. 3	5.85	5.58
7	719	Stn. 3	8.53	167	1.68	17.26	2.50	3.81	5.053	1.98	Stn. 3	3.81	3.44
7	720	Stn. 3	8.53	215	1.68	16.91	2.72	2.98	2.422	1.95	Stn. 3	2.98	2.53
7	712	Stn. 4	11.58	171	1.22	15.60	3.82	1.09	1.578	1.80	Stn. 6	2.19	2.19
7	706	Stn. 5	14.33	54	0.76	20.93	0.07	0.26	0.904	1.54	Stn. 6	1.95	1.95
7	721	Stn. 6	17.07	68	1.37	--	--	1.21	-1.297	0.77	Stn. 6	1.21	0.182
8	1300	Stn. 3	8.53	236	1.68	11.03	6.74	3.53	3.410	1.86	Stn. 3	3.53	3.30
8	1300	Stn. 4	11.58	234	1.22	5.35	11.31	1.45	0.998	1.30	Stn. 6	2.26	2.27
8	1300	Stn. 5	14.33	81	1.07	19.85	1.20	0.23	-0.271	0.91	Stn. 6	1.85	0.383
8	1300	Stn. 6	17.07	76	1.37	16.48	2.91	1.63	-1.165	0.71	Stn. 6	1.63	-0.045

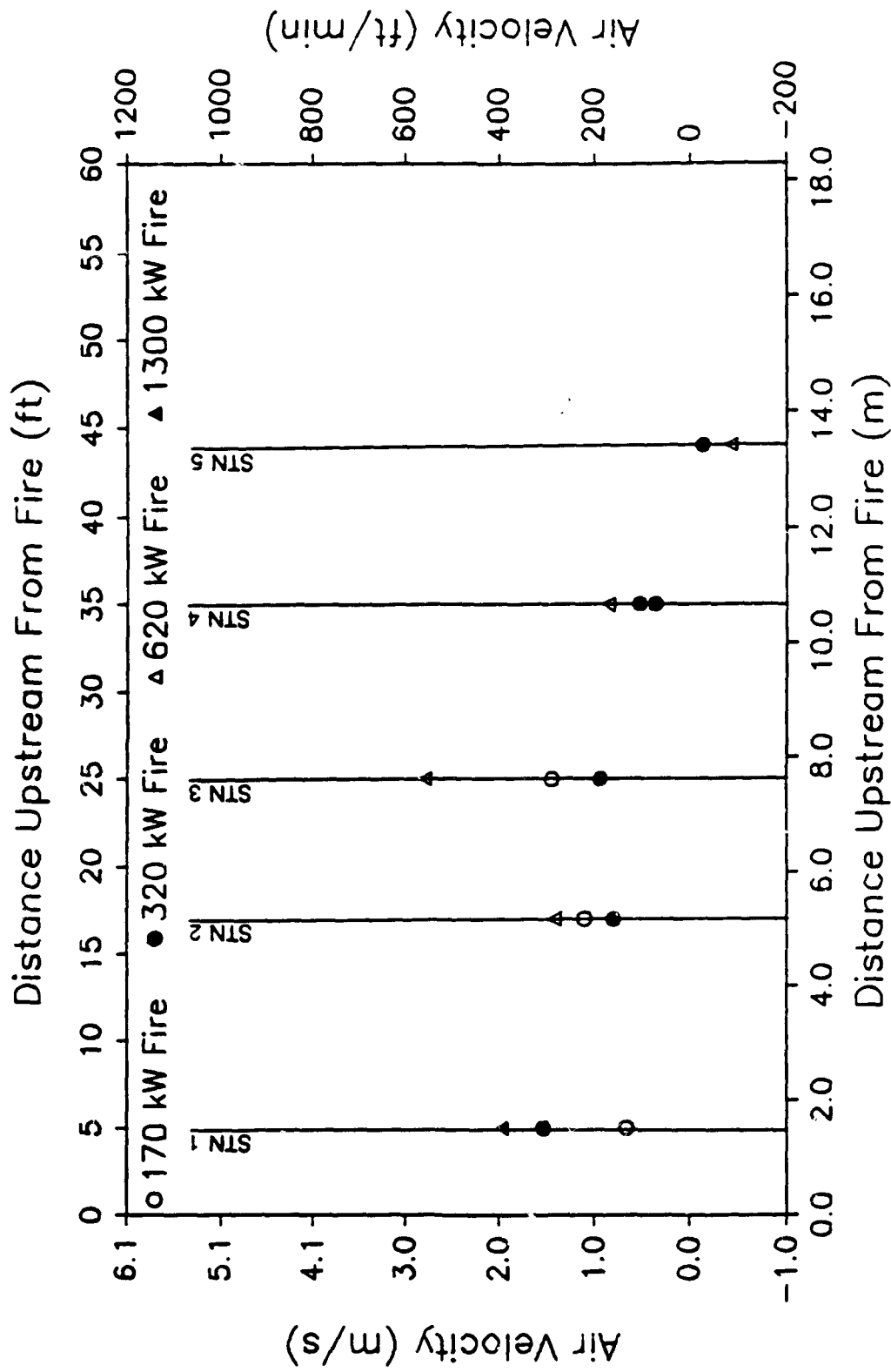


Fig. 6 – Required air velocity to halt upstream smoke migration during horizontal corridor tests with fire in location 1

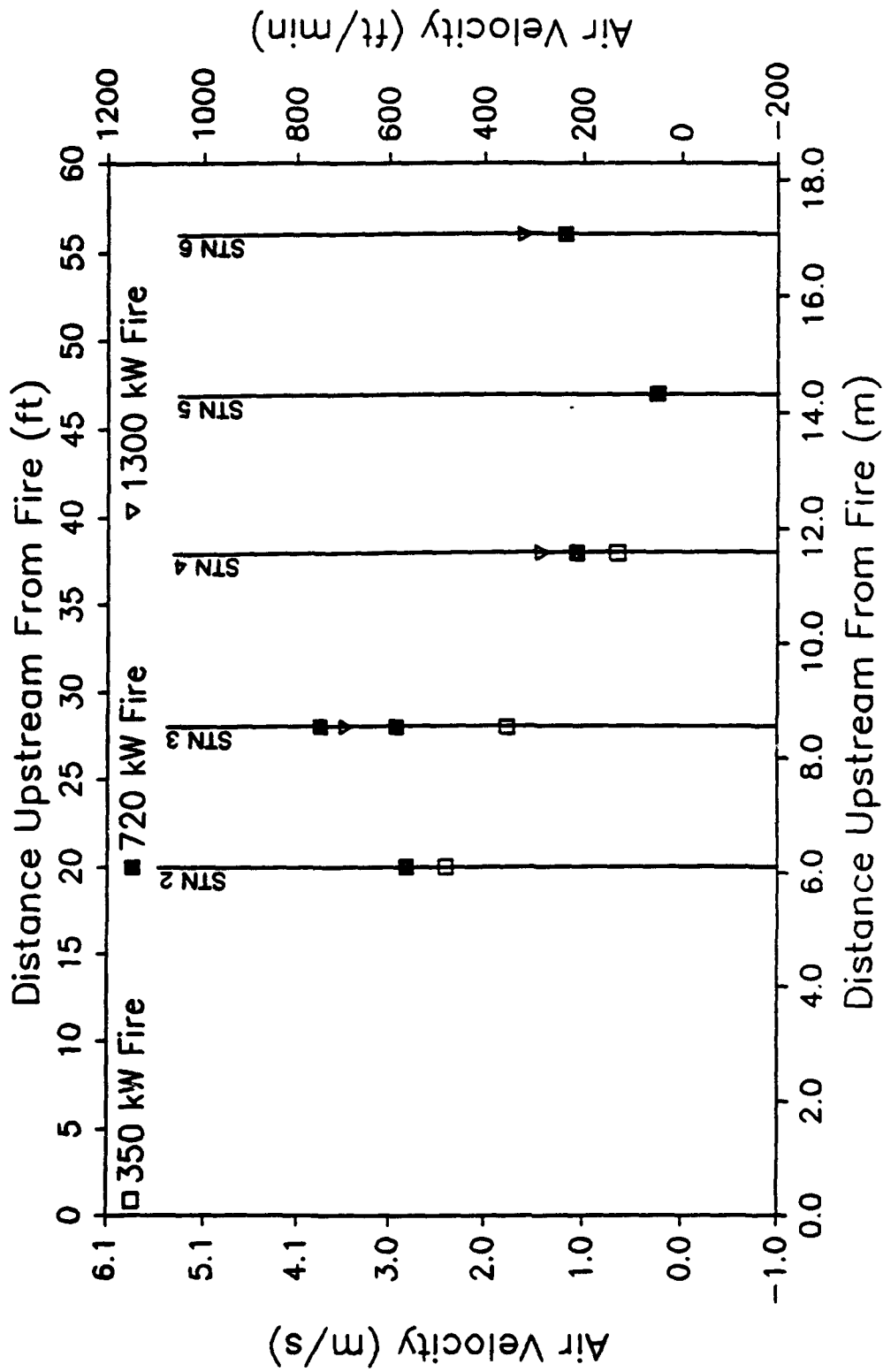
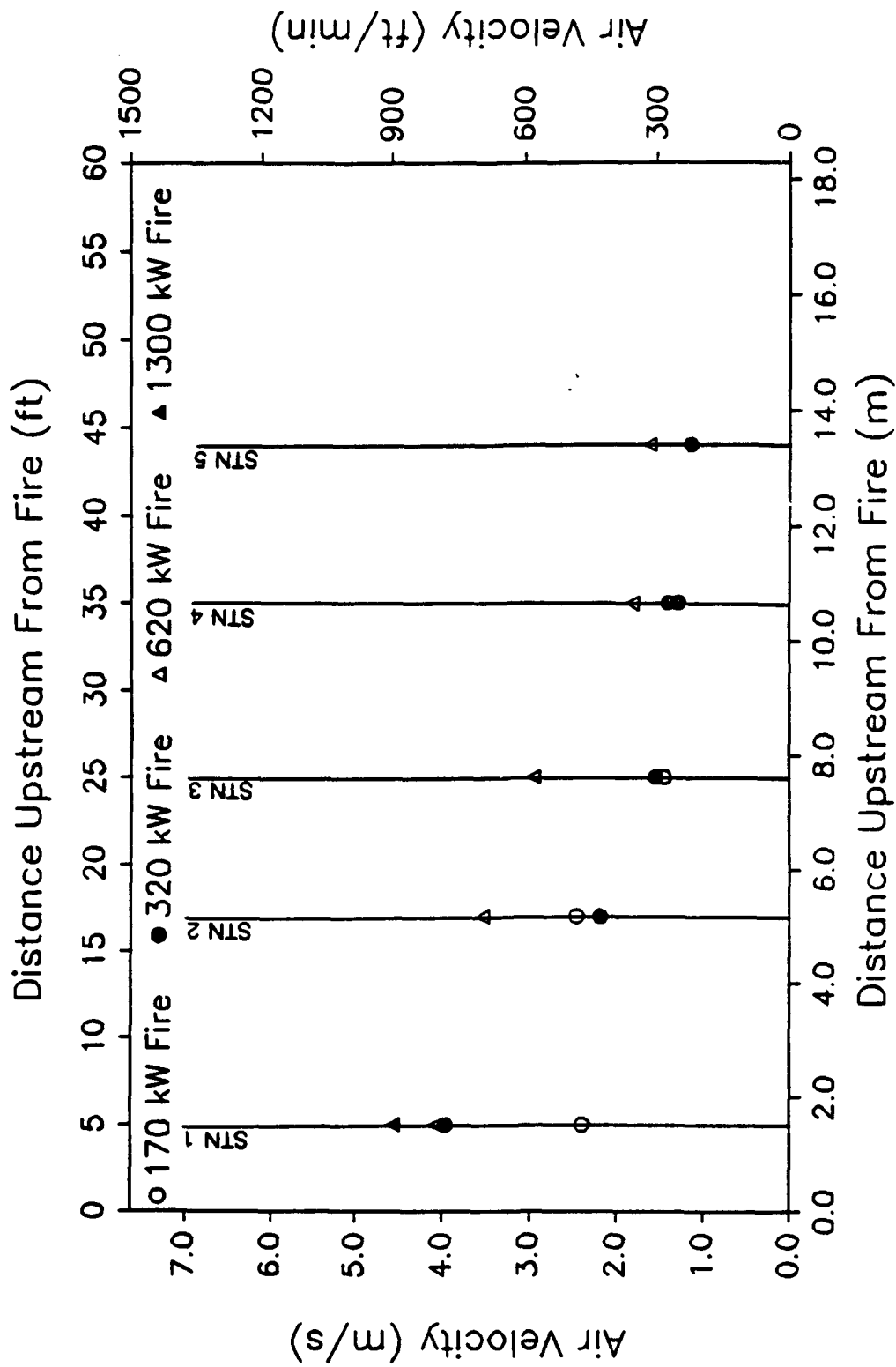


Fig. 7 – Required air velocity to halt upstream smoke migration during horizontal tests with fire in location 2



**Fig. 8** – Required air velocity at station 6 to halt smoke migration during horizontal corridor tests with fire in location 1

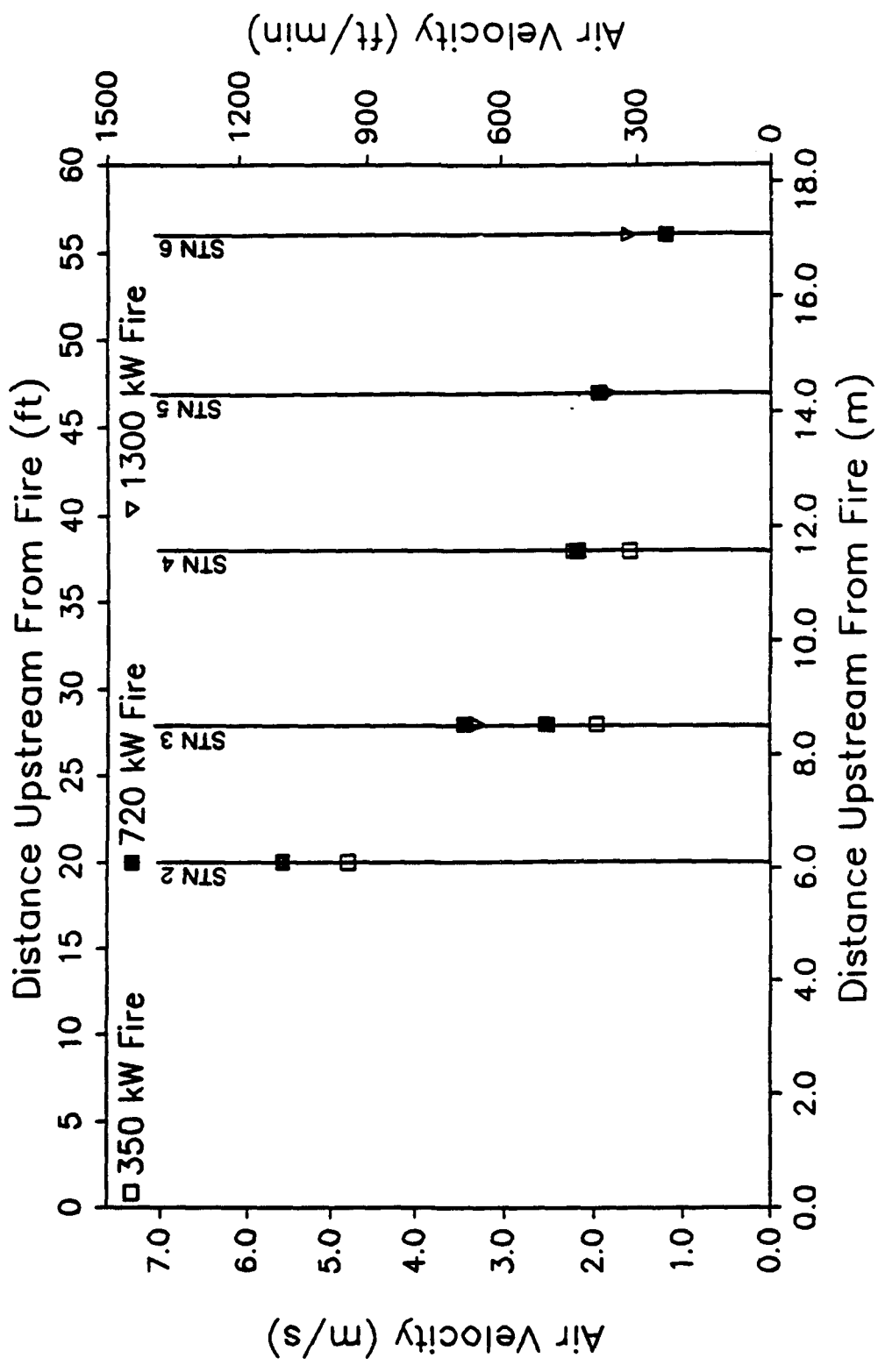
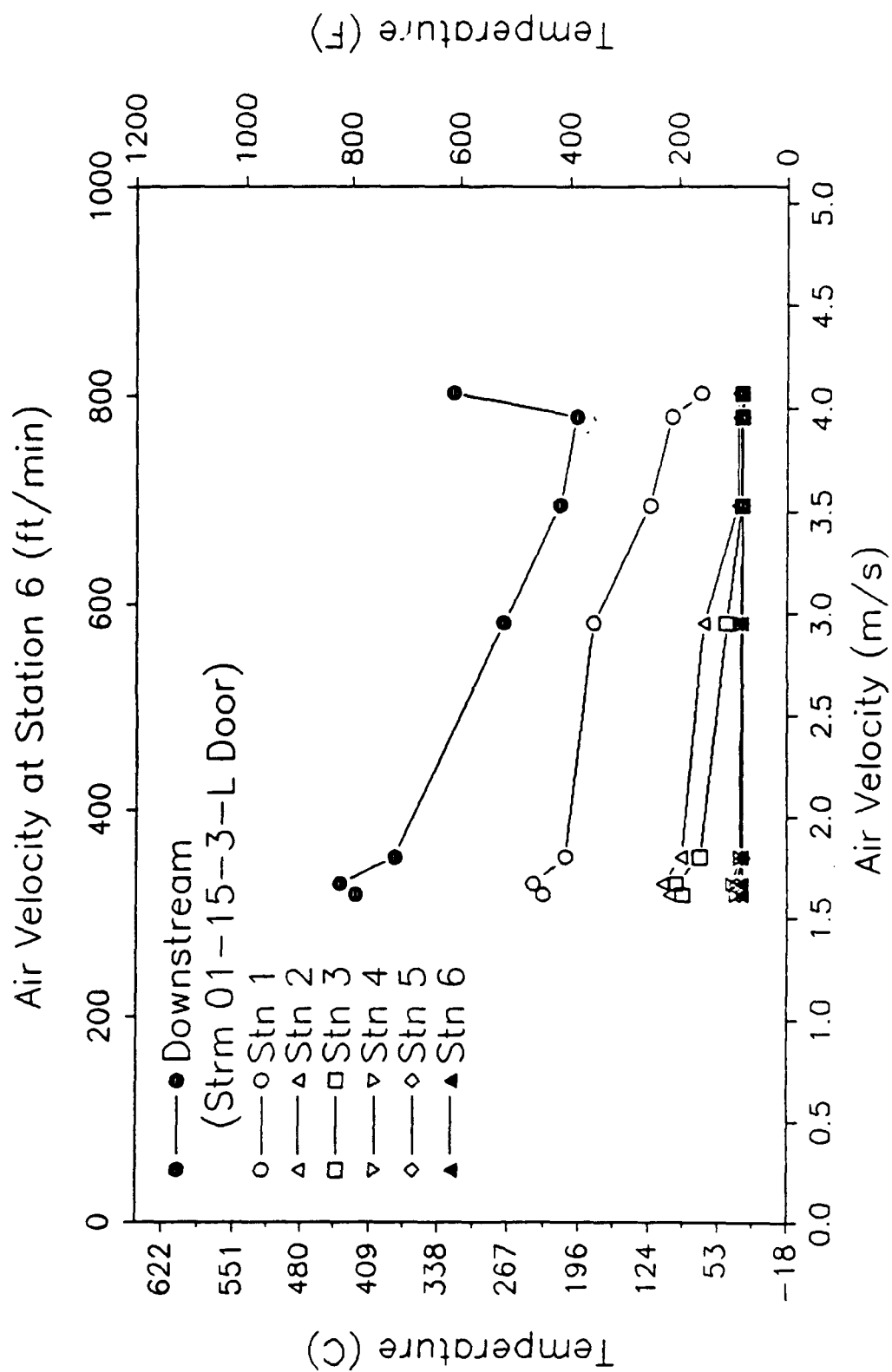


Fig. 9 - Required air velocity at station 6 to halt upstream smoke migration during horizontal tests with fire in location 2



**Fig. 10** – Air Velocity effects on upstream and downstream average temperatures in horizontal corridor with 620 kW fire in location 1

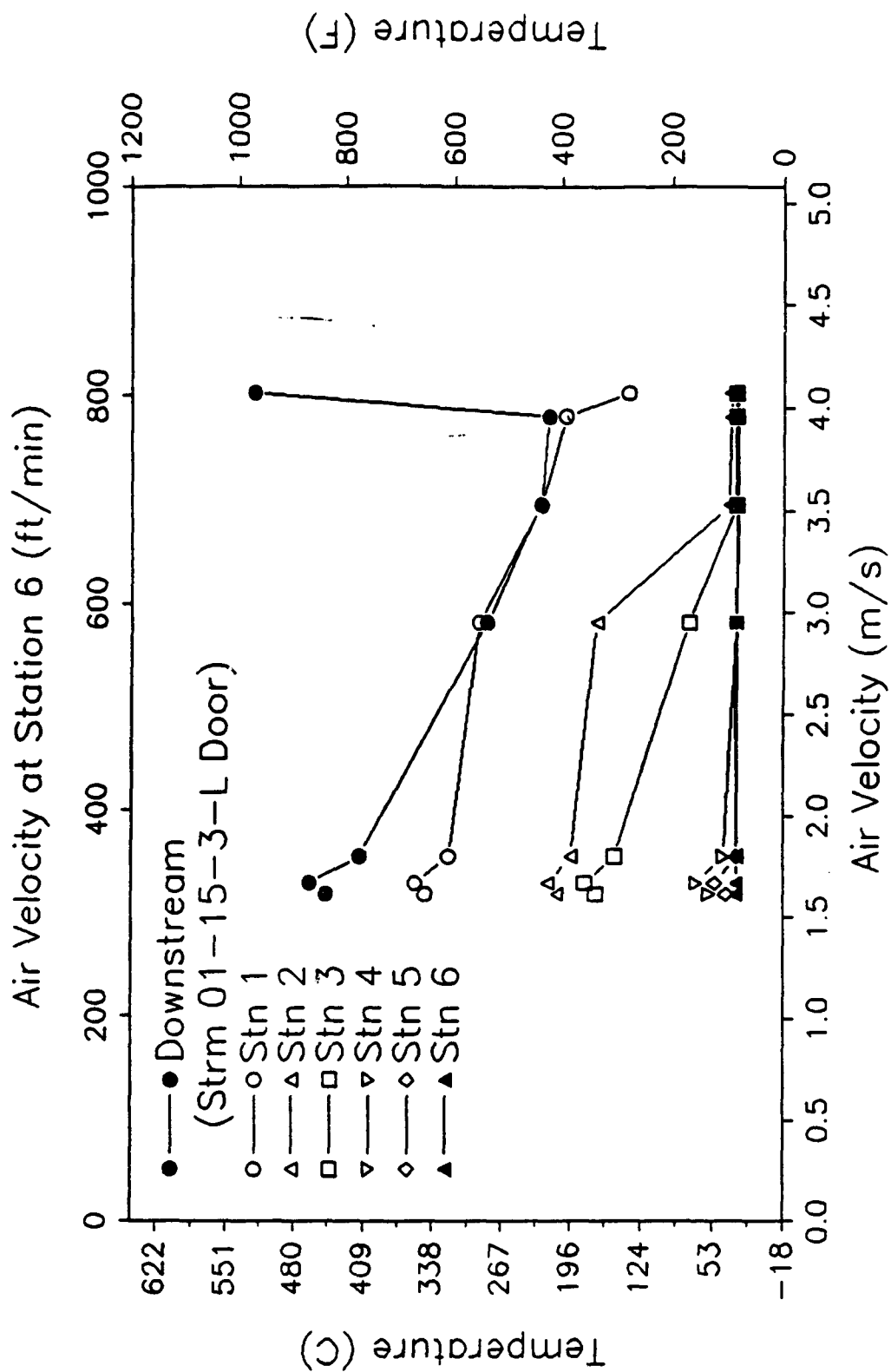
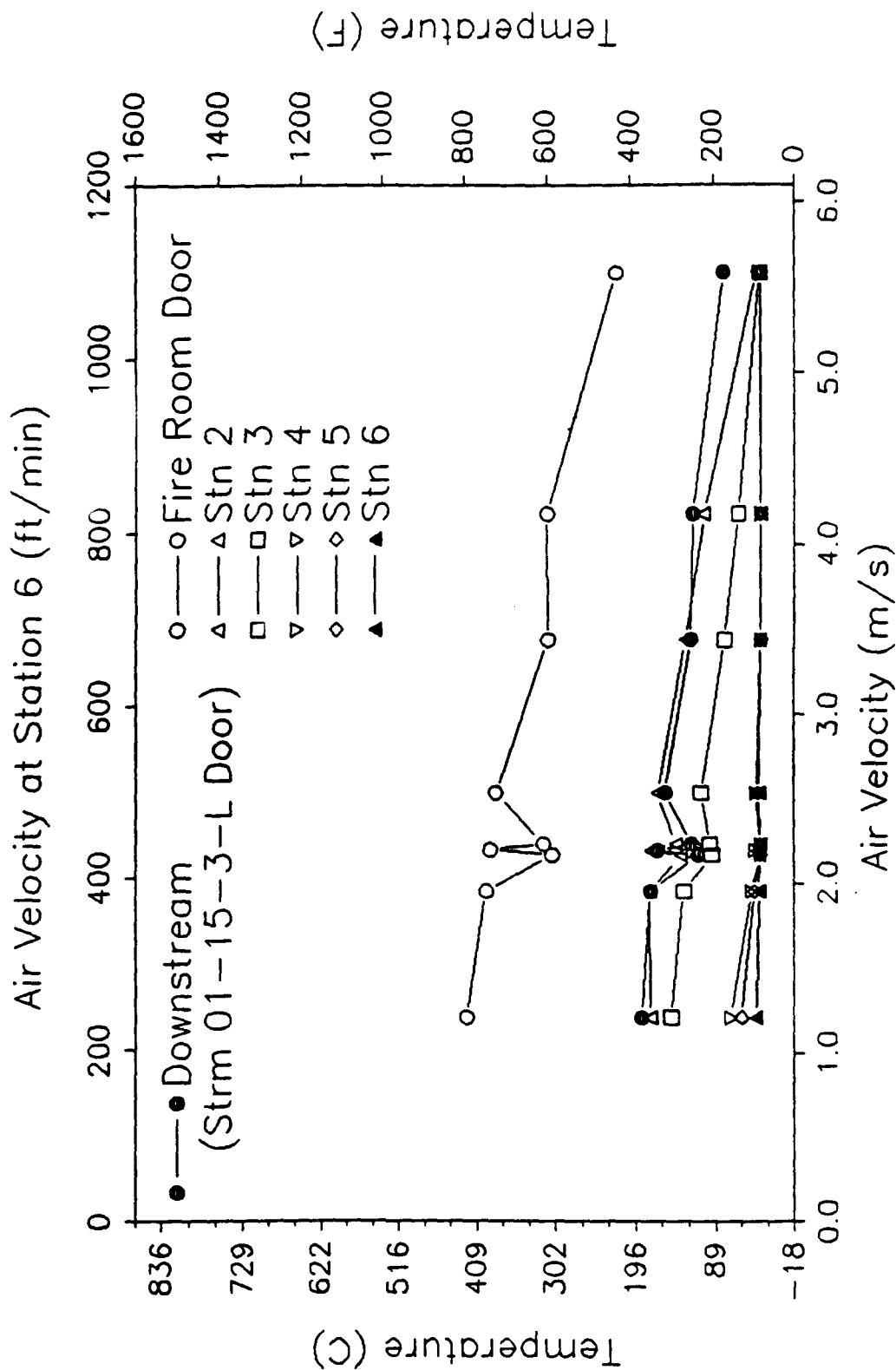
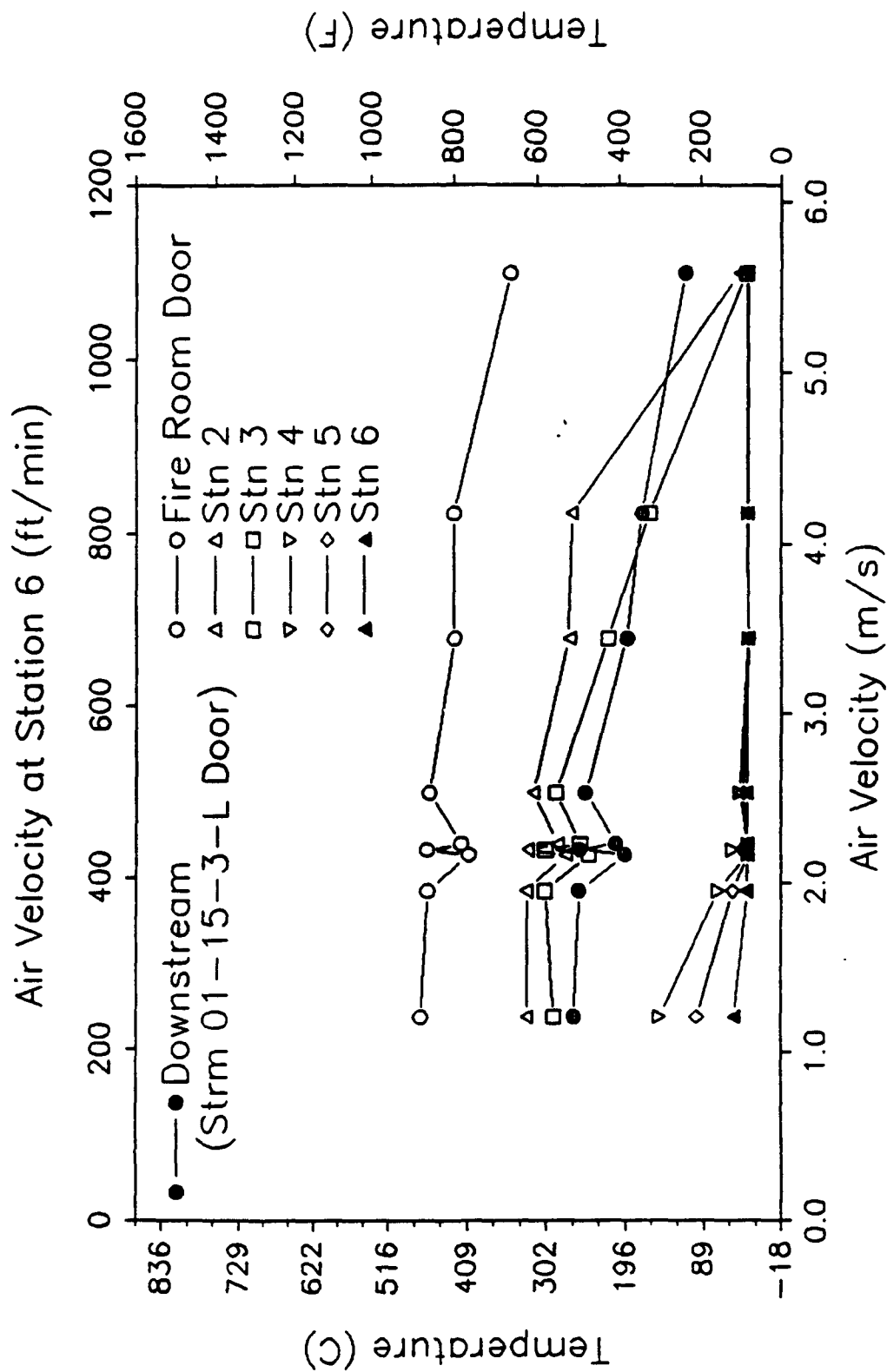


Fig. 11 – Air Velocity effects on upstream and downstream maximum temperatures in horizontal corridor with 620 kW fire in location 1



**Fig. 12** — Air Velocity effects on upstream and downstream average temperatures in horizontal corridor with 720 kW fire in location 2





**Fig. 13** – Air Velocity effects on upstream and downstream maximum temperatures in horizontal corridor with 720 kW fire in location 2

The Froude numbers,  $Fr_{TD}$ , based on the hot layer temperature and depth at the station preceding the smoke location and the opposing air velocity at the smoke location are shown in Figures 14 and 15 for test fires in location 1 and 2, respectively. The arches at stations 3 and 6 cause the Froude numbers determined at these locations to be higher than the other locations near them due to the reduction in flow area in the arch. The maximum Froude number determined was 1.35 at station 3 for the 620 kW fire in location 1. If stations 3 and 6 are excluded, the maximum Froude number determined was 0.80 at station 1 for the 320 kW fire in location 1.

Figures 16 and 17 show the determined Froude numbers,  $Fr_{Cl}$ , based on the temperature difference at the ceiling level (highest thermocouple in the tree at the station preceding the smoke front) as suggested from the correlation of Heskestad and Spaulding [5]. The maximum Froude number determined using this method was 0.88 at station 3 for the 720 kW fire in location 2. Excluding stations 3 and 6, the maximum was 0.59 at station 2 for the same 720 kW fire. The correlation of Heskestad and Spaulding [5] for apertures in vertical walls (Eq. 5) is tested for application to this horizontal corridor in Figures 18 and 19. As there were no apertures in the test corridor except at station 3 and 6, and as the buoyant force was determined where there was some interaction between the smoke and air flows, this correlation was not expected to apply without some modification.

Figures 20 and 21 show Froude number determinations,  $Fr_Q$ , similar to the Thomas [3] no smoke back flow correlation. In these determinations the buoyancy force was derived from the fire size, corridor width and downstream average air temperature which was determined at the starboard room (stateroom 01-15-3-L) door. The maximum Froude number was 1.68 at station 3 for the 720 kW fire in location 2 and 1.28 at station 2 for the 350 kW fire in location 2 with station 3 and 6 excluded.

The determination of  $Fr_Q$  was repeated using the station 6 air flow in Figures 22 and 23. The Froude numbers are high as a result of the increase in flow area after the archway at station 6 is cleared. The maximum Froude number determined was 2.51 at station 1 for the 320 kW fire in location 1.

## **7.2 Results for Vertical Trunk Smoke Movement Test Series**

The results of the tests involving vertical trunk flows are given in Table 3. The hot gas layer temperature and depth was determined using the thermocouple trees in the center of the trunk and on the side of the trunk running the entire height. The hot gas layer was defined in the same manner as used in the horizontal tests. The opposing air velocity was determined at the smoke location. The pressure differential at the same location as the velocity determination is also included in Table 3. The concentration (percent by volume) of both oxygen and carbon dioxide was determined at the smoke location and is given in Table 3. This table also presents the hand held anemometer readings, which were all taken at the main deck hatch and the determined air flow readings from the bi-directional probes at that same location for comparison. The pressure differential at the main deck hatch is also presented in Table 3. These

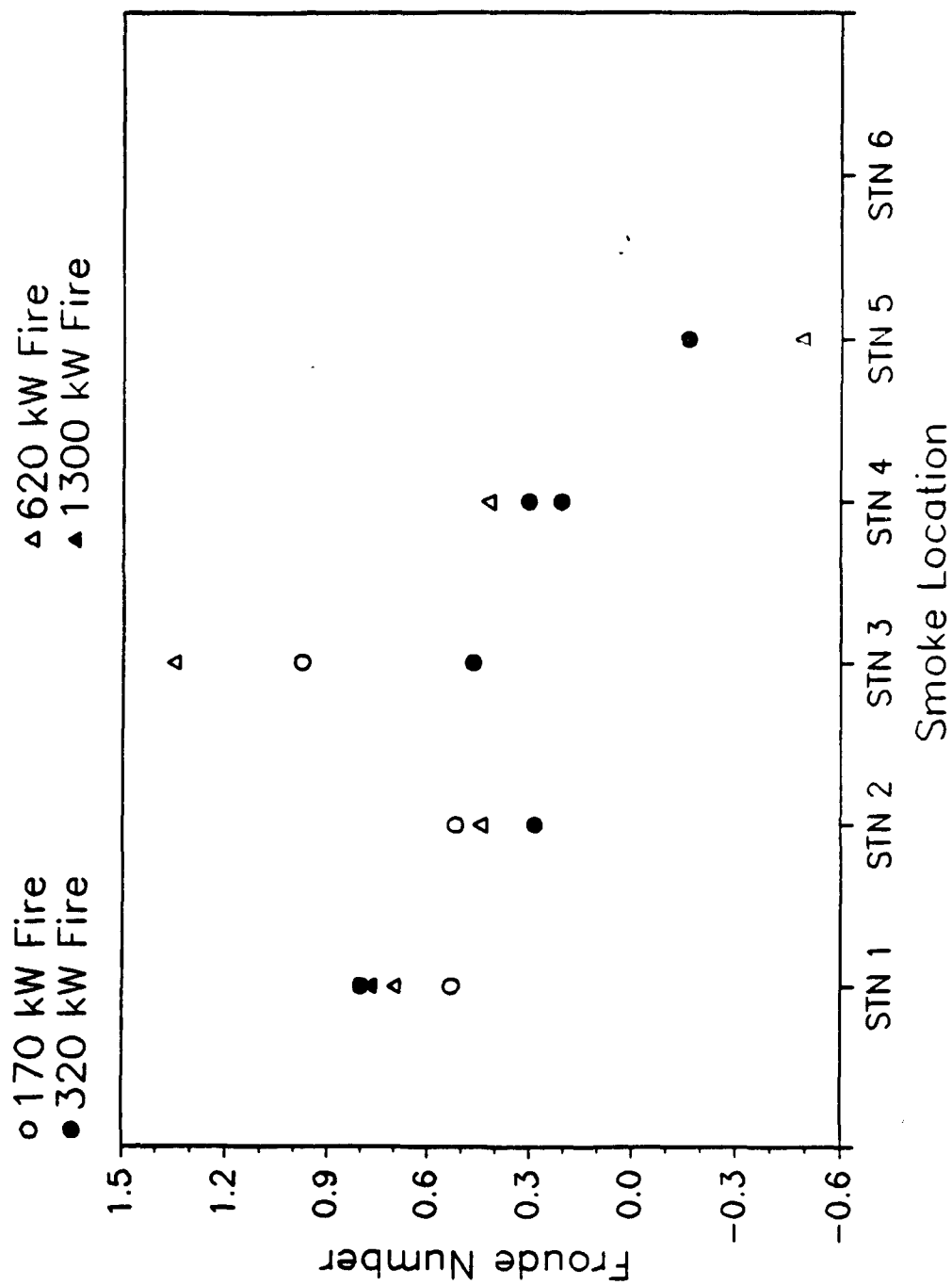


**Fig. 14** – Froude Number correlation based on hot layer temperature depth and average velocity at smoke location with fire in location 1

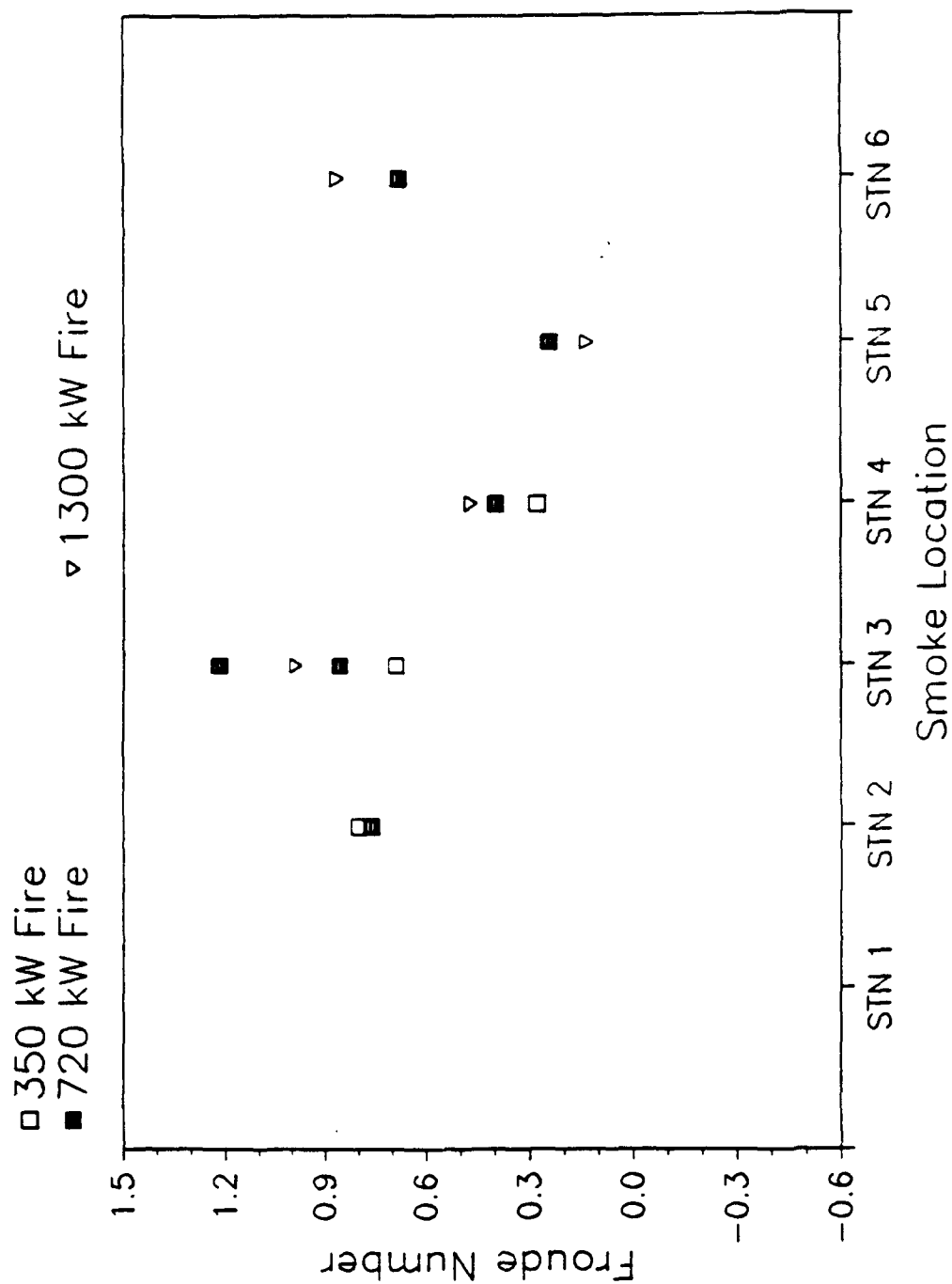


**Fig. 15** – Froude Number correlation based on hot layer temperature depth and average velocity at smoke location with fire in location 2

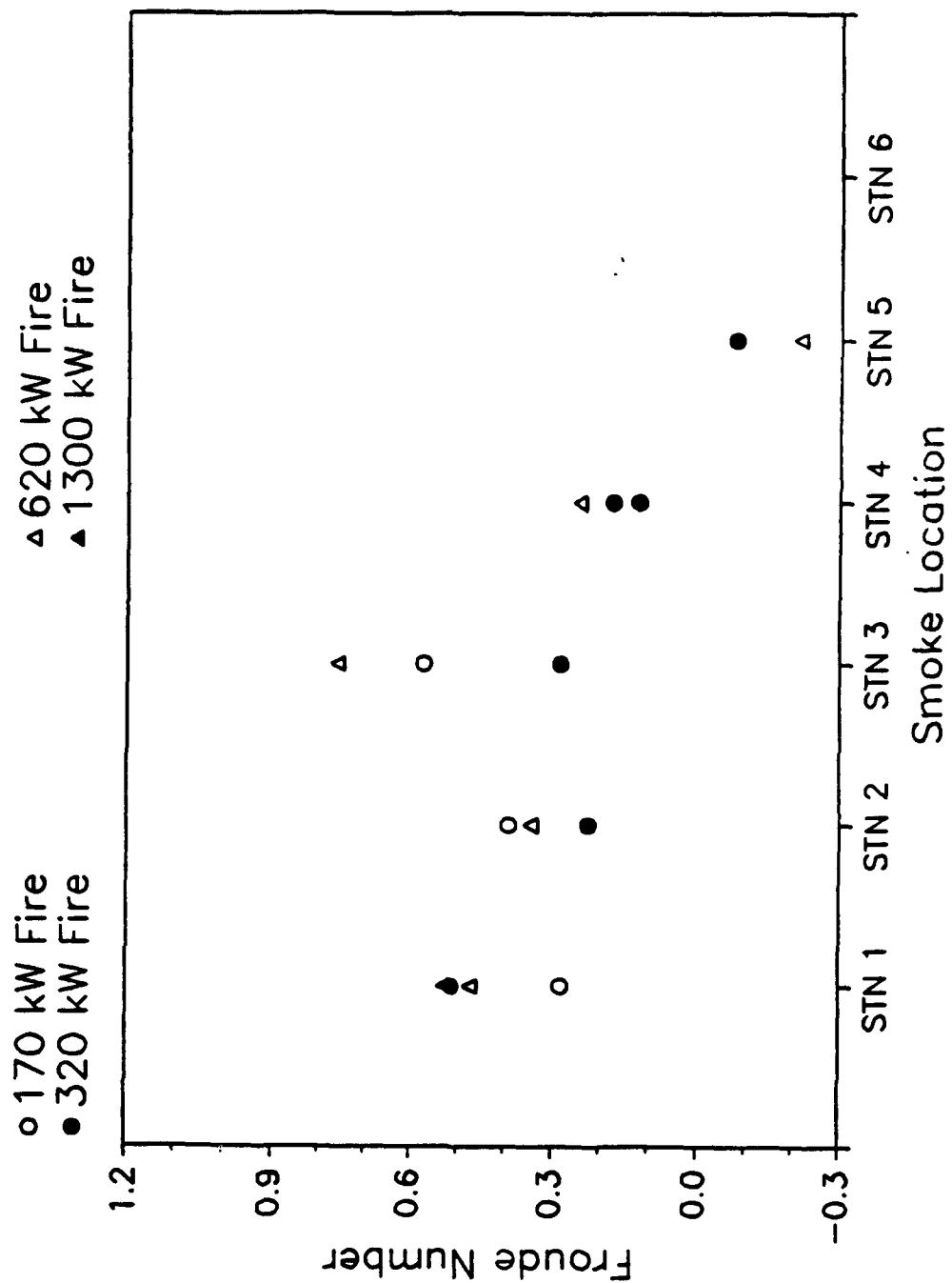


Fig. 16— Froude Number correlation based on ceiling temperature difference and velocity at smoke location with fire in location 1

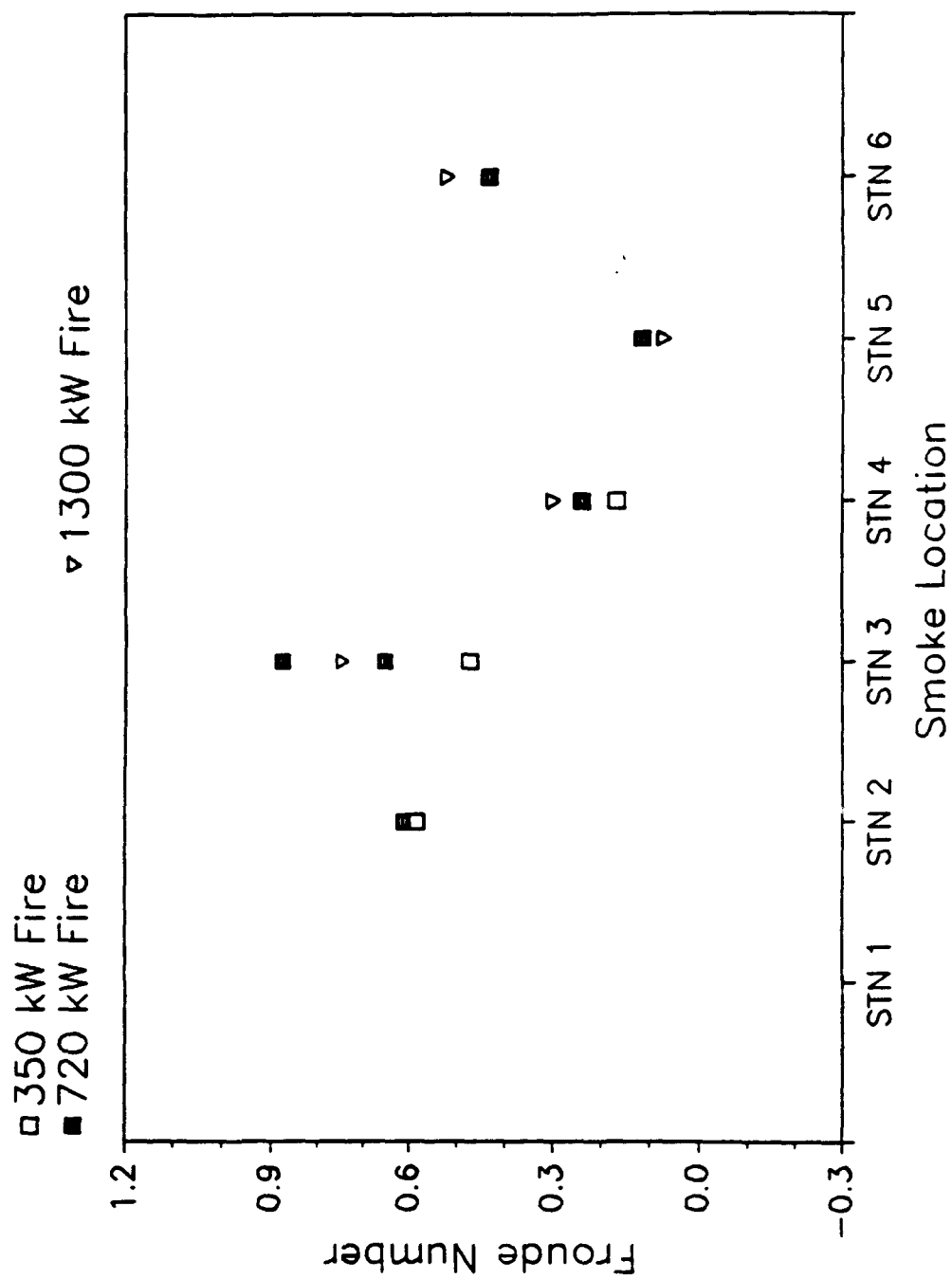
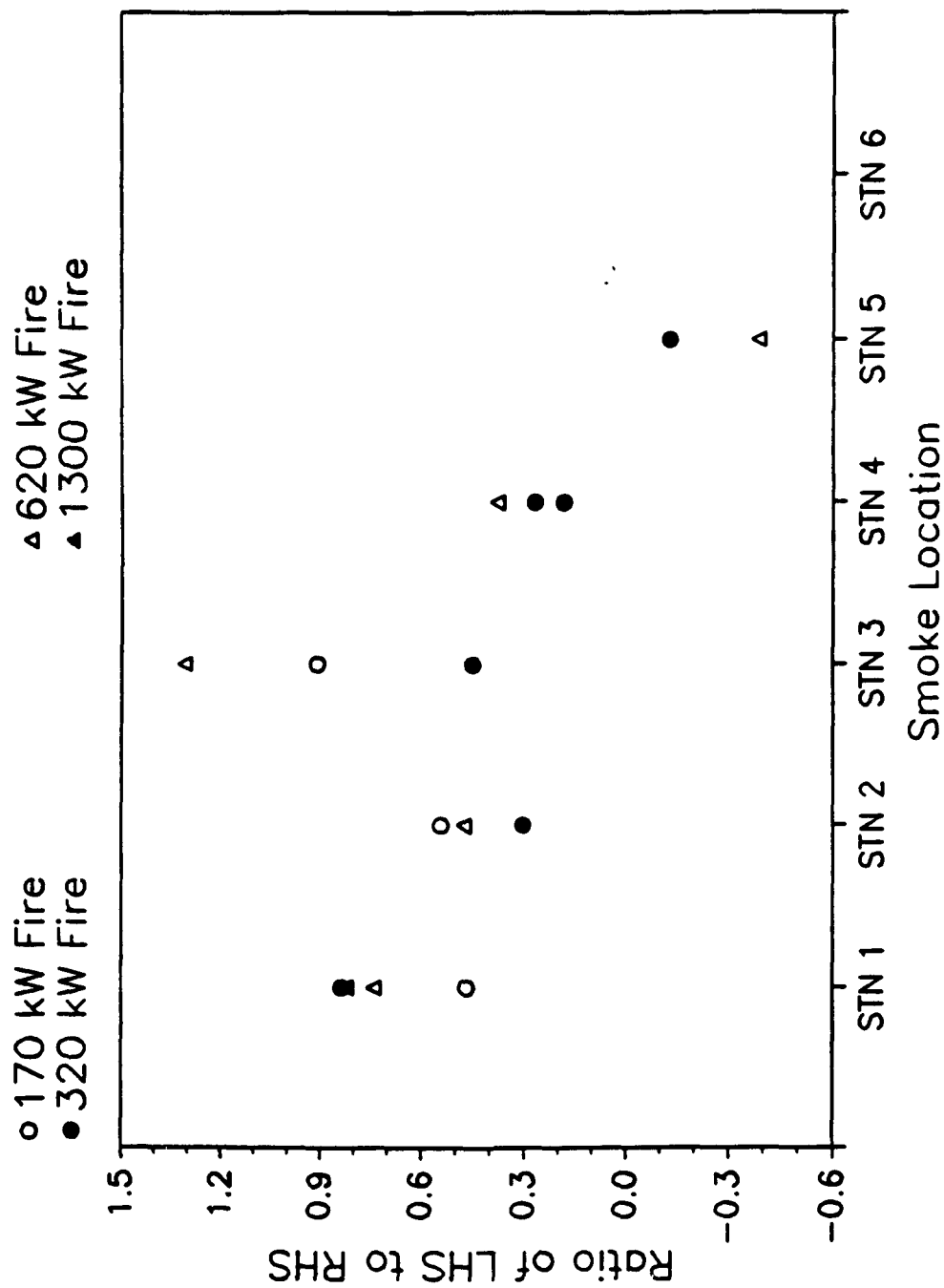
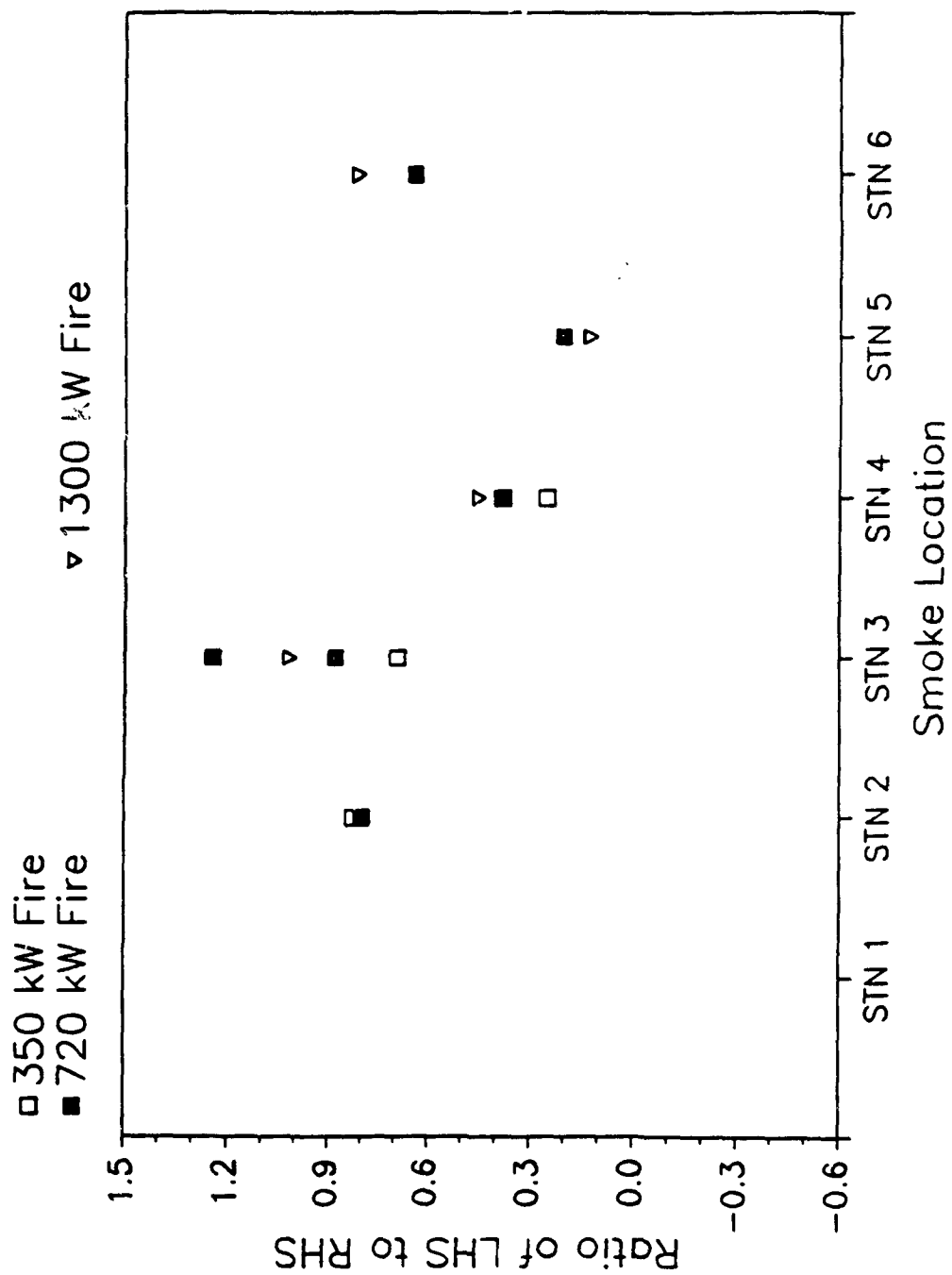


Fig. 17 – Froude Number correlation based on ceiling temperature difference and velocity at smoke location with fire in location 2



**Fig. 18** – Check of Heskestad and Spaulding correlation during horizontal corridor tests with fire in location 1



**Fig. 19** — Check of Heskestad and Spaulding correlation during horizontal corridor tests with fire in location 2



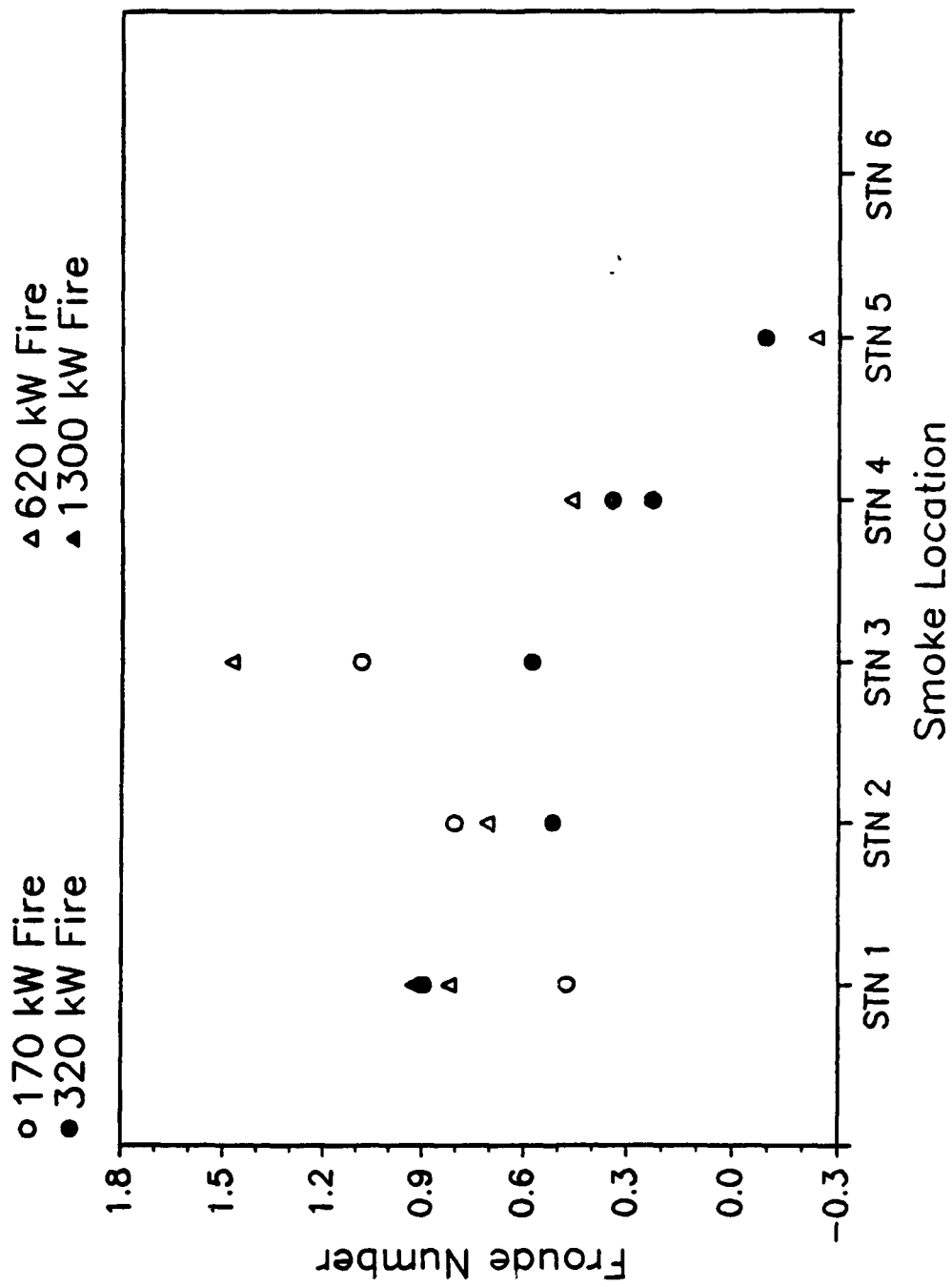


**Fig. 20** – Froude Number correlation based on fire size, downstream temperature and velocity at smoke location with fire in location 1

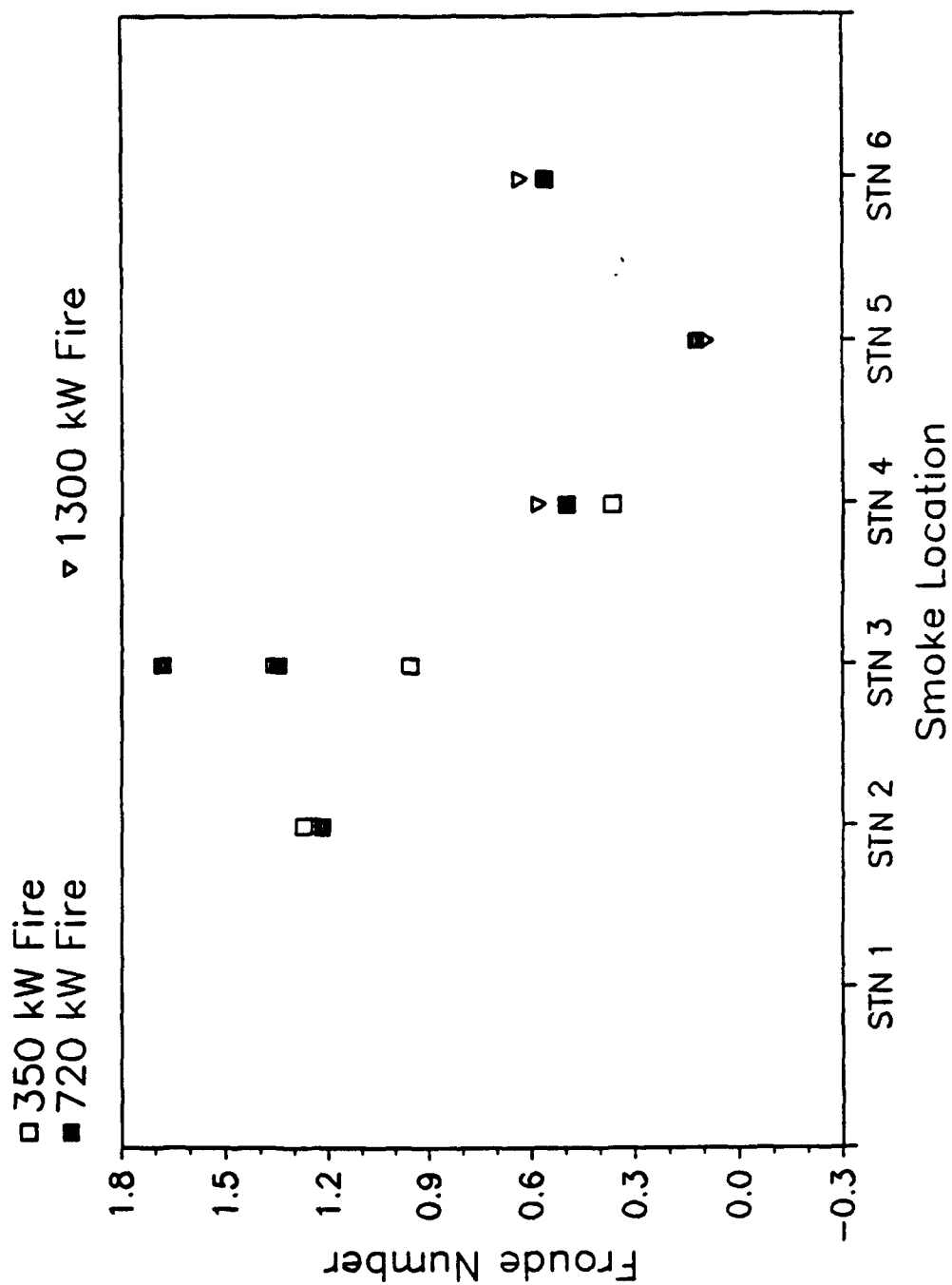


Fig. 21 – Froude Number correlation based on fire size, downstream temperature and velocity at smoke location with fire in location 2

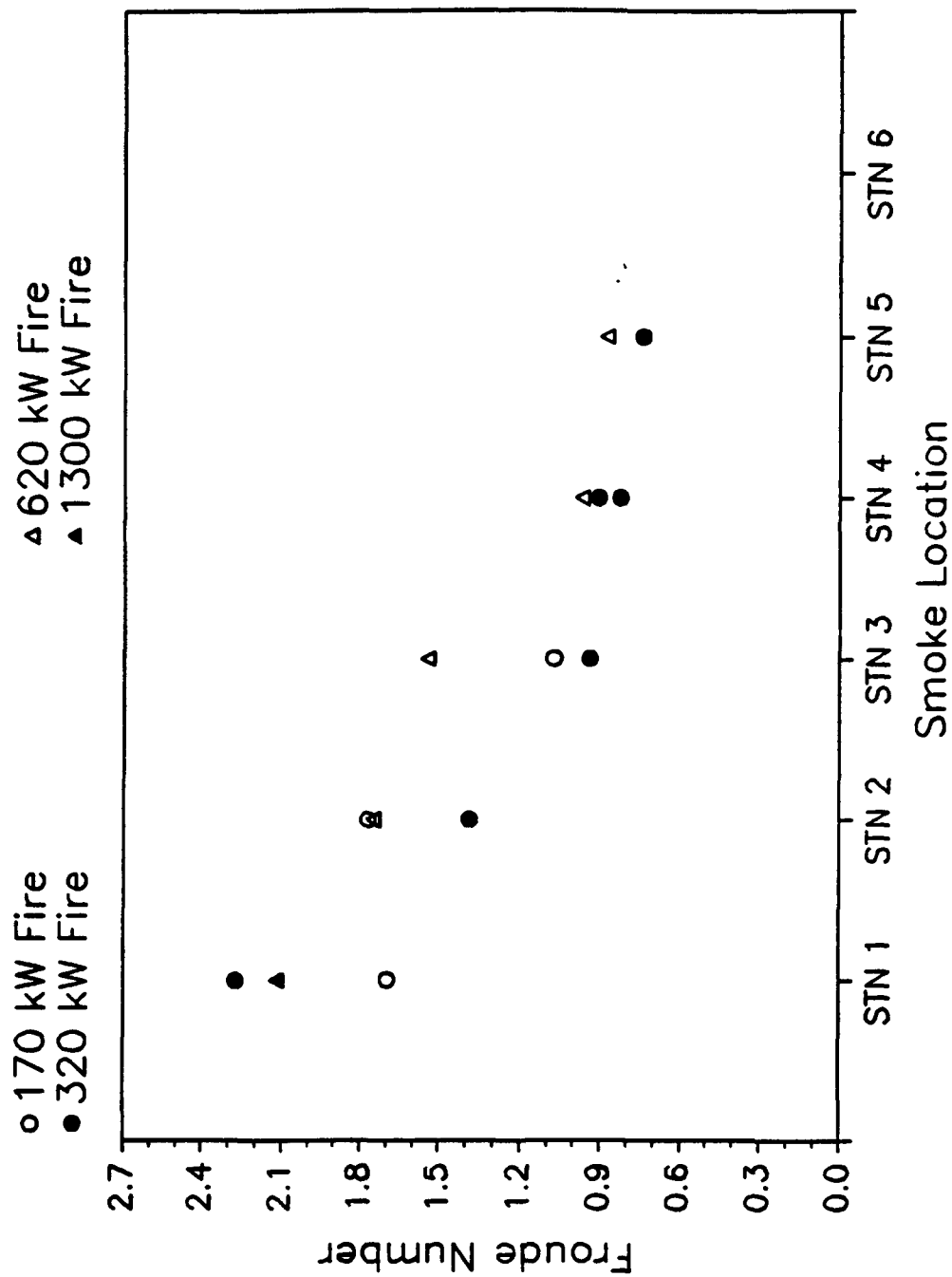


Fig. 22 – Froude Number correlation based on fire size, downstream temperature and velocity at station 6 with fire in location 1

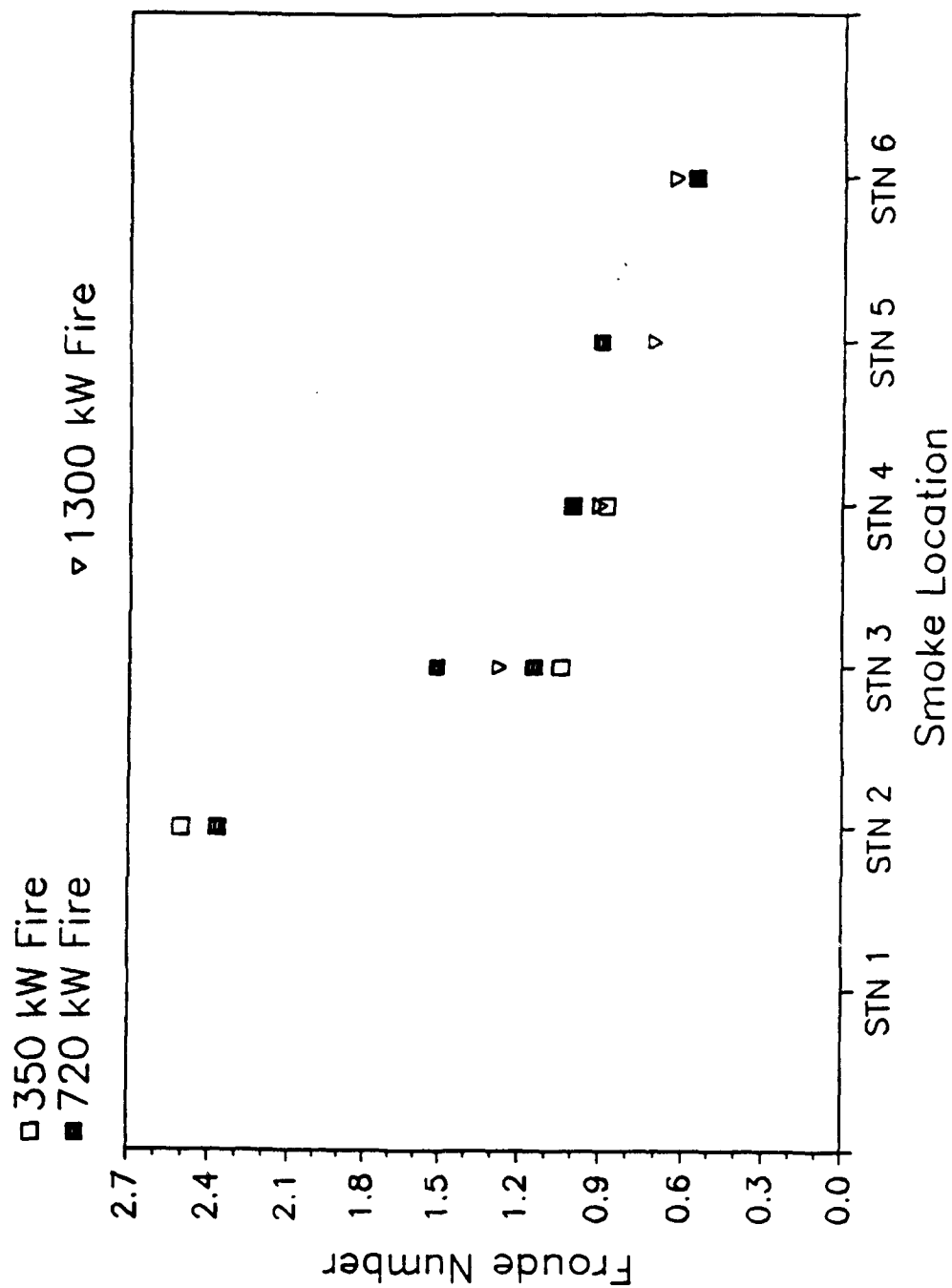


Fig. 23 – Froude Number correlation based on fire size, downstream temperature and velocity at station 6 with fire in location 2

Table 3. Shipboard Experimental Results: Vertical Trunks

Test No.	Fire Size (kW)	Smoke Loc.	Trunk Dist (m)	Trunk Temp (°C)	Side Depth (m)	Side Temp (°C)	Main Depth (m)	3Deck Hatch (°C)	Hatch (°C)	O <sub>2</sub> (%)	CO <sub>2</sub> (%)	Vel (m/s)	$\Delta P$ (Pa)	Vel <sub>h</sub> (m/s)	Vel <sub>h</sub> Loc.	Vel <sub>h</sub> (m/s)	$\Delta P_h$ (Pa)
10	274	3DKH	4.27	111	2.74	64	3.96	29	35	19.10	1.67	1.23	2.912	1.06	MDK H	1.60	1.969
10	273	MDKH	7.32	129	6.40	109	5.79	66	145	20.57	0.24	0.22	1.366	0.46	MDK H	0.22	1.366
11	662	3DKH	4.27	153	3.35	100	3.96	33	56	18.56	2.33	1.03	2.763	1.11	MDK H	1.65	1.824
11	662	MDKH	7.32	154	6.40	139	5.79	62	162	19.76	0.70	0.94	1.812	0.52	MDK H	0.94	1.812
12	1300	3DKH	4.27	179	2.74	107	3.96	34	60	17.85	2.57	2.35	4.876	1.83	MDK H	2.81	5.102
13	1300	3DKH	4.27	182	2.74	111	3.96	35	50	17.22	2.48	2.14	4.829	1.69	MDK H	2.59	4.057
13	1300	MDKH	7.32	185	6.40	168	5.79	50	129	20.42	0.00	2.11	3.933	1.06	MDK H	2.11	3.933
14	193	3DKH	2.74	144	3.35	203	3.96	28	66	19.92	1.29	2.39	0.480	1.56	MDK H	2.27	4.032
14	182	MDKH	5.79	121	5.79	209	4.57	31	149	20.89	0.10	0.14	0.694	0.60	MDK H	0.14	0.694
14	328	3DKH	2.74	283	3.35	334	3.96	29	112	19.23	1.86	2.62	0.918	1.61	MDK H	2.58	4.455
14	325	MDKH	5.79	194	5.79	322	4.57	34	211	21.06	0.00	0.34	1.521	0.71	MDK H	0.34	1.521
15	668	3DKH	2.74	406	3.35	369	3.96	31	140	19.29	1.98	3.95	3.756	1.94	MDK H	3.77	9.682
15	672	MDKH	5.79	297	5.79	363	5.79	37	346	21.03	0.00	1.71	2.263	0.93	MDK H	1.71	2.263
15	1036	MDKH	5.79	409	5.79	490	5.79	41	485	21.01	0.01	1.80	2.763	1.04	MDK H	1.80	2.763
16	340	3DKH	2.74	245	3.35	299	3.96	28	78	18.84	2.14	2.66	1.339	1.60	MDK H	2.74	5.451

measurements give an indication of the variation in required air flow to hold the smoke at the various locations in the trunk.

The opposing air velocity required to halt upstream smoke migration is shown in Figures 24 and 25 for the test fires in locations 1 and 2 respectively. Figures 26 and 27 show the required air flow at the main deck hatch. For fires in location 1 (offset from the trunk entrance) there is not a great difference in the flow velocity required to halt the upstream smoke migration at the third deck hatch or the main deck hatch, approximately 1 m/s (195 ft/min) or less, while for fires in location 2 (directly under the third deck hatch) this difference is approximately 2 m/s (395 ft/min).

Figures 28 through 31 shown the effects of increased air flow through the test trunk on both upstream and downstream temperatures for the 650 kW fire in location 1 and the 670 kW fire in location 2. The mid-point temperature is the average of the temperature 1.5 m (5 ft) above the lower hatch on the center and side trunk trees.

The Froude numbers,  $Fr_{TD}$ , based on the hot gas layer temperature and depth determined from the thermocouple tree in the center of the trunk and the opposing air velocity at the smoke location are shown in Figures 32 and 33. Figures 34 and 35 show  $Fr_{TD}$  determined from the side trunk thermocouple tree. The maximum Froude number determined for the main deck hatch was 0.26 for the 1300 kW fire at location 2. The maximum for the third deck hatch was 0.66 for the 670 kW fire in location 2.

Figures 36 through 41 give the Froude numbers,  $Fr_{CI}$ , based on the temperature difference at the height of the smoke location (third or main deck hatch levels) for each of the two fire locations as determined from the thermocouple tree in the center of the trunk, the tree in the side of the trunk, and the string of thermocouples in the two hatches, respectively. The maximum Froude number determined was 1.6 at the lower hatch for the 1300 kW fire in location 1 based on the hatch tree. The Froude numbers based on the hatch trees had significantly greater scatter than those based on the either of the trunk trees. The maximum Froude number based on either trunk tree was 0.99 at the main deck hatch for the 340 kW fire in location 2 determined from the side tree. The maximum for the lower hatch based on a trunk tree was 0.96 for the 1300 kW fire in location 1 based on the center tree. The greater scatter in the  $Fr_{CI}$  as compared to  $Fr_{TD}$  is due to the increased requirement for precision in determining the location of the smoke front in  $Fr_{CI}$ . The average temperature and depth in the previous method obscures some of the differences in the actual smoke front locations between tests.

Froude number determinations,  $Fr_Q$ , similar to that of Thomas' [3] no back flow correlation, both with the opposing air velocity measured at the smoke location and with the opposing air velocity measured at the main deck hatch, are shown in Figures 42 through 45. As the flow area in either hatch was smaller than the flow area at either fire location, the determined Froude number is high in comparison to Thomas [3] correlation in spite of the limited upstream smoke migration. The maximum Froude number determined was 1.83 at the lower hatch for the 670 kW fire in location 2 with the opposing air velocity determined at the lower hatch (1.75 with the air velocity determined

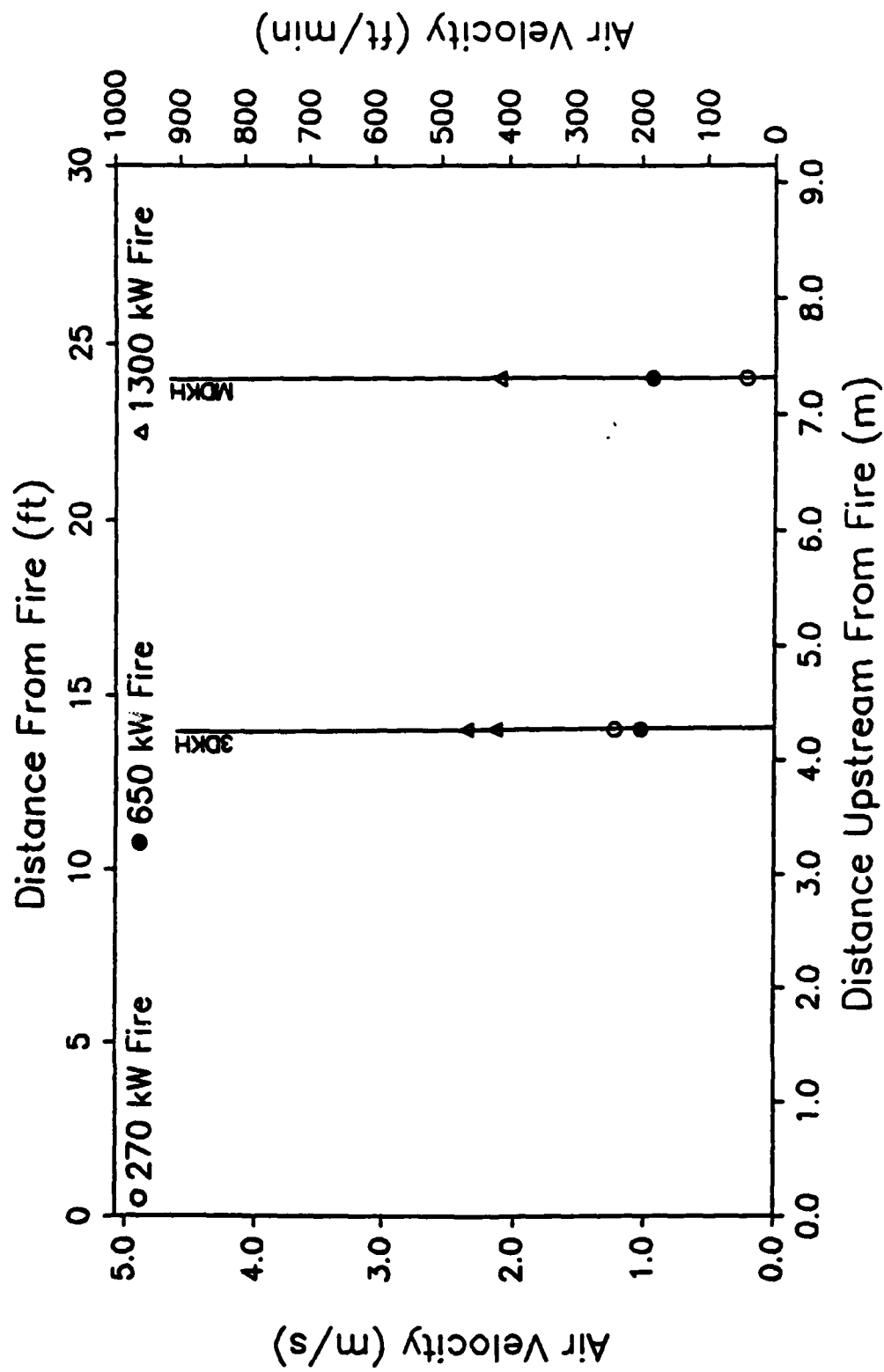


Fig. 24 – Required air velocity to halt upstream smoke migration during vertical trunk tests with fire in location 1

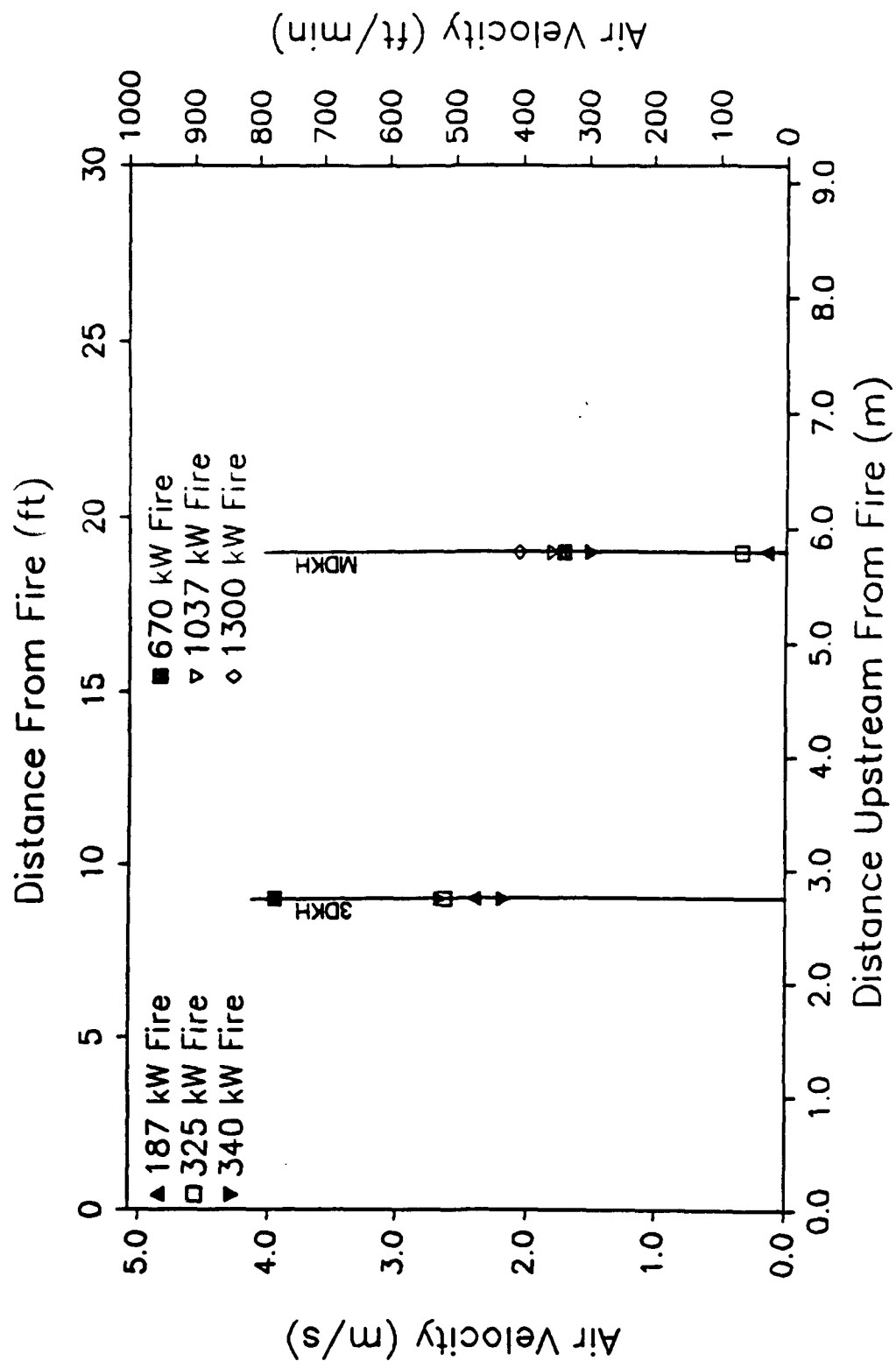
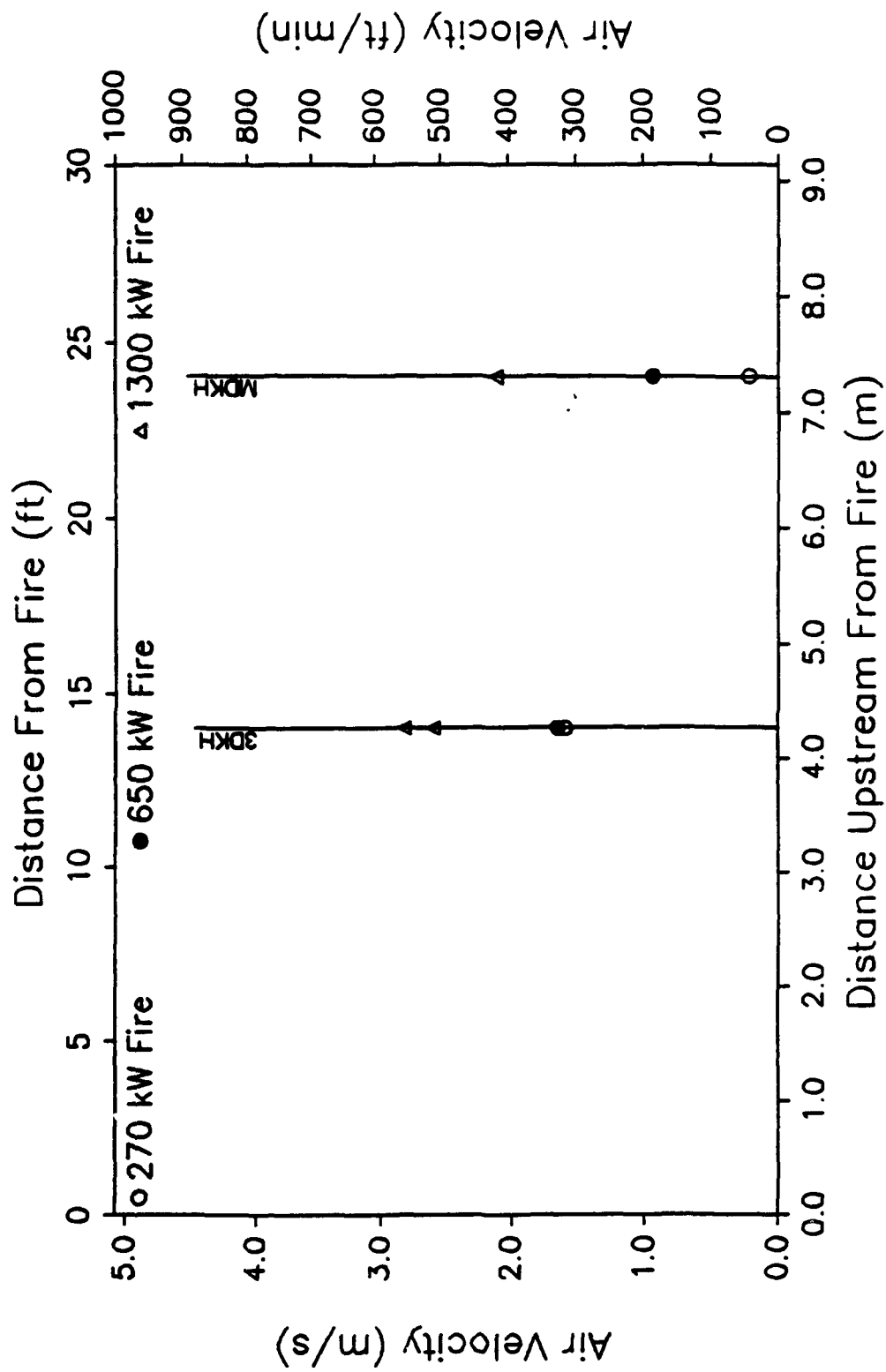
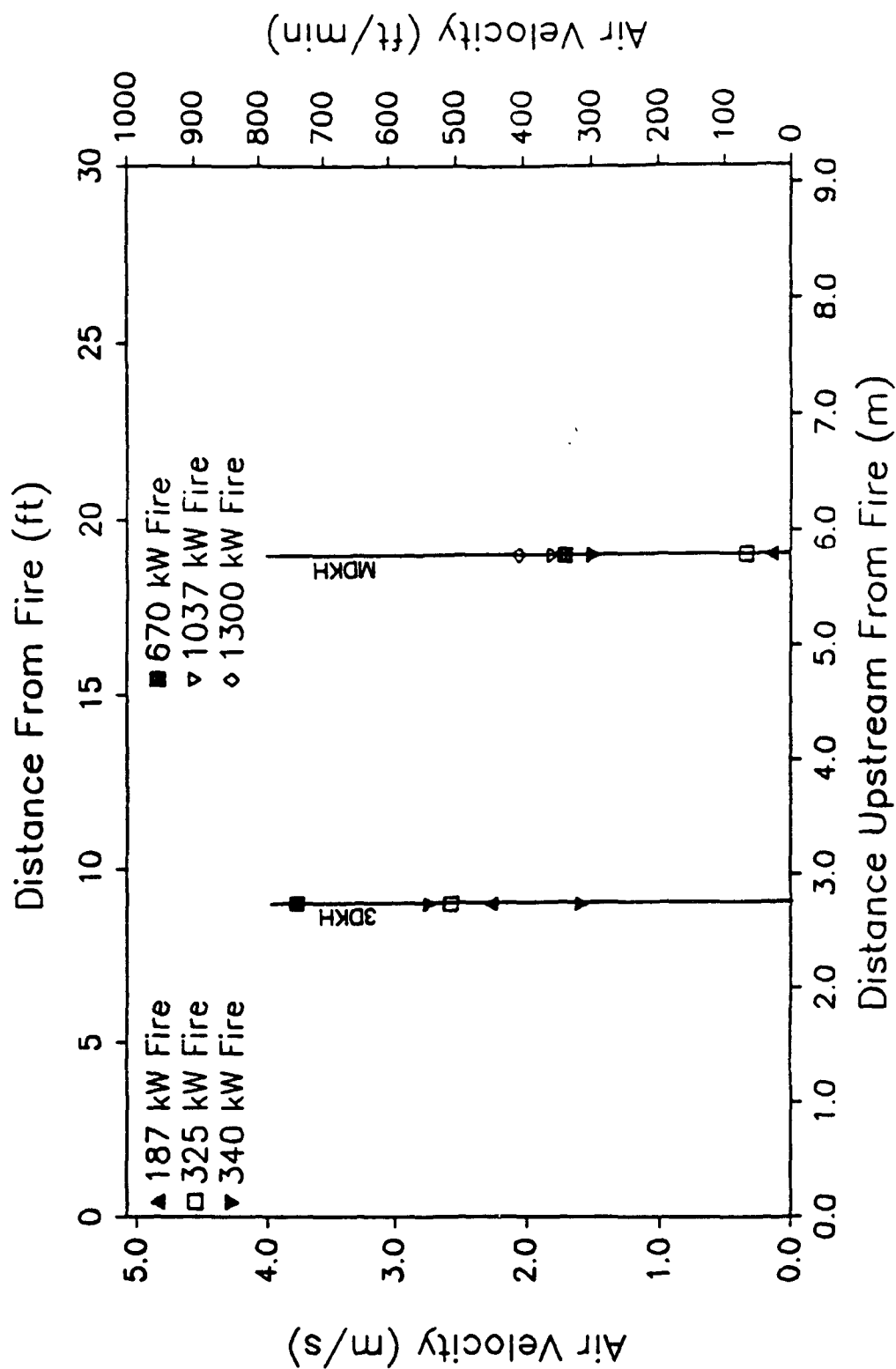


Fig. 25 – Required air velocity to halt upstream smoke migration during vertical tests with fire in location 2





**Fig. 26** – Required air velocity at main deck hatch to halt smoke migration during vertical trunk tests with fire in location 1



**Fig. 27** – Required air velocity at main deck hatch to halt upstream smoke migration during vertical tests with fire in location 2

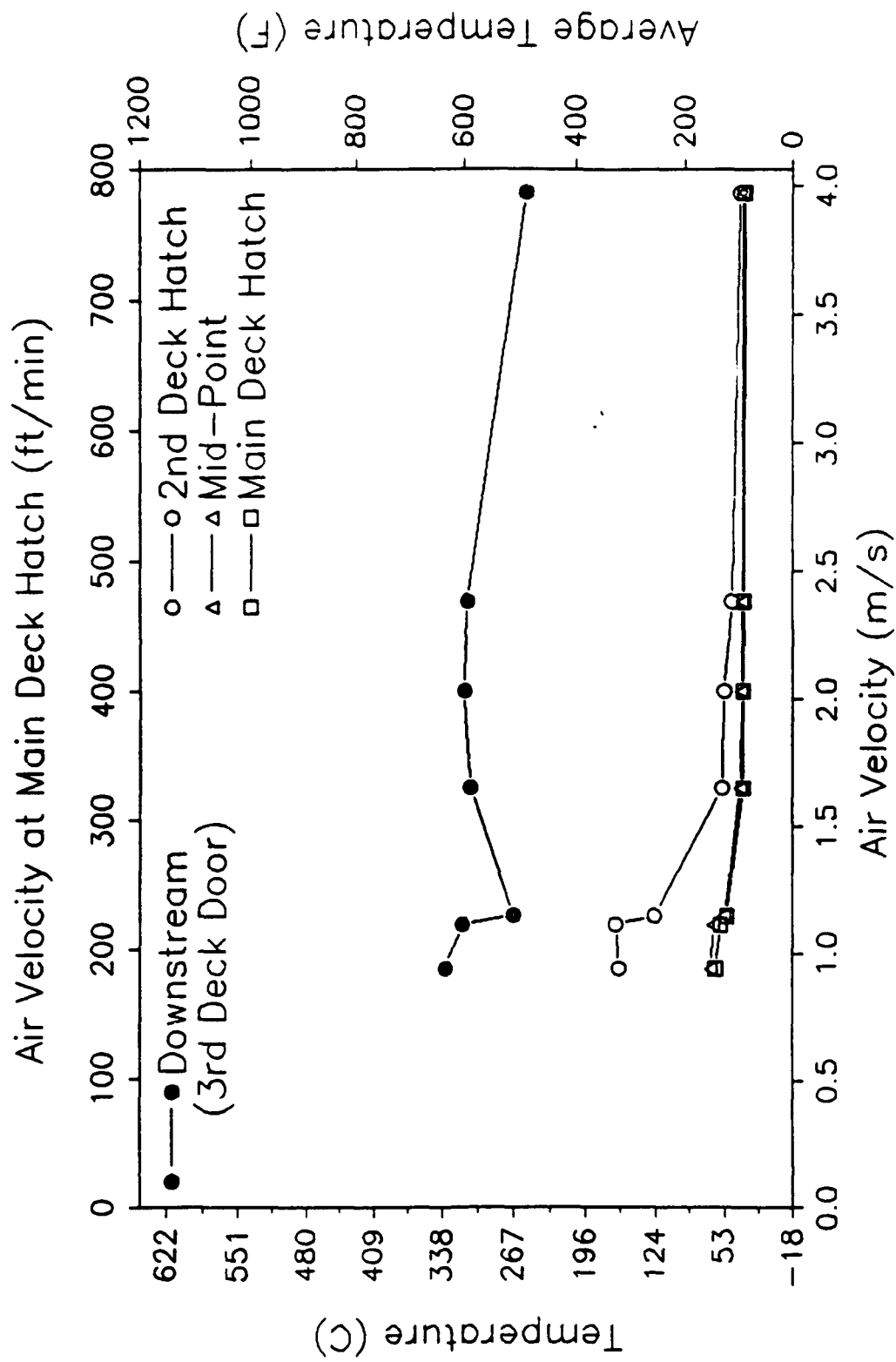


**Fig. 28** – Main deck hatch air velocity effects on average temperatures with 650 kW fire in location 1

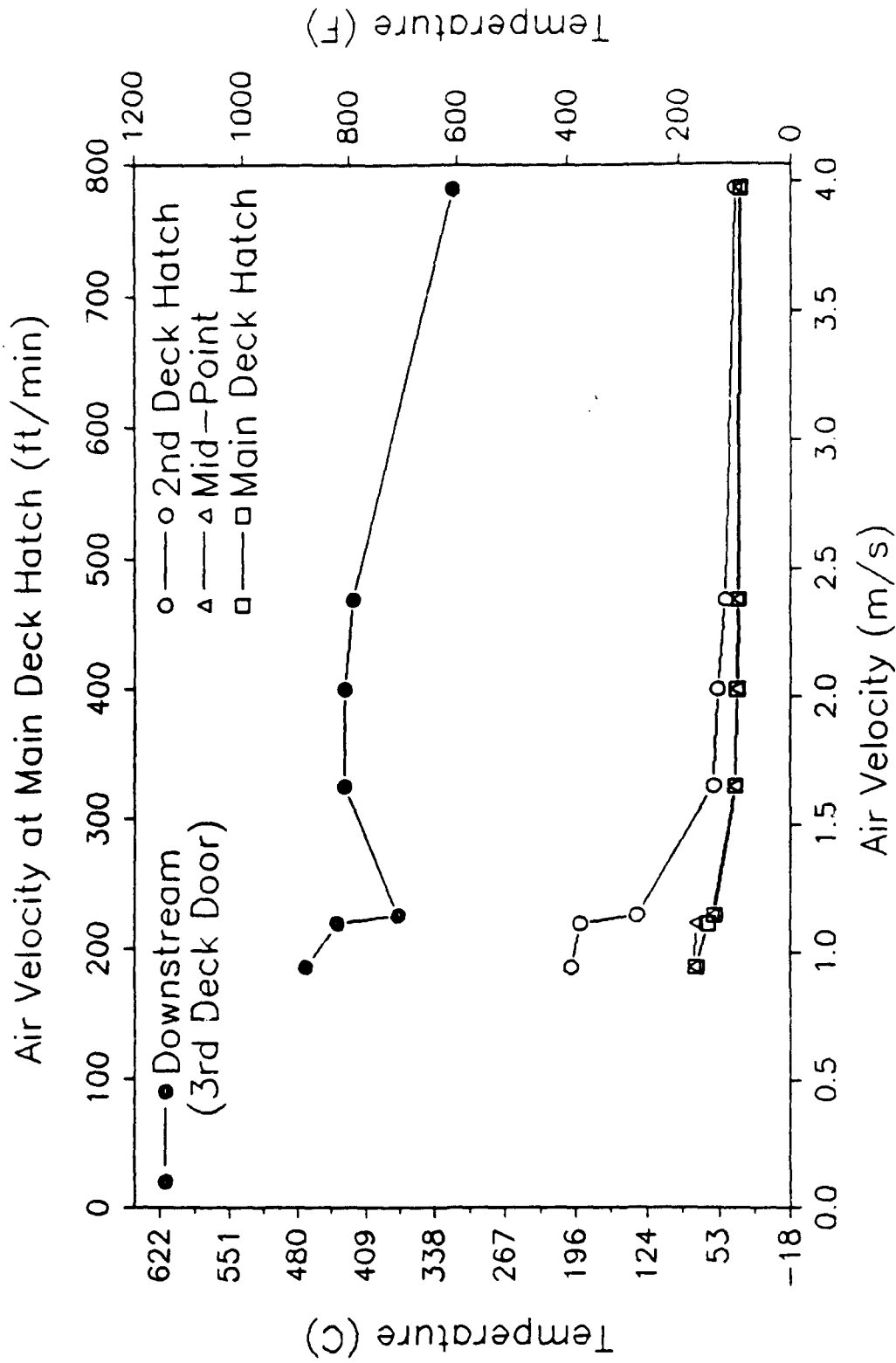


**Fig. 29** – Main deck hatch air velocity effects on maximum temperatures with 650 kW fire in location 1

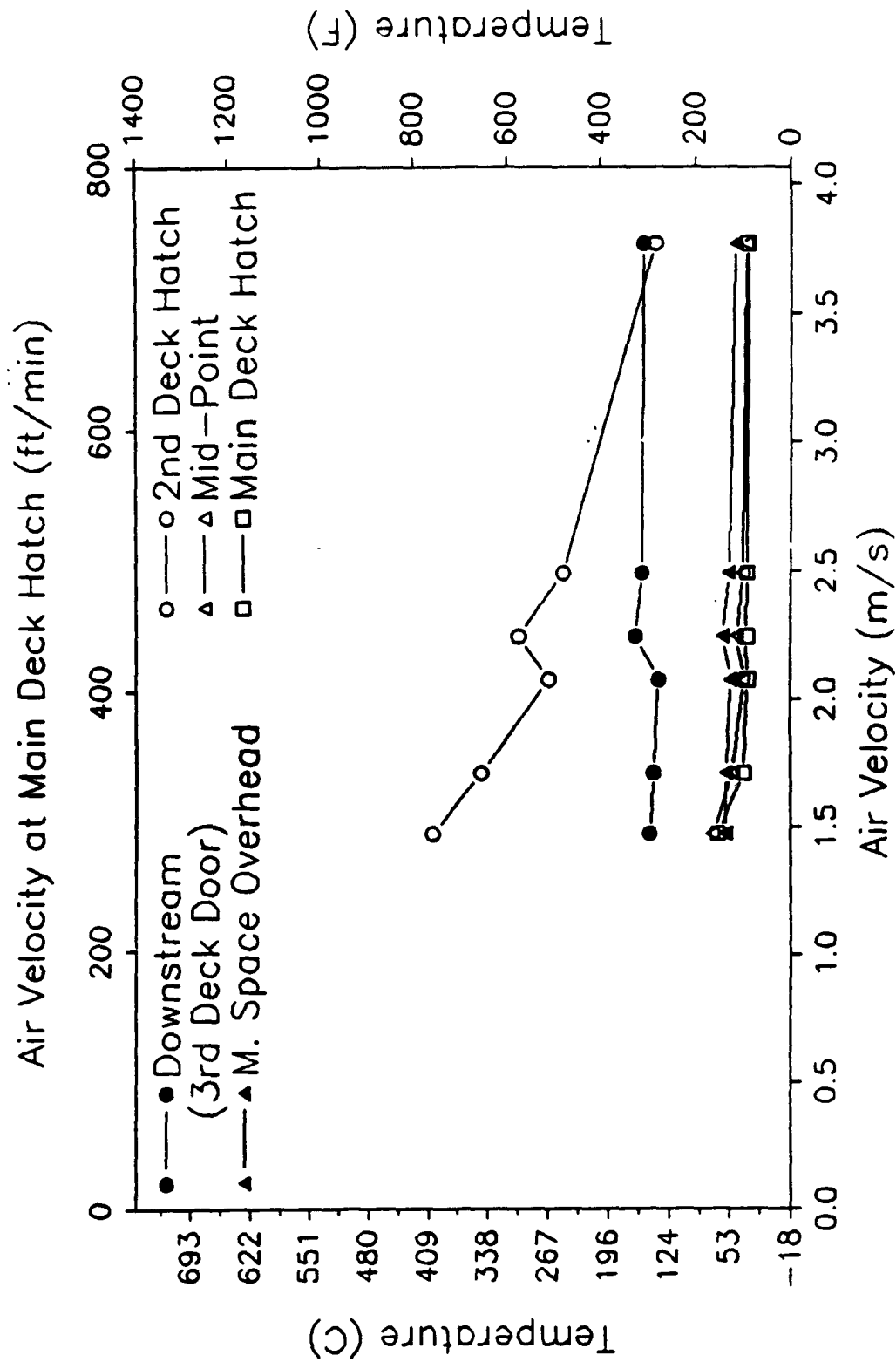
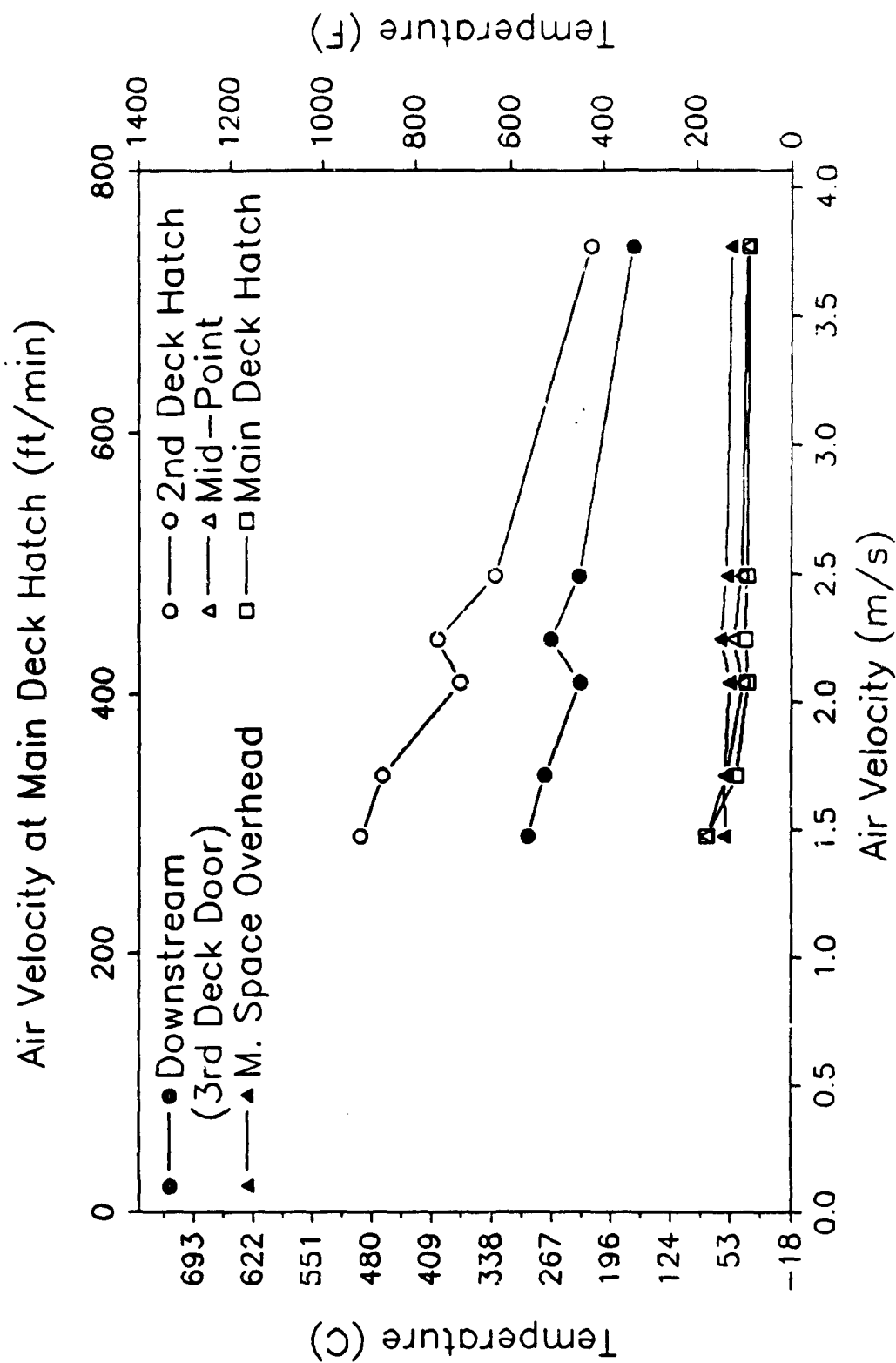


Fig. 30 — Main deck hatch air velocity effects on average temperatures with 670 kW fire in location 2



**Fig. 31— Main deck hatch air velocity effects on maximum temperature with 670 kW fire in location 2**

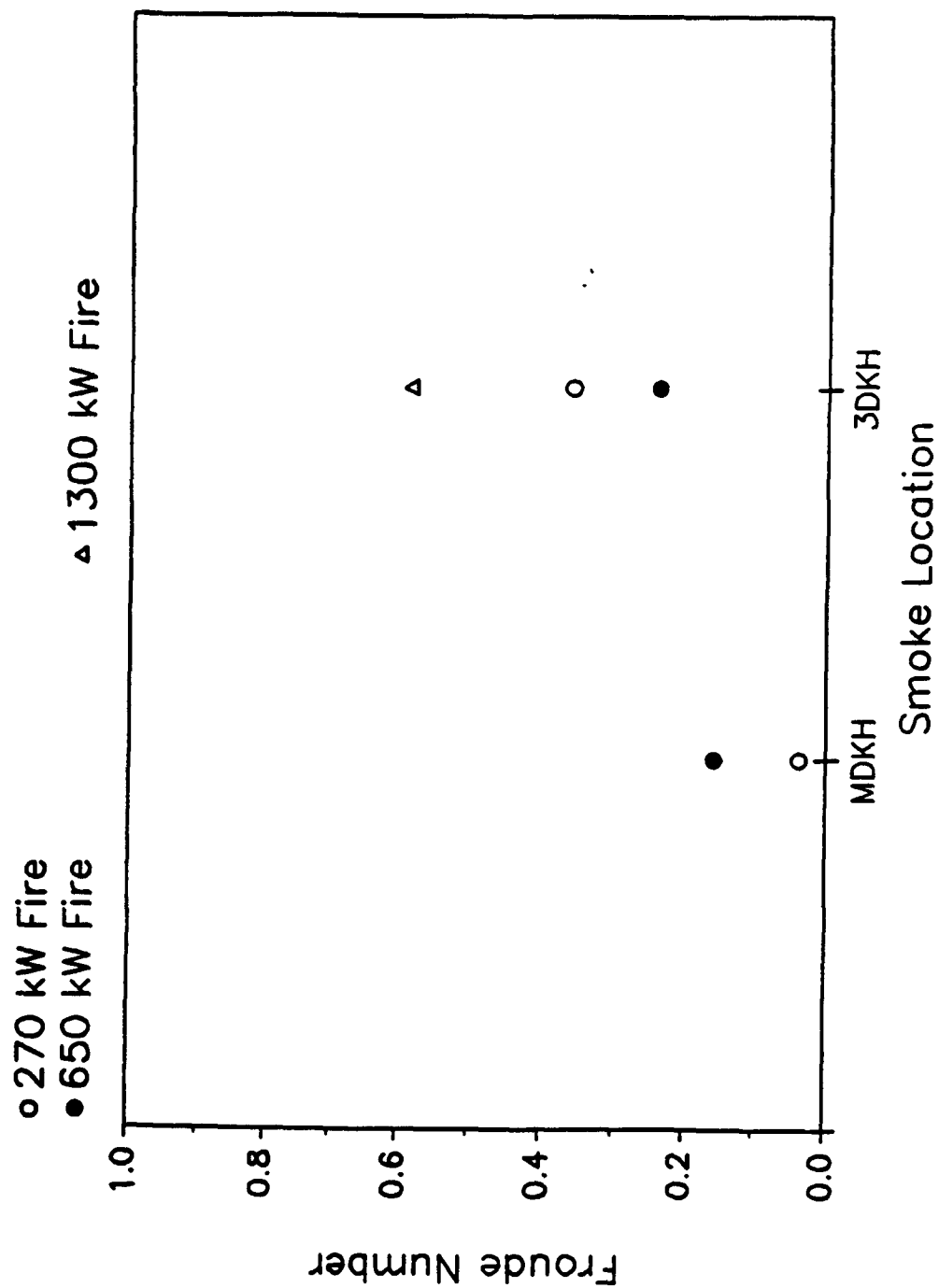


Fig. 32— Froude Number correlation based on center (trunk) tree hot layer temperature, depth and average velocity at smoke location with fire in location 1

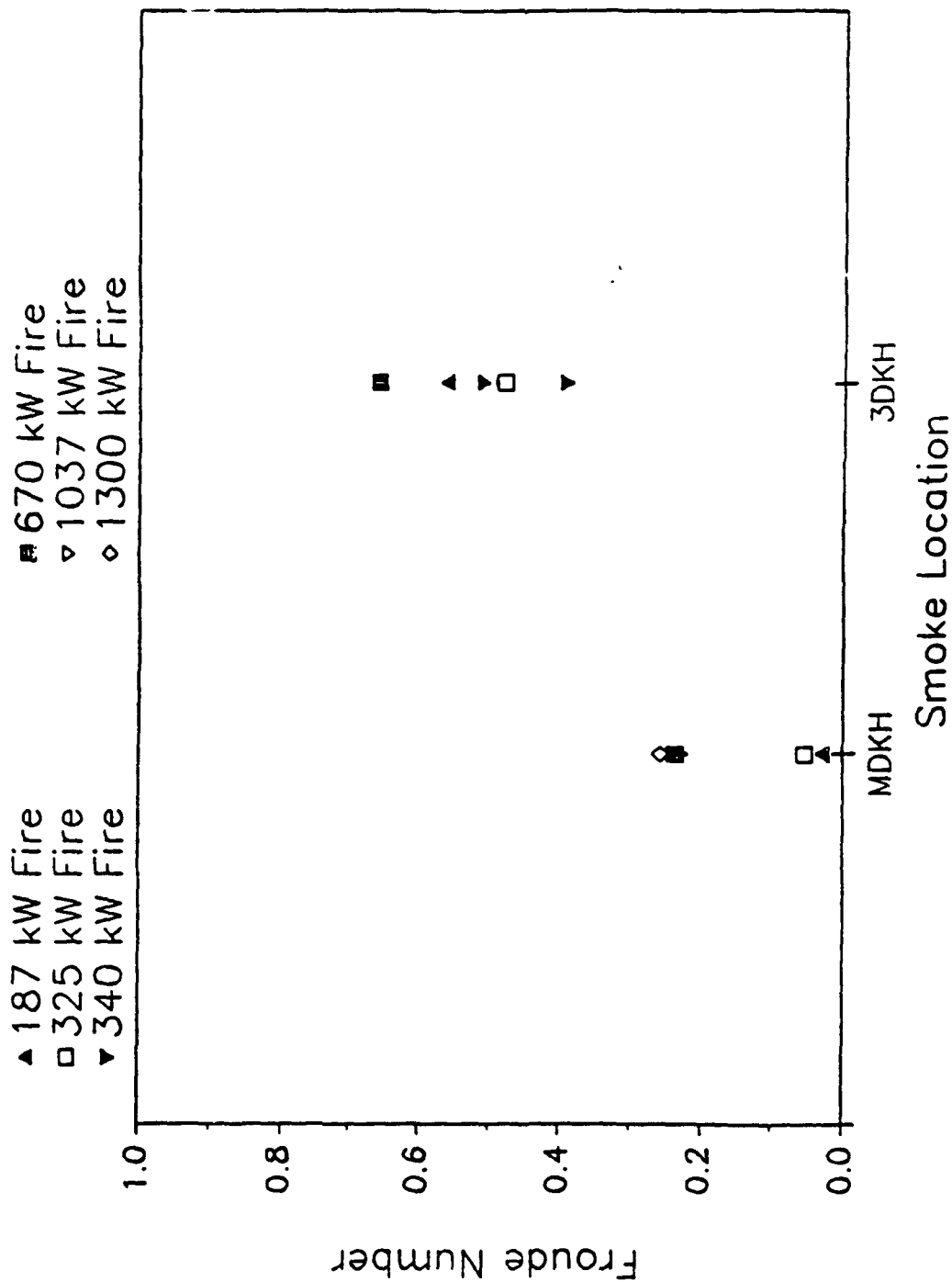
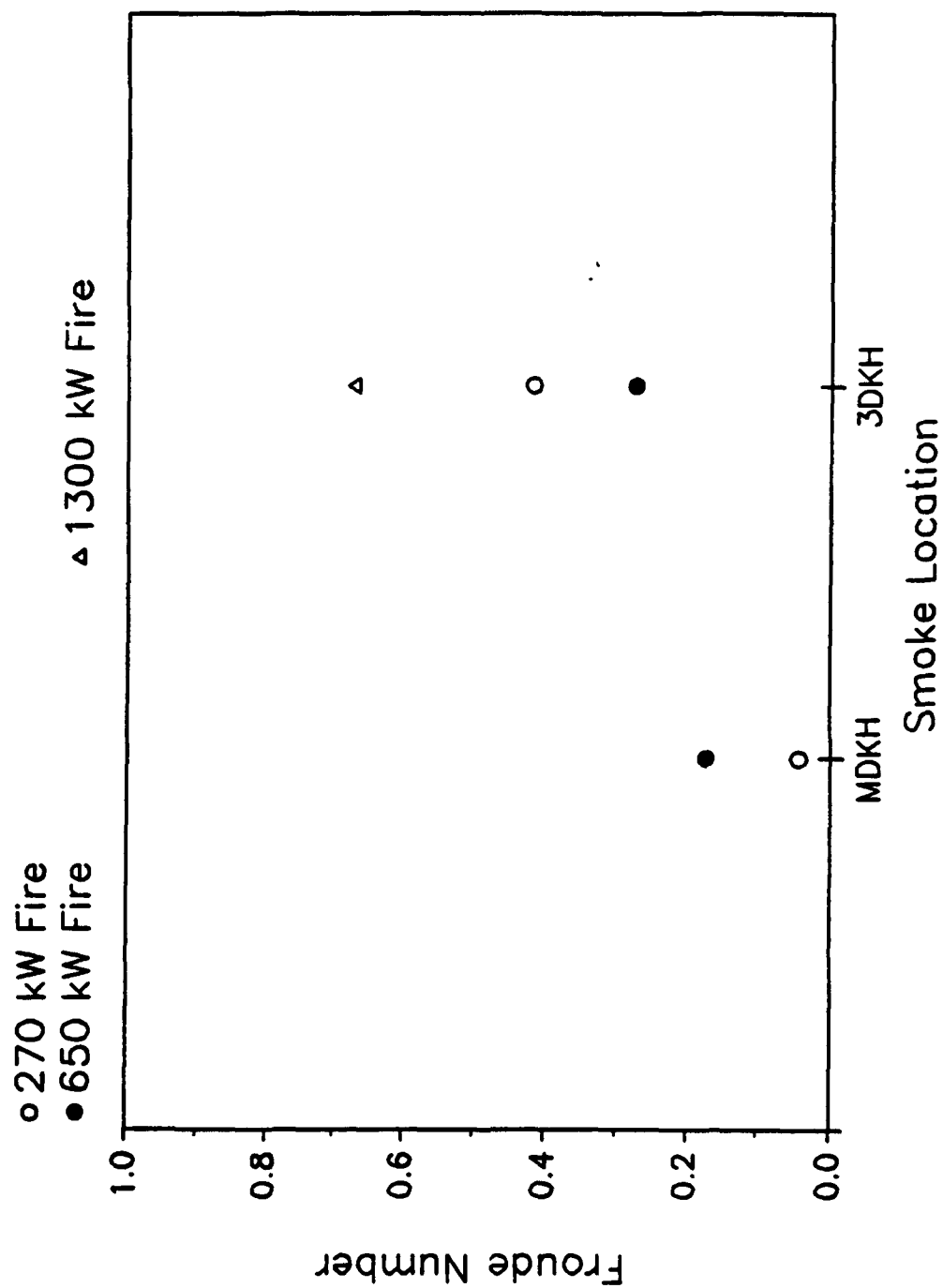


Fig. 33 - Froude Number correlation based on center (trunk) tree hot layer temperature, depth and average velocity at smoke location with fire in location 2





**Fig. 34**— Froude Number correlation based on side trunk tree hot layer temperature, depth and average velocity at smoke location with fire in location 1

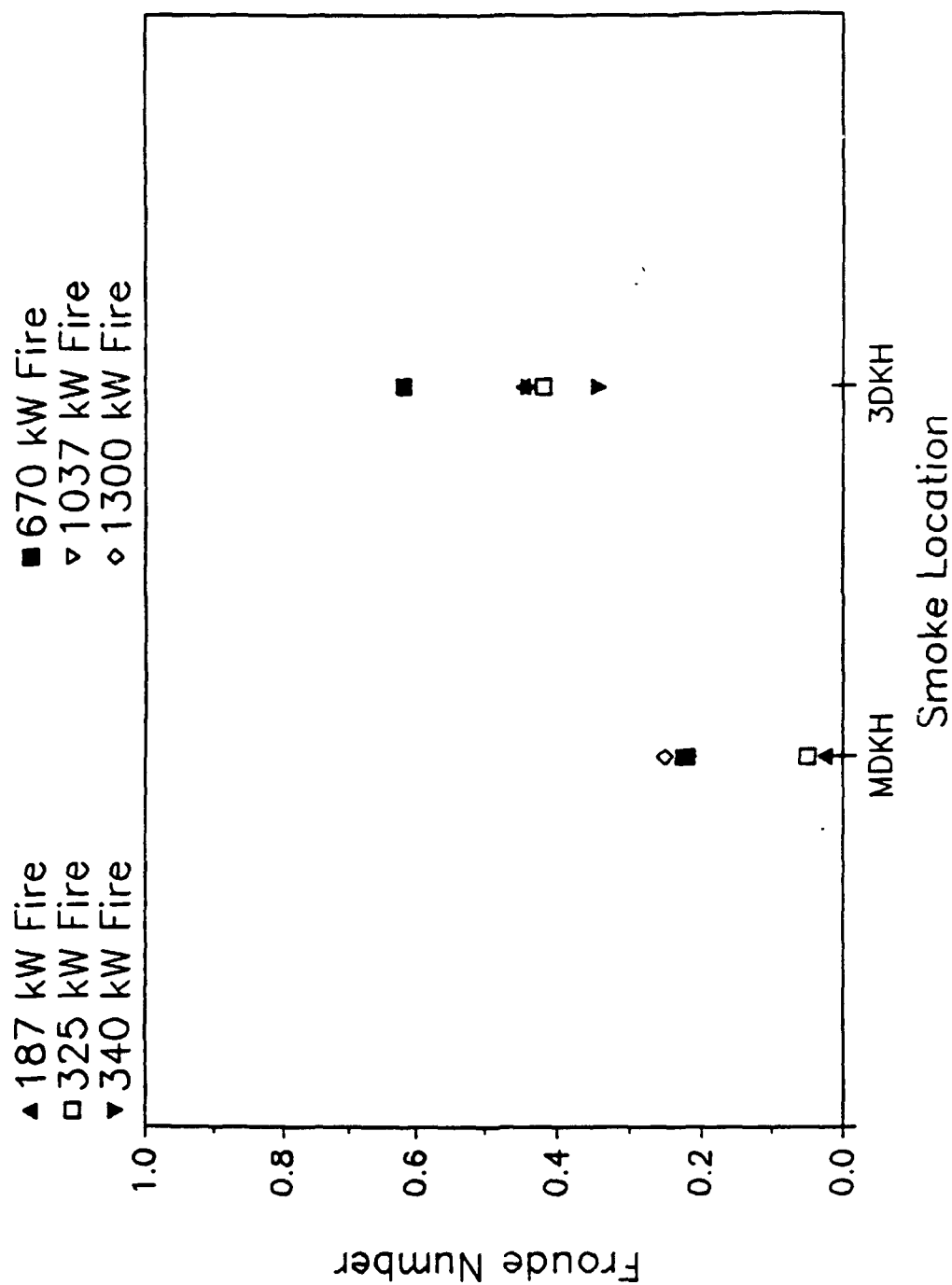
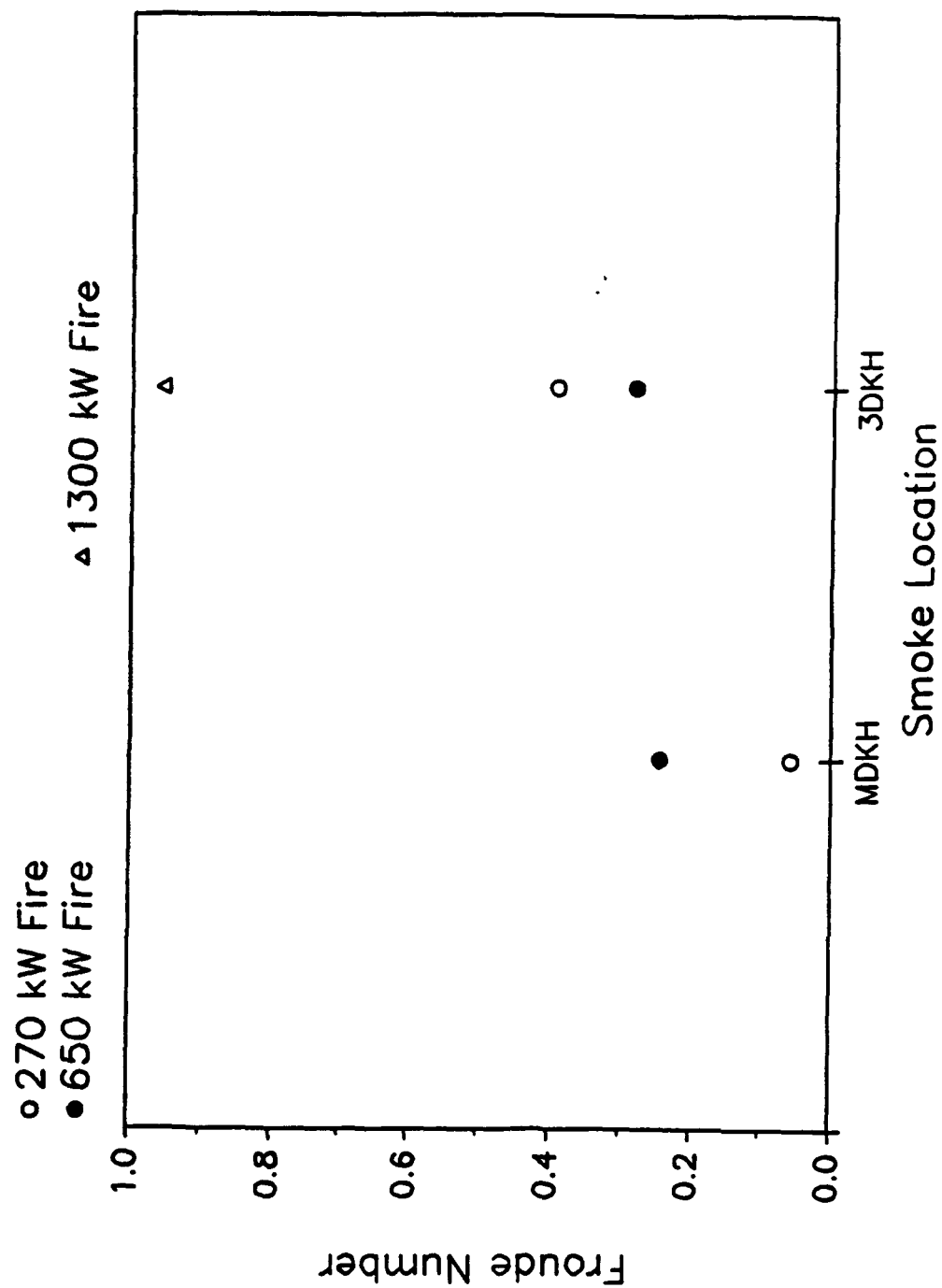


Fig. 35— Froude Number correlation based on side trunk tree hot layer temperature, depth and average velocity at smoke location with fire in location 2



**Fig. 36** – Froude Number correlation based on center trunk tree temperature difference, height and velocity at smoke location with fire in location 1

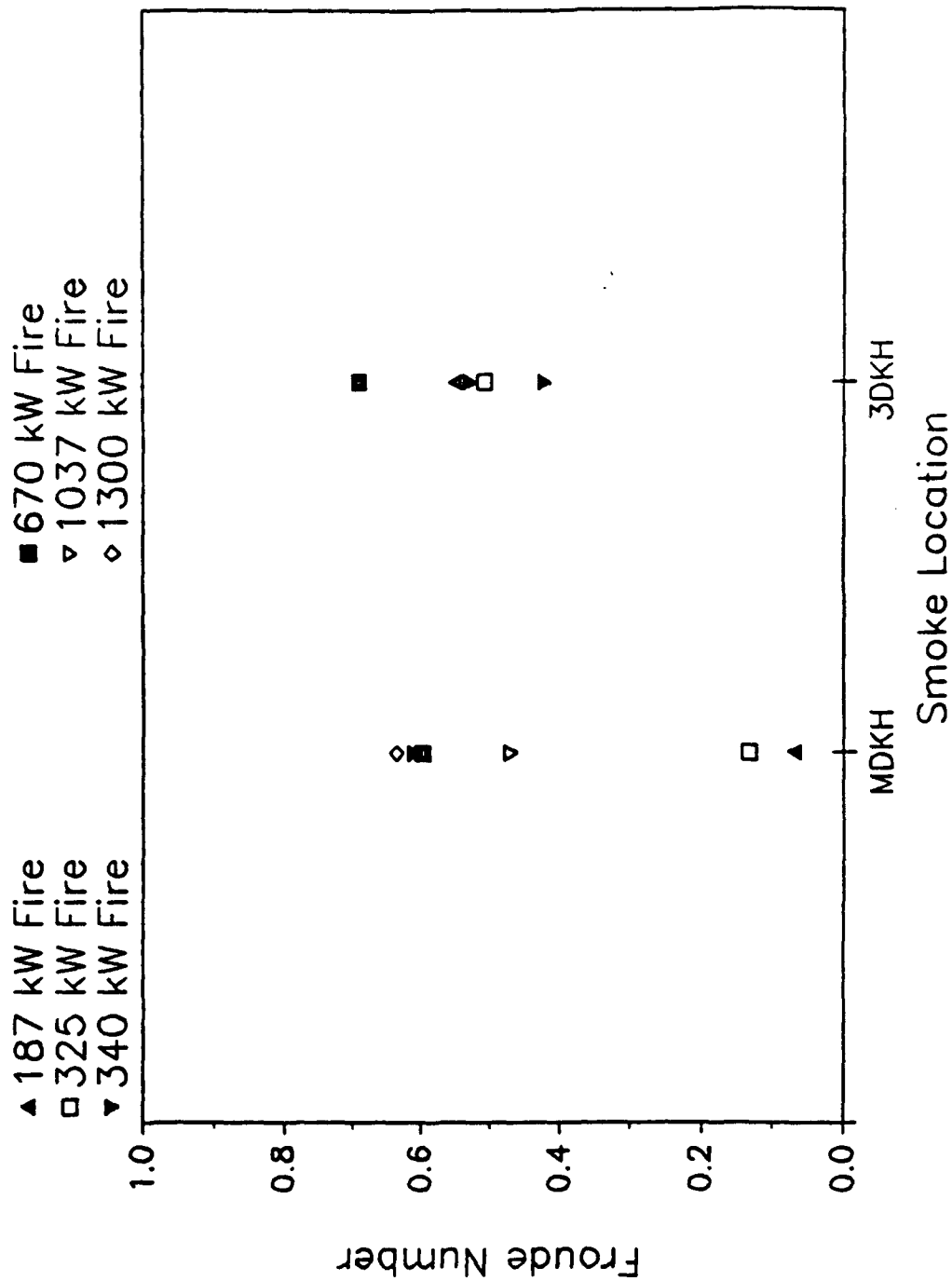


Fig. 37 – Froude Number correlation based on center trunk tree temperature difference, height and velocity at smoke location with fire in location 2

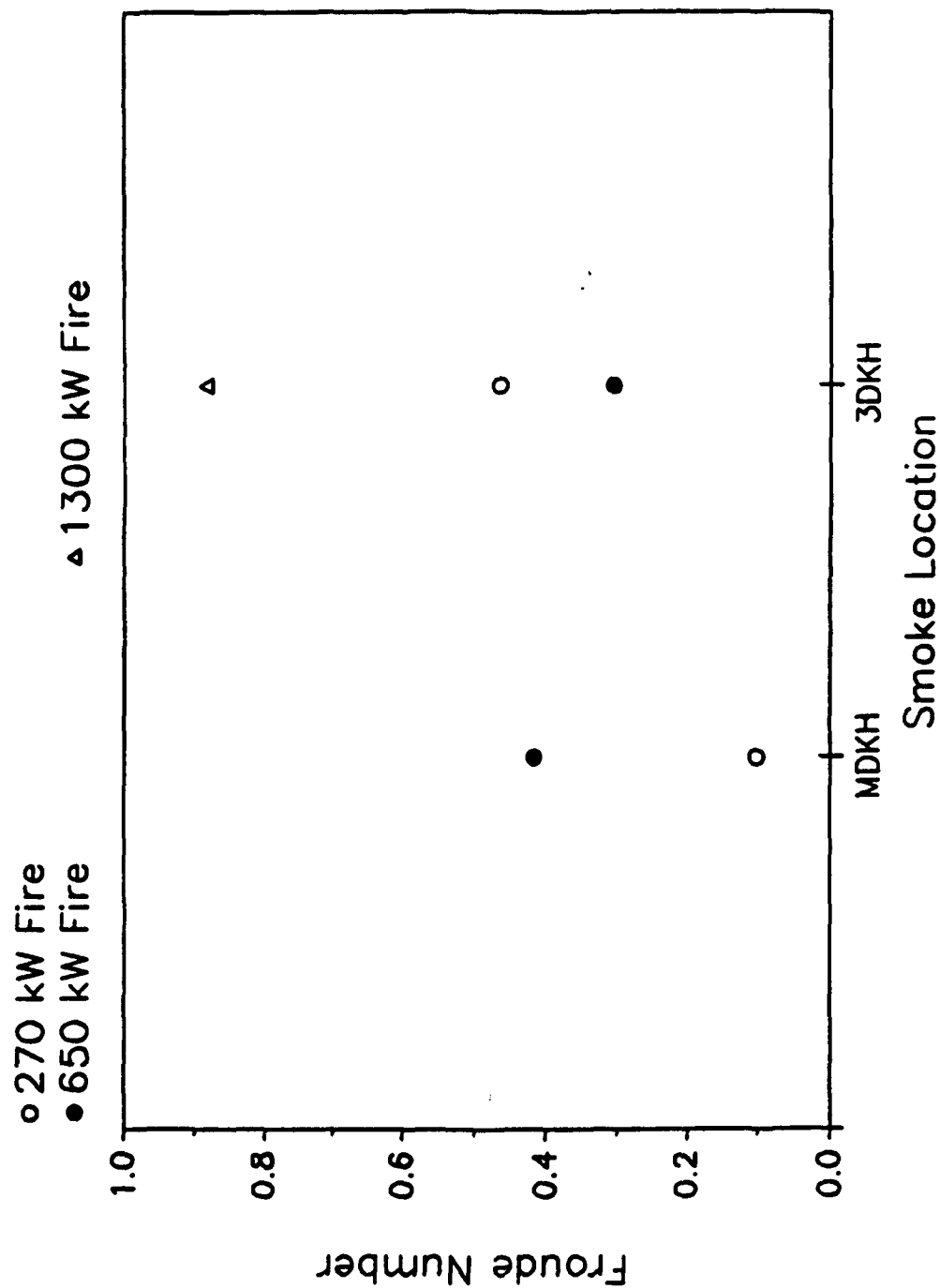


Fig. 38 – Froude Number correlation based on side trunk tree temperature difference, height and velocity at smoke location with fire in location 1

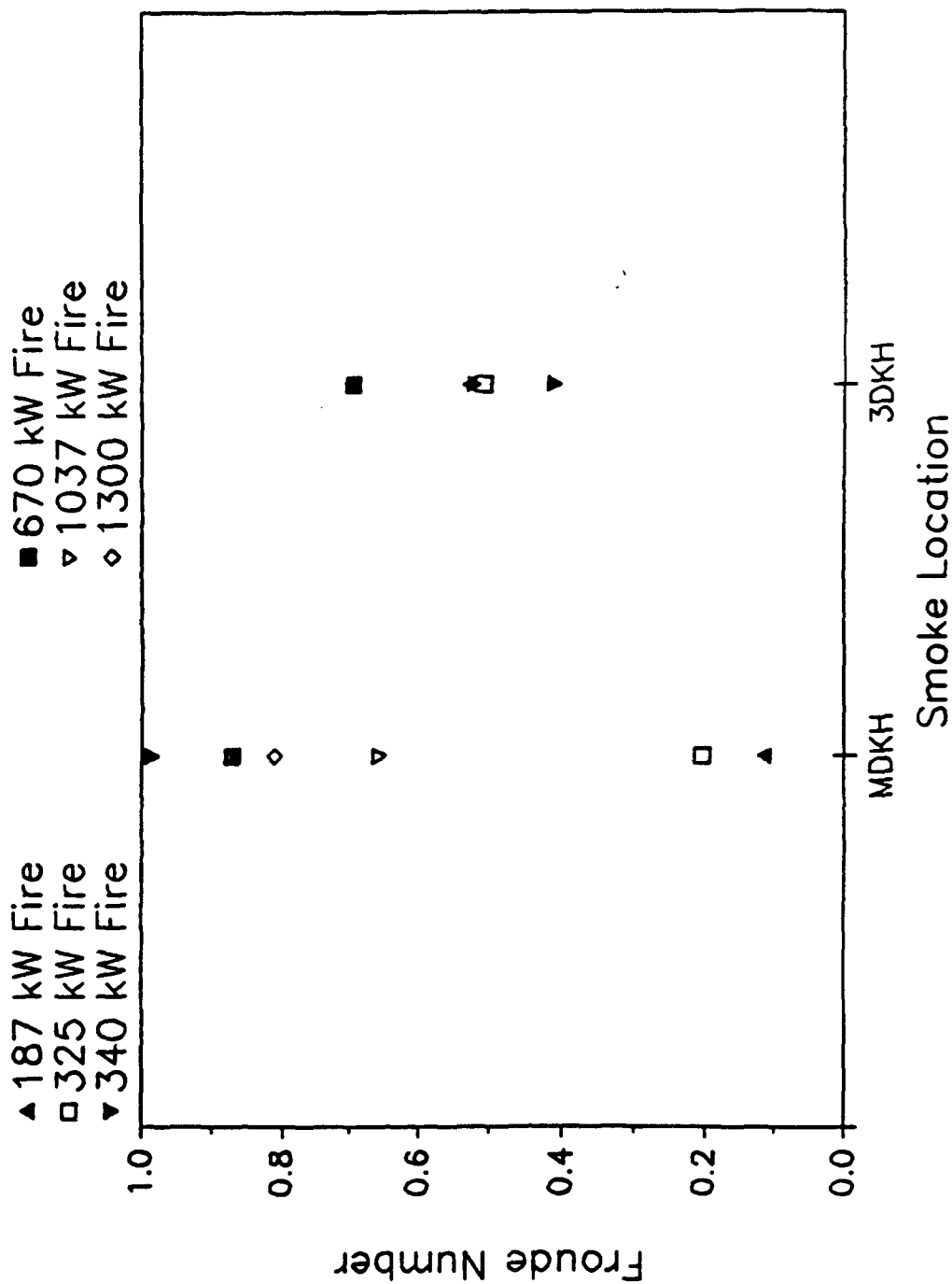


Fig. 39 – Froude Number correlation based on side trunk tree temperature difference, height and velocity at smoke location with fire in location 2

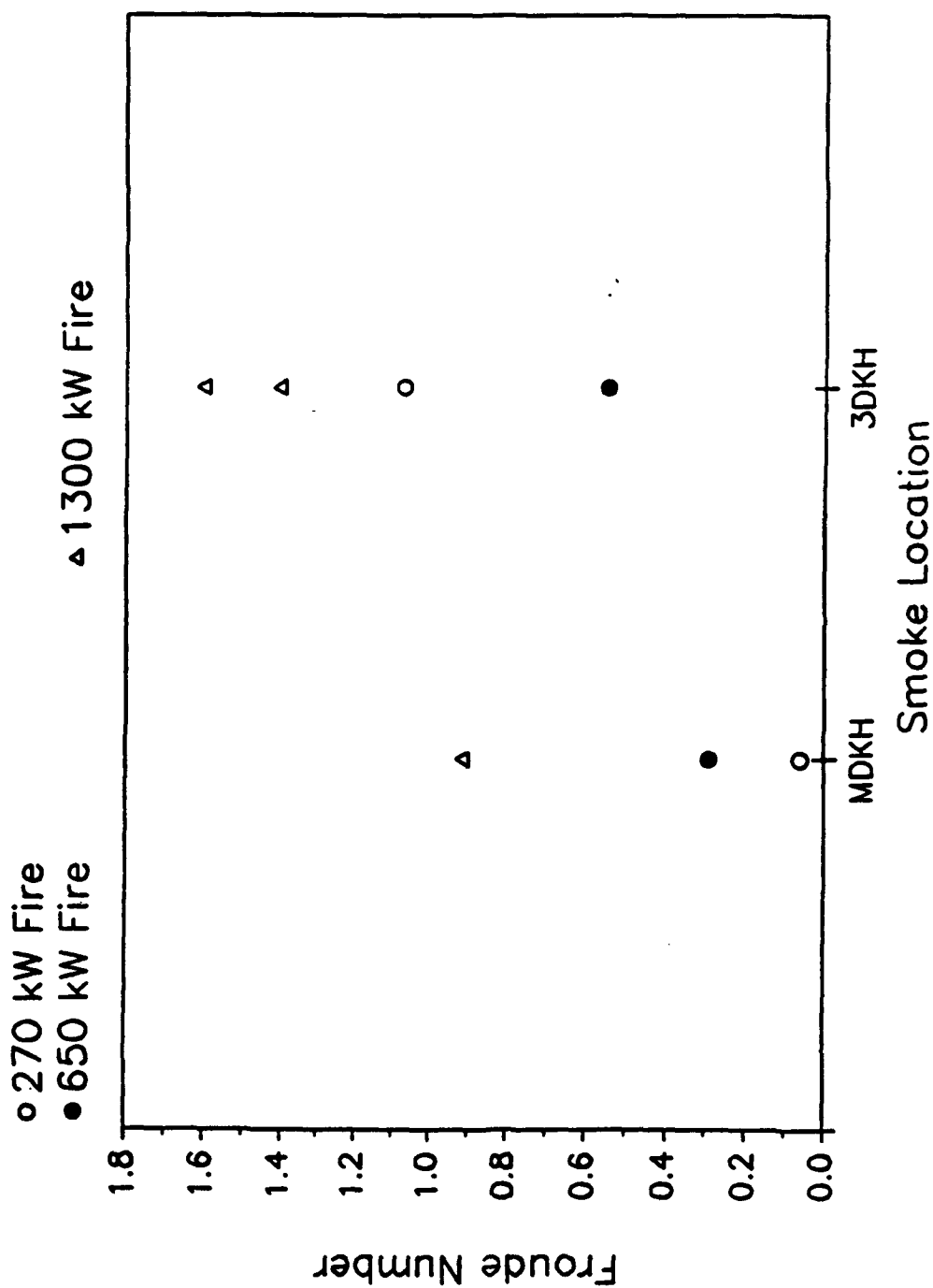


Fig. 40— Froude Number correlation based on hatch trees temperature difference, height and velocity at smoke location with fire in location 1

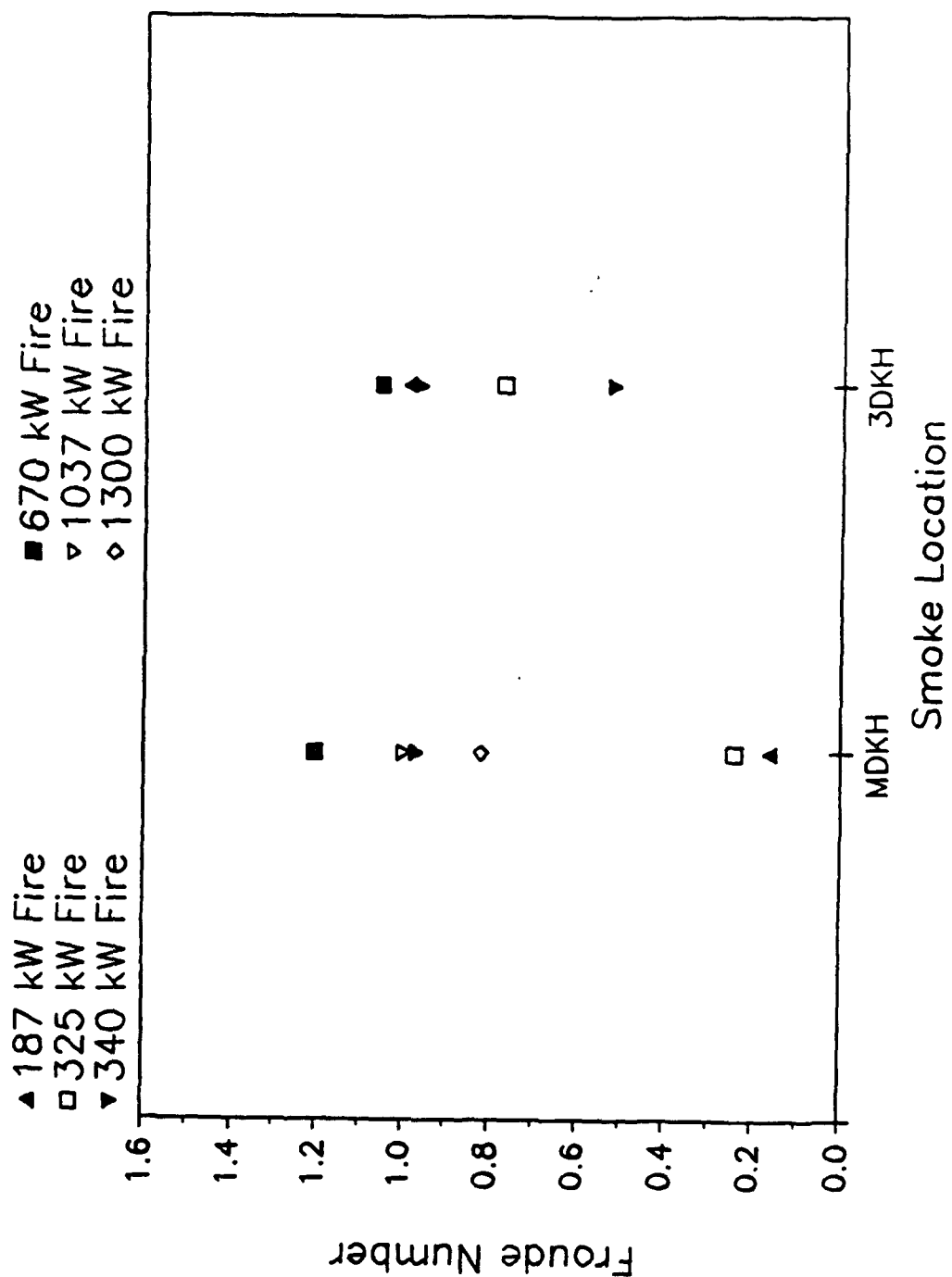


Fig. 41 – Froude Number correlation based on hatch trees temperature difference, height and velocity at smoke location with fire in location 2



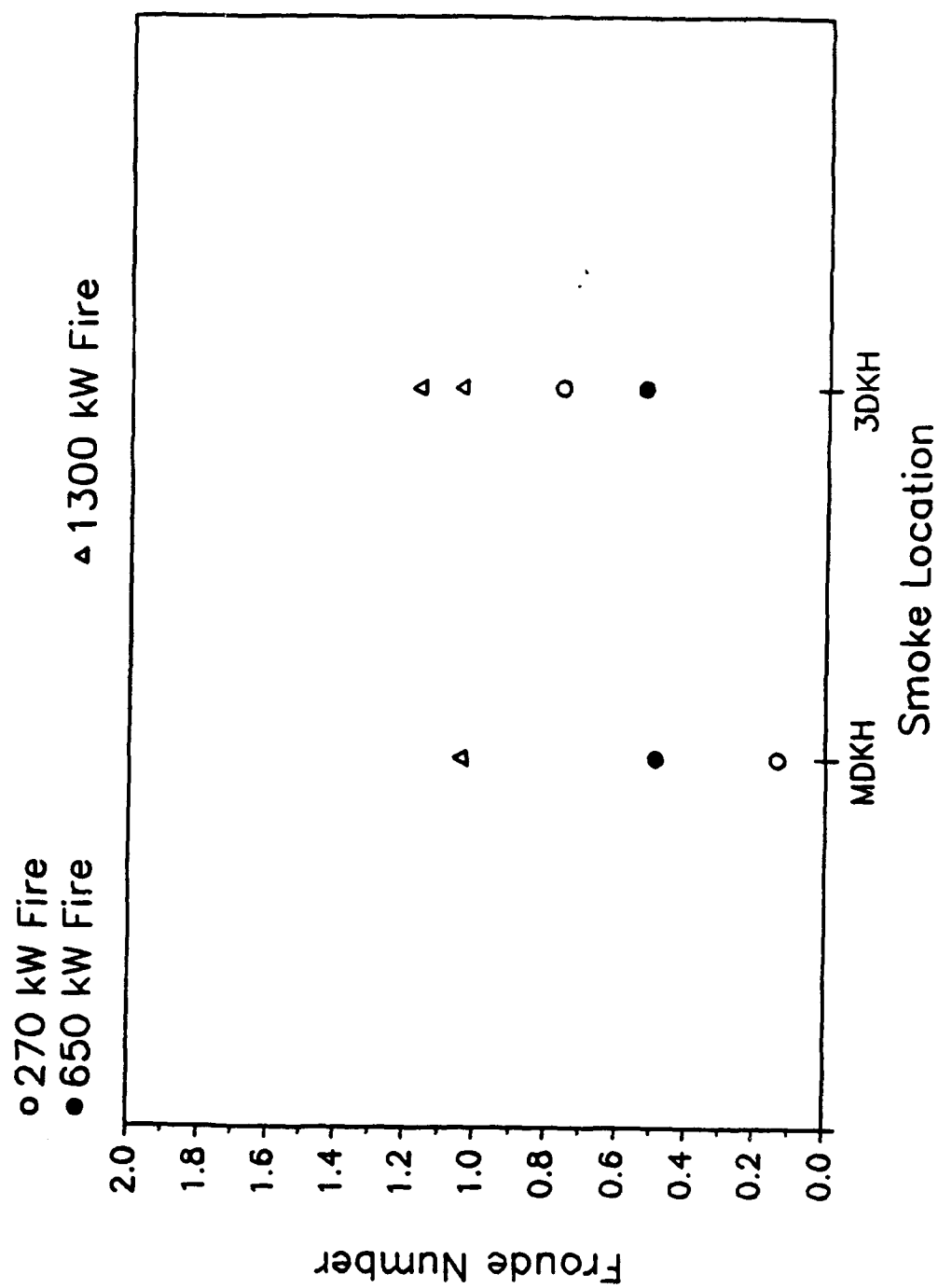


Fig. 42 – Froude Number correlation based on fire size, downstream temperature and velocity at smoke location with fire in location 1

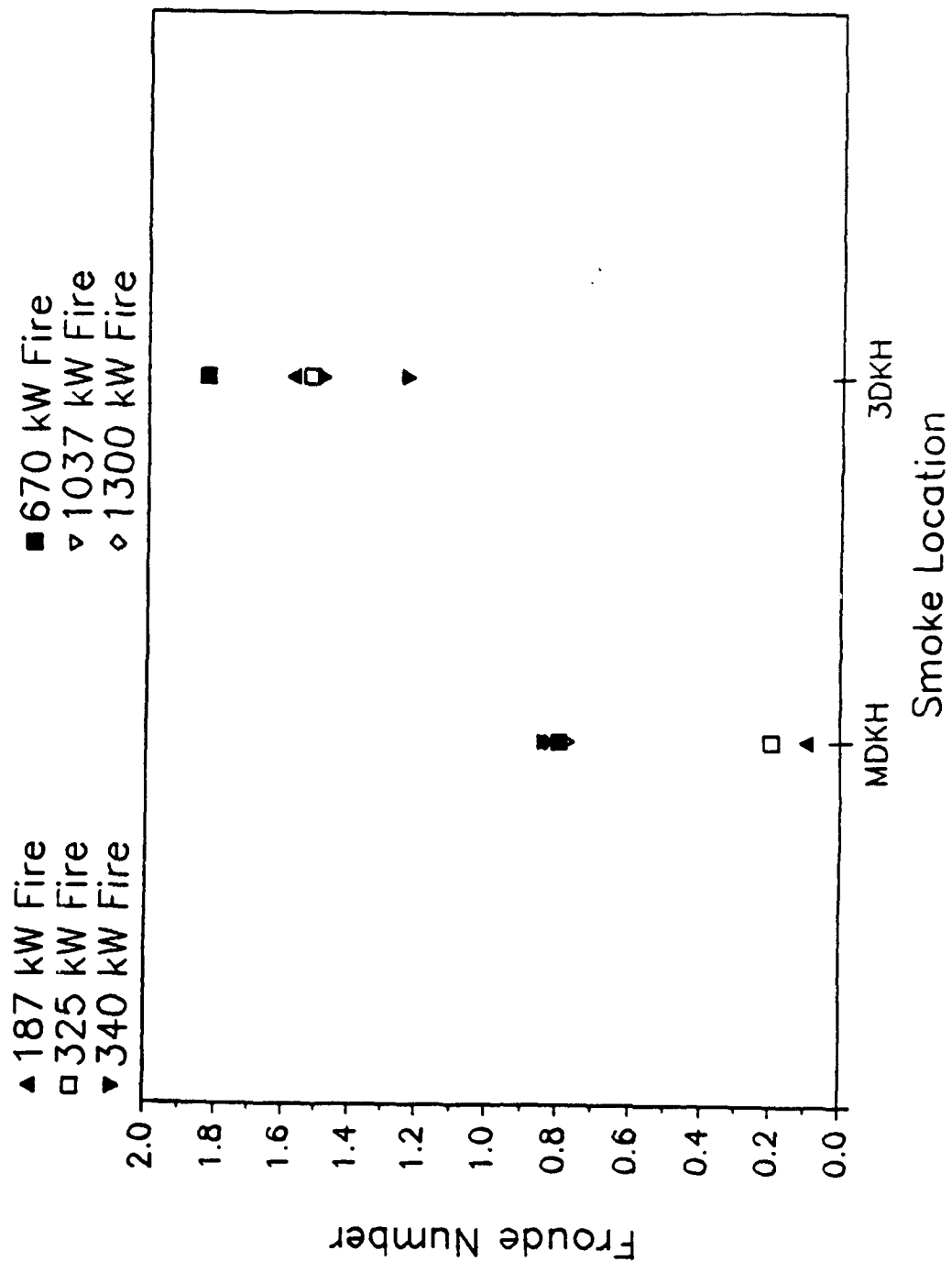


Fig. 43 – Froude Number correlation based on fire size, downstream temperature and velocity at smoke location with fire in location 2

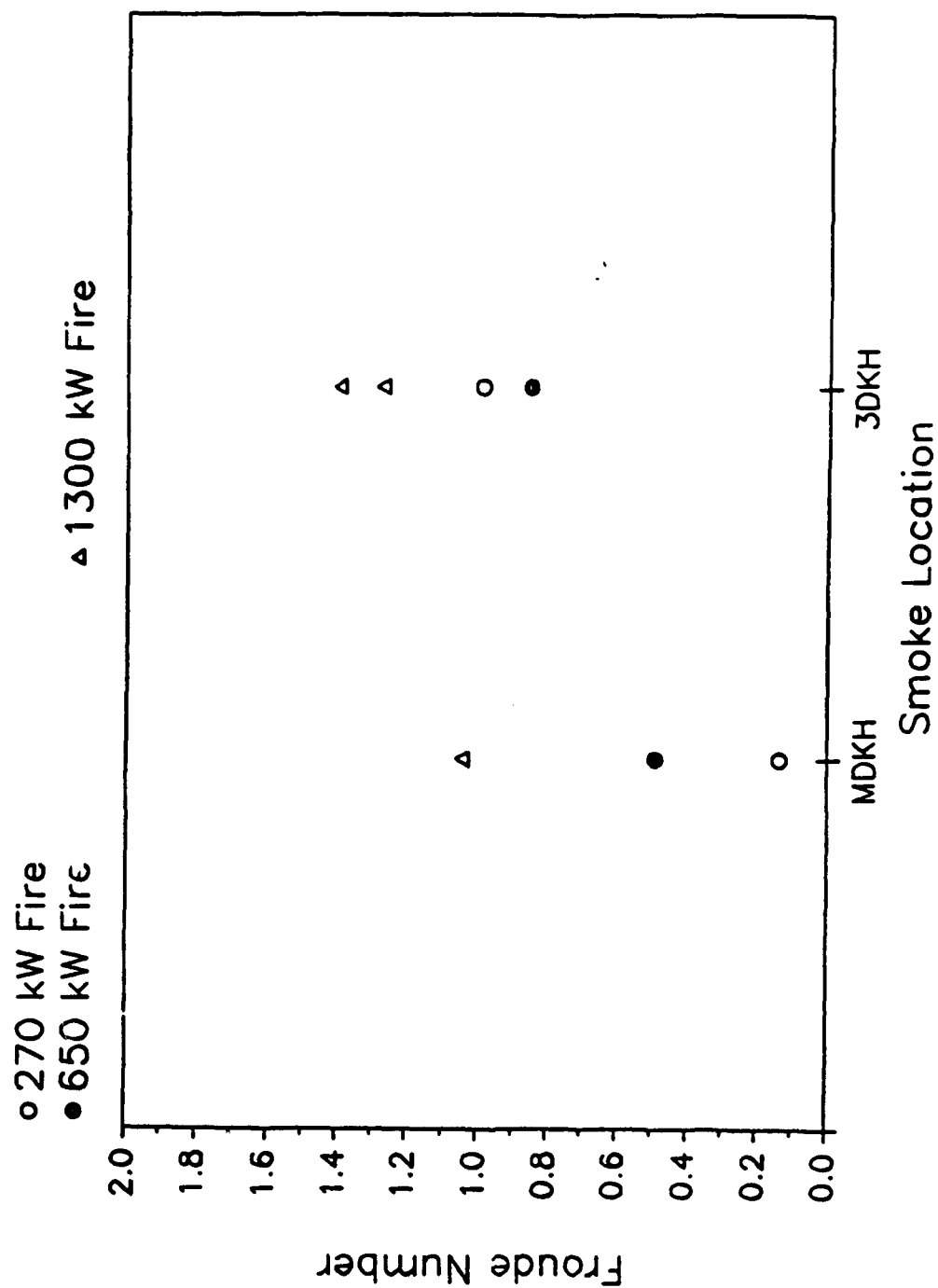


Fig. 44 – Froude Number correlation based on fire size, downstream temperature and velocity at main deck hatch with fire in location 1

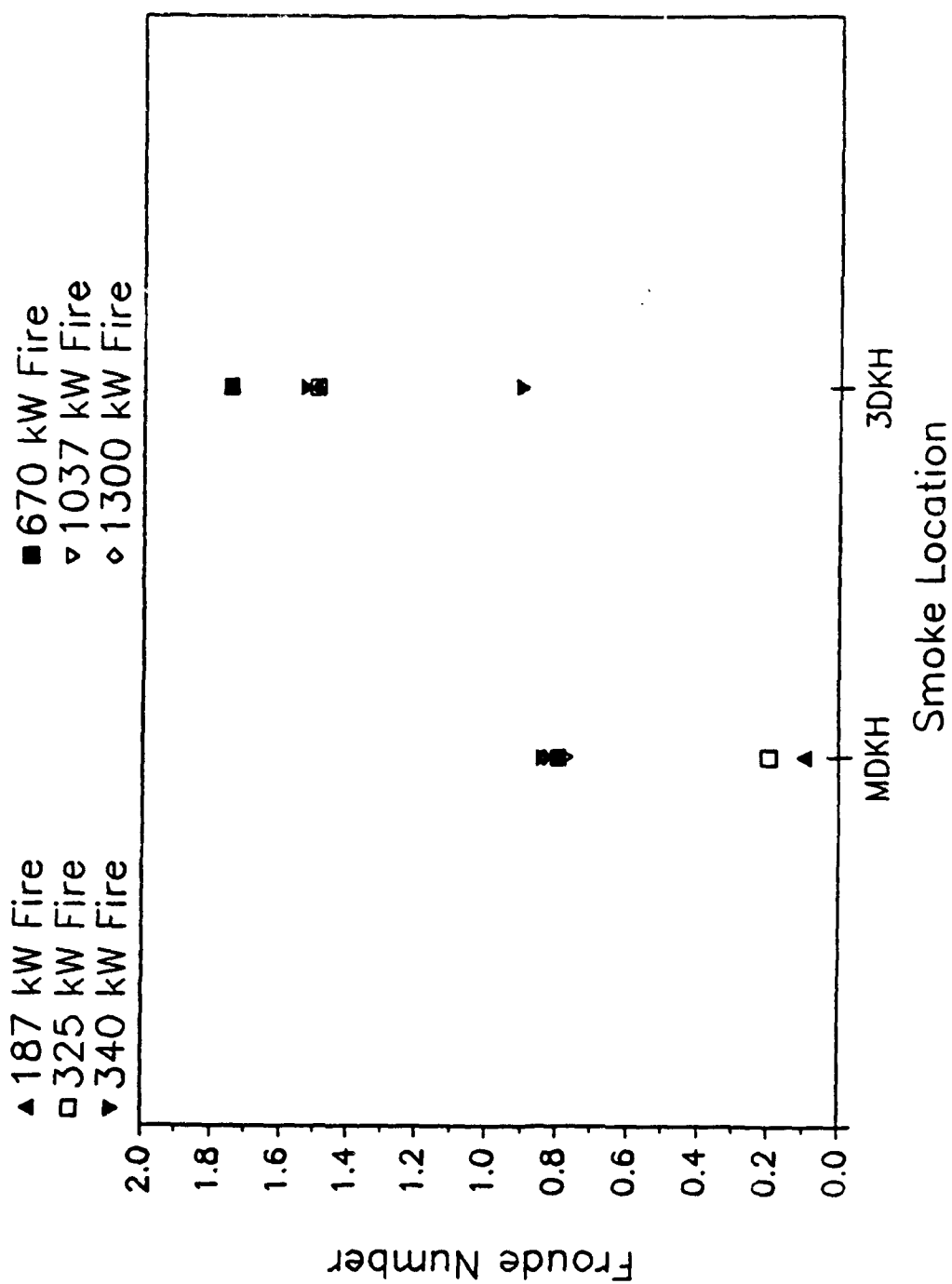


Fig. 45— Froude Number correlation based on fire size, downstream temperature and velocity at main deck hatch with fire in location 2

at the main deck hatch). The maximum Froude number determined at the main deck hatch was 1.05 for the 1300 kW fire in location 1.

## **8.0 DISCUSSION**

These results clearly demonstrate the efficacy of counterflow air velocity in preventing upstream smoke migration in both horizontal and vertical geometries. Simplified theoretical models (Froude modeling) have been demonstrated to apply in approximate terms in a complicated shipboard flow path. Hence, computer-based mathematical modeling could be used to evaluate the counterflow air velocity required to prevent smoke migration for any fire size in any ship geometrical configuration. As a very approximate rule of thumb, air velocities through door openings on the order of 2-3 m/sec (393-500 ft/min.) will eliminate or severely limit upstream smoke migration. This translates to a flow requirement of approximately 2 to 3 m<sup>3</sup>/sec (4000 - 6000 ft<sup>3</sup>/min) volumetric air flow rate requirement.

Lower values will severely restrict upstream smoke migration and will halt smoke migration after the smoke has travelled a certain distance and cooled. The relationship between fire size, counter flow air velocity and upstream smoke travel distance is approximately given by the Froude number correlations.

The counterflow air requirement could be provided by the use of exhaust fans as well as supply fans. In either event, both supply and exhaust flow paths must be provided. In addition, the supply fan must generate sufficient pressure at the required flow to account for pressure losses along the supply path (in this case passageways) as well as to move the expanded volume of hot smoke down the exhaust path to an overboard vent.

Provision of adequate air flow rates could be accomplished by reconfiguring normal ship's ventilation fans, machinery space fans, and/or portable blowers. The advantages of using supply air are (1) fan and opening configuration can be set away from the fire/smoke source and (2) the fans will not be exposed to elevated temperatures. The issue of adequate fan supply pressure and subsequent induced pressure differential at the fan source and in the supply and exhaust air may have particular impact on the use of portable blowers.

The primary risk of using forced ventilation in counterflow smoke control relates to increasing fire size and temperatures downstream of the fire location. In some cases, however, the increased air flow rates dilute and cool the smoke in the exhaust system. These tests did not evaluate the impact of counterflow air supply on fire spread rate in a passageway; these fires were of a fixed size.

The risk of increased fire spread rate is obviously mitigated if the forced air flow permits rapid location and extinguishment of the fire. This well known firefighting tradeoff is clear. If one wishes to vent smoke in any fashion, air must be supplied.

In order to assess the threat of increased fire spread rate or enhanced burning caused by the provision of supply air, it is useful to treat two separate cases: one in which the fire is in a compartment opening onto a passageway; the other where the passageway itself is involved in the fire.

Consider the case where the fire is located in a compartment. In this case, the compartment is supplied air by the buoyant flows associated with the fire. The same forces that cause smoke to spread outside of the compartment cause combustion air to be drawn through openings. These openings exist in the form of open doors, door louvres, supply and exhaust ducts, cable penetrations, cracks around doors, and other openings. One effect of forced air flow down a passageway is providing clean air with 21 percent oxygen concentration. The other effect is a positive pressure that may, depending on other leakage paths in the compartment, force air into the compartment. Assume that the only openings to the compartment lie along the bulkhead that is exposed to the forced counterflow air movement. In this case, since there is no other exhaust path, there is little effect of air supplied down the corridor. This holds true whether the door is open or closed unless the entire passageway leading to the compartment is severely oxygen depleted.

A more realistic case is that small leakage paths exist throughout the compartment. In this case, the net positive pressure in the passageway forces air into the space and through openings between the passage and the compartment and it simultaneously forces smoke and heated gases out through other leaks. This net inflow of air will provide additional combustion air in a quantity driven by the size of the leakage paths. Note that without this externally induced positive pressure, leaks high in the space will exhaust smoke from the compartment, and leaks at lower elevations will draw air by virtue of normal buoyancy forces. The provision of forced supply air in the passageway redirects this natural flow in and out of the compartment essentially substituting forced pressure differences for natural buoyancy driven pressure differences. The impact of forced air in this case is completely dependent on the size of the leaks and the induced pressure difference. It will, in general, be a very slight impact.

The potentially more troublesome case is a fire in the passageway. In this case, the exhaust path downstream of the fire is relatively large (or there would be no counterflow air movement), and hence, the supply air in the passage forms a wind tunnel which can accelerate the rate of fire spread downstream. The rate of increased fire spread has never been evaluated. However, the ability to form a completely smokefree access path to the fire will greatly reduce the time required for a firefighting team to find and extinguish the fire. This tradeoff needs to be quantified for the case of fires in passageways.

## **9.0 CONCLUSIONS**

The application of air flow or pressurization techniques, commonly used to clear the means of egress in buildings, to keep important shipboard passageways and trunks clear of smoke has been shown to have significant promise. In these tests, relatively

modest air velocities were able to limit the migration of smoke in either the horizontal corridor or the vertical trunk.

The concept of forced counterflow air movement to limit smoke spread and form a smokefree path to the fire has been demonstrated. There is a clear predictable relationship between fire size and required air flow velocity.

This approach requires configuring both a supply and exhaust path into the area where smoke is to be moved as well as the provision of a forced supply or exhaust source. The risk of increased fire growth and/or spread is greatest where the fire is located directly in the supply/exhaust path (e.g., in a passageway). The balance between fire spread and greatly reduced extinguishment time must be further evaluated.

Attempts to generalize the results of these tests through a Froude number correlation were hampered by the complicated flow patterns of both the smoke and opposing air. Therefore, only modest generalizations can be made, i.e., a Froude number,  $Fr_{TD}$ , of 1.35 is sufficient to hold smoke in a horizontal corridor when the buoyancy is based on the hot layer average temperature and depth 2.4 m (8 ft). As a rule of thumb, air flow velocities on the order of 2.5 m/s (8.3 ft/s) will be sufficient to prevent smoke migration against relatively severe fires located directly in the passageway. Other fire locations will require lower air velocity requirements.

## 10.0 RECOMMENDATIONS FOR FUTURE RESEARCH

Based on these results, it is recommended that additional work be performed to evaluate the following issues:

- (1) The ability of damage control teams to reconfigure ship's ventilation systems to provide supply (or exhaust) flow and to establish supply and exhaust flow paths;
- (2) The risk of increased fire spread caused by counterflow air movement needs to be further studied and quantified;
- (3) The use of portable blowers for providing an adequate supply air (pressure and flow) should be evaluated and quantified;
- (4) The impact of smokefree access paths on the effectiveness of damage control teams should be quantified;
- (5) The tradeoff between improved firefighting effectiveness and potential increases in fire growth rates requires quantification; and
- (6) Firefighting doctrine and guidance should be prepared if the concept can be practically used by damage control teams with minimum risk.

## 11.0 REFERENCES

1. National Fire Protection Association, "Recommended Practice for Smoke Control Systems," NFPA No. 92A, Batterymarch Park, Quincy, MA, 1988.
2. Carey, R.B., "Smoke and Toxic Gas Control System for Navy Ships," DTRC Report DTNSRDC/SME-85/101, February 1986.
3. Thomas, P. H., "The Movement of Smoke in Horizontal Passages Against an Air Flow," Fire Research Note No. 723, Fire Research Station, Borehamwood, Herts, England, 1968.
4. Klote, J. H., and Fothergill, J. W., Jr., "Design of Smoke Control Systems for Buildings," NBS Handbook 141, U.S. Dept. of Commerce, Washington, D.C., July 1983.
5. Heskestad, G., and Spaulding, R. D., "Inflow of Air Required at Wall and Ceiling Apertures to Prevent Escape of Fire Smoke," FMRC Technical Report J.I. OQ4E4.RU 070 (A), Factory Mutual Research Corporation, Norwood, MA, July 1989.
6. Carhart, H. W., and Williams, F. W., "The Ex-USS SHADWELL — Full Scale Fire Research and Test Ship," NRL Memorandum Report 6074, Revised January 20, 1988.
7. Dwyer Instruments, Inc., "The Dwyer Catalog of Controls and Gages," Michigan City, Indiana, 1988.
8. Segeler, C. G., Editor in Chief, *Gas Engineers Handbook*, First Edition, Industrial Press Inc., New York, NY, 1965.
9. DiNenno, P. J., Editor in Chief, *SFPE Handbook of Fire Protection Engineering*, National Fire Protection Association, Batterymarch Park, Quincy, MA, 1988.